



Calhoun: The NPS Institutional Archive DSpace Repository

Theses and Dissertations

1. Thesis and Dissertation Collection, all items

1975

A superconducting synchronous torque-compensated motor for naval applications.

Reynerson, Donald Martin

Massachusetts Institute of Technology

<http://hdl.handle.net/10945/21074>

Downloaded from NPS Archive: Calhoun



<http://www.nps.edu/library>

Calhoun is the Naval Postgraduate School's public access digital repository for research materials and institutional publications created by the NPS community.

Calhoun is named for Professor of Mathematics Guy K. Calhoun, NPS's first appointed -- and published -- scholarly author.

Dudley Knox Library / Naval Postgraduate School
411 Dyer Road / 1 University Circle
Monterey, California USA 93943

A SUPERCONDUCTING SYNCHRONOUS TORQUE-
COMPENSATED MOTOR FOR NAVAL APPLICATIONS

Donald Martin Reynerson

UNIVERSITY LIBRARY
UNIVERSITY POSTGRADUATE SCHOOL
MONTEREY, CALIFORNIA 93940

A SUPERCONDUCTING
SYNCHRONOUS TORQUE-COMPENSATED
MOTOR FOR NAVAL APPLICATIONS

by

DONALD MARTIN REYNERSON
"

BSEE, MEE, NORTH CAROLINA STATE UNIVERSITY
(1968)

SUBMITTED IN PARTIAL FULFILLMENT OF THE
REQUIREMENTS FOR THE DEGREE OF
NAVAL ARCHITECT
AND THE DEGREE OF
MASTER OF SCIENCE IN MECHANICAL ENGINEERING
at the

MASSACHUSETTS INSTITUTE OF TECHNOLOGY
JUNE, 1975

A SUPERCONDUCTING SYNCHRONOUS TORQUE-COMPENSATED MOTOR
FOR NAVAL APPLICATIONS

by

DONALD MARTIN REYNERSON

Submitted to the Department of Ocean Engineering on May 9, 1975, in partial fulfillment of the requirements for the degree of Naval Architect and the degree of Master of Science in Mechanical Engineering.

ABSTRACT

Modern naval vessels, which depend more on a reduction in the displacement per shaft horsepower than an increase in the lift/drag ratio to improved performance, must increasingly turn to propulsion systems with characteristically high power densities. Systems planned for or currently employed in high performance craft all have inherent disadvantages which require new approaches. One such approach is the use of electrical propulsion systems which allow operational flexibility and an ease of power transfer not found in many other systems. The utilization of superconducting materials in the field windings of propulsion machines significantly improves the power density of the system while retaining other advantageous characteristics of electrical propulsion systems.

Many superconducting motors either in the conceptual or prototype stages of development, require the superconducting field winding to transfer machine torque to the naval craft which, in turn, requires a substantial structural interface between the superconducting element and the environment. Such a structural interface results in a significant heat leak into the cryogenic components reducing system efficiency. Other designs place the cryogenic element on the rotor, requiring a rotating liquid transfer coupling and all of the technical complexities that such an element entails.

This thesis proposes the use of a dual field motor; the main power producing field to be superconducting, and an ambient temperature concentric compensating field configured to remove the load torque from the cryogenic element. Both fields are wound on the stator, thus eliminating the liquid transfer problem; the three-phase armature is wound on the rotor. A mathematical model is developed and the size and parameters for a 22,700 horsepower motor are determined. The resulting model is analyzed and various modes of control discussed.

Thesis Supervisor: Philip Thullen
Title: Associate Professor of Mechanical Engineering

Thesis Reader: Clark Graham
Title: Associate Professor of Marine Systems

ACKNOWLEDGEMENTS

To a large degree, the culmination of three years of study is expressed in this thesis, and without the continuing assistance over this period of several individuals, completion of this work would have been impossible. My sincere appreciation is extended to Professor Philip Thullen who patiently supervised and guided the development and preparation of this work. I am also indebted to Dr. Thomas A. Keim for his frequent and always thorough explanations of the many questions which arose during the course of this undertaking.

The author is especially grateful to his wife, Ann, whose patience and understanding under often trying conditions during the years at M.I.T. was at times monumental. Special thanks to Mrs. Sandra Margeson who assumed the tedious and time consuming responsibility of preparing this thesis.

This work was supported in part by the Office of Naval Research, Contract #N00014-75-C-0497.

TABLE OF CONTENTS

	<u>PAGE</u>
Title Page	1
Abstract	2
Acknowledgements	3
Table of Contents	4
I. Introduction	5
II. Physical Description of Motor	23
III. Theoretical Characteristics and Rating Expressions	27
IV. Results	40
V. Discussion of Results and Conclusions	51
VI. Recommendations	58
Appendix A. Field Analysis	59
Appendix B. Machine Inductances	94
Appendix C. Internal Torque Expressions	113
Appendix D. Machine Sizing and Losses	124
Appendix E. Derivation of Machine Characteristics and Rating Expressions	132
Appendix F. Program Listing	144
References	156

I. INTRODUCTION

The use of superconducting field windings in synchronous machines is now an accepted and experimentally substantiated technique, and it is evident that these machines have the greatest potential applications where weight and power density are of significance in the system design philosophy. Because of the inherent weight and volume savings and system flexibility associated with superconducting power generation and utilization, superconducting machines present an attractive alternative in the design of naval propulsion systems.

As progress is made from lower to higher performance water-borne vehicles, increases in speed are entirely attributable to increases in the shaft horsepower per ton displacement rather than to improvements in the vehicle lift-drag ratios. In addition, hull structure and propulsion plant together have in past designs accounted for an average of 60% of the light ship weight, and future marine engineering studies, especially those in the naval systems domain, should concentrate on such developments as superconducting machines which promise significant weight and volume savings and superior acoustical performance. Electric power trains, because of their flexibility, are particularly attractive in advanced ship concepts such as SWATH, hydrofoils, and surface effect vehicles which require power transmission in strictly confined spaces and transmission trains which change direction abruptly.

All of the superconducting synchronous motors now either in the conceptual or prototype phases of development, utilize a rotating superconducting field winding which requires cryogenic fluid transfer to the rotating member. Many designs also require the superconducting field winding to transmit machine torque to the ship hull which requires a substantial structural interface between the cryogenic elements and the ship's hull. This results in significant thermal leakage to the low temperature machine components.

The motor evaluated herein will have a stationary superconducting field winding and an ambient temperature rotating armature winding, the armature being the central, interior member (see Figure 1). The field winding is surrounded by a solid, iron flux return path, operating in a magnetically saturated condition. A third direct current ambient temperature winding is provided to assume the load torque and relieve the superconducting field winding of this duty. This design eliminates the need for a rotating cryogenic transfer coupling and will substantially reduce the structural interface between the superconducting field and its environment.

The compensating field winding, if feasible, may be located either between the armature and main field or between the main field and shield. This thesis will examine both configurations and draw the appropriate conclusions from the analytical results.

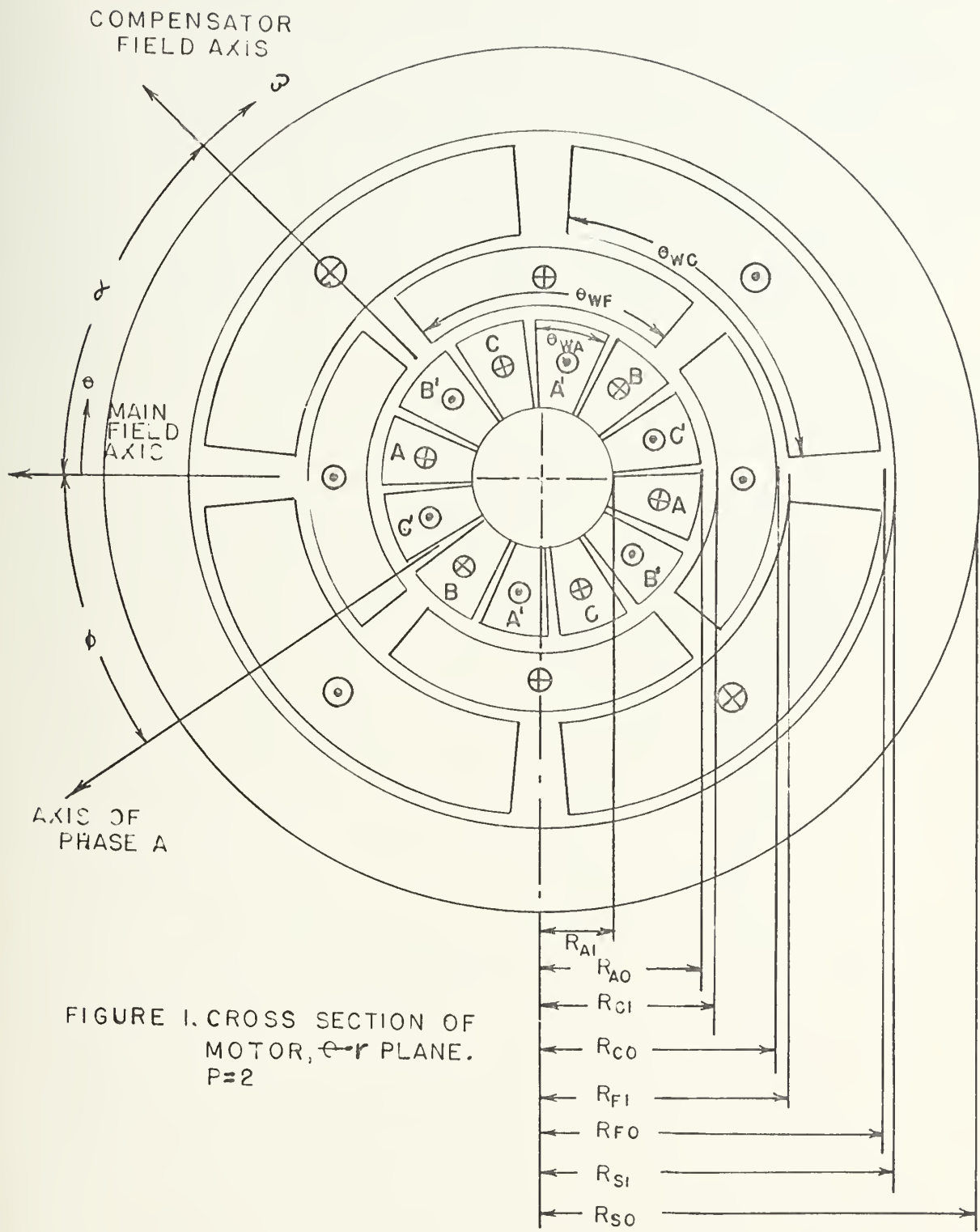


FIGURE 1. CROSS SECTION OF
MOTOR, ~~FOR~~ PLANE.
P=2

This paper develops the motor in a conceptual framework with emphasis on naval applications and high performance vehicles. Figures 2, 3, and 4 depict three possible applications to naval ship systems that are currently considered "state-of-the-art" to the naval architect and marine engineer. The motor developed herein may find useful applications both in these systems and many of those to be conceived in the future.

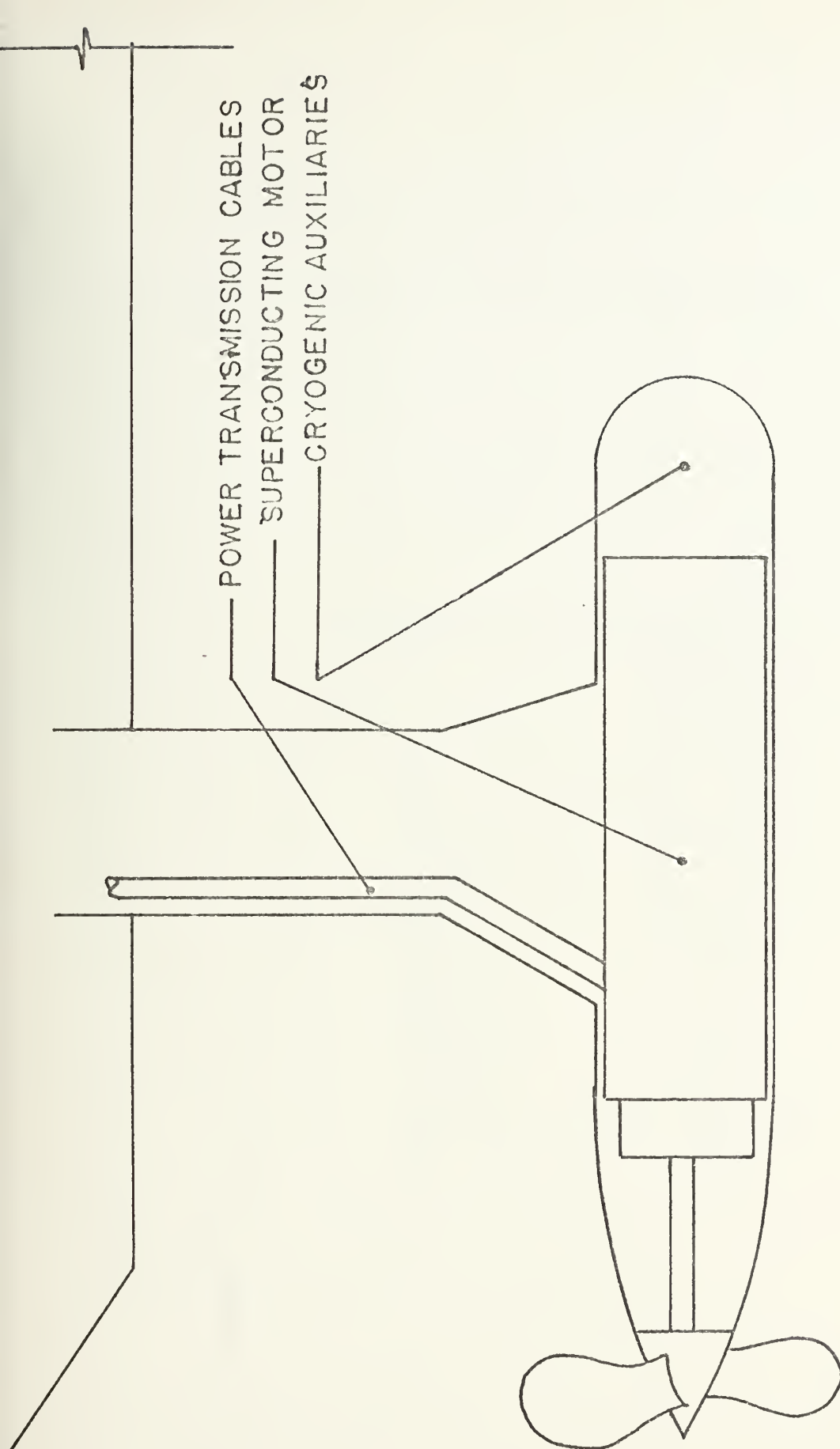


FIGURE 2. HYDROFOIL APPLICATION

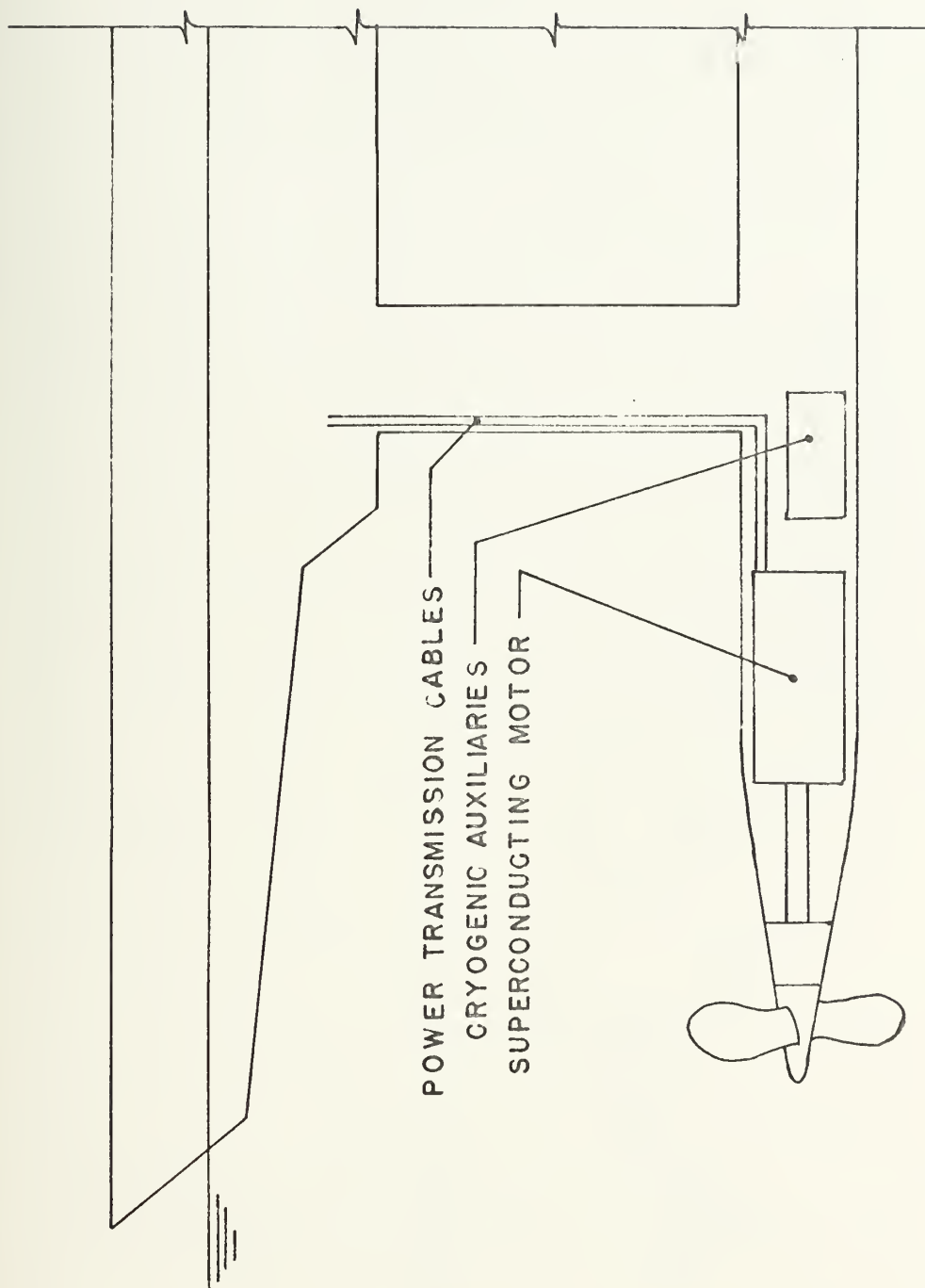


FIGURE 3. SMALL WATERPLANE AREA-TWIN HULL (SWATH) APPLICATION.

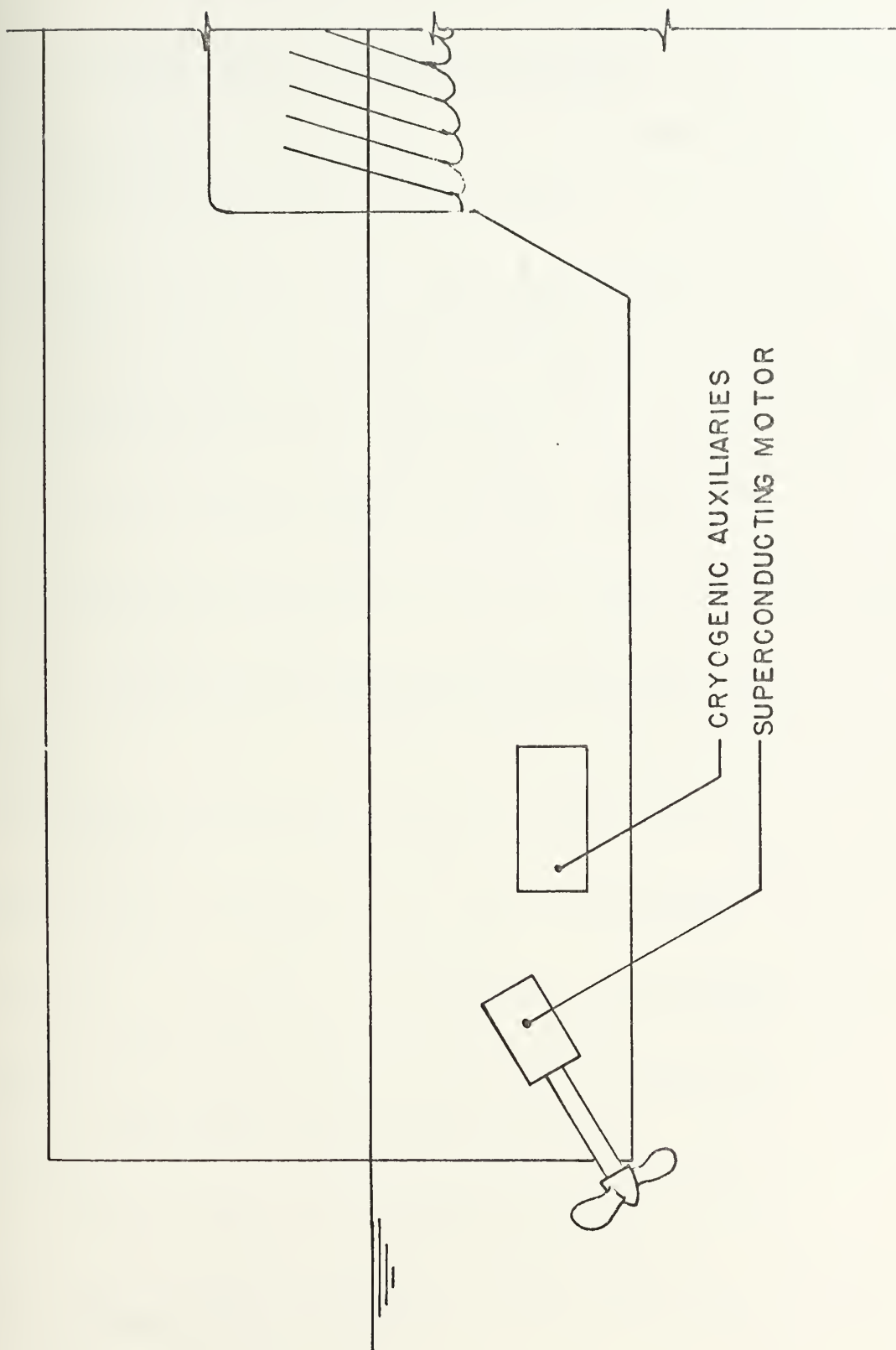


FIGURE 4. SURFACE EFFECT SHIP(SES) APPLICATION.

LIST OF FIGURES

	<u>PAGE</u>
1. Cross Section of Torque-Compensated Superconducting Motor, $\theta-r$ Plane	7
2. Hydrofoil Application	9
3. Small Waterplane Area-Twin Hull (SWATH) Application	10
4. Surface Effect Ship (SES) Application	11
5. Cross Section of Torque-Compensated Superconducting Motor, $r-z$ Plane	24
6. Idealized Support Structure for Superconducting Field Element	25
7. Field Density Capability Plot, $\alpha=90^\circ$, Underexcited Mode	28
8. Field Density Capability Plot, $\alpha<90^\circ$, Overexcited Mode	29
9. Voltage-Current Relationships for Overexcited and Underexcited Compensated Motors	31
10. λ as a Function of Power Factor Angle, ψ	36
11. J_a as a Function of J_f for a Fixed Power Factor; Overexcited Mode	37
12. J_a as a Function of J_f for a Fixed Power Factor; Underexcited Mode	38
13. J_c as a Function of Horsepower for Machines with Compensator Inside of Field	41
14. J_c as a Function of Horsepower for Machines with Compensator Outside of Field	43
15. σ_m as a Function of Horsepower for Machines with Compensator Outside of Field	45
16. J_c as a Function of J_a for Selected Motor Described in Table 3	47

17. Horsepower as a Function of J_a for Selected Machine Described in ^a Table 3	48
18. α as a Function of J_a for Selected Machine Described in Table 3 ^a	49
A1. Field Winding Angular Dependence of Current Density	70
A2. Field Winding Pole Face	74
A3. Schematic of Machine Shield Showing Parameters Used to Derive α_o	78
B1. Single Turn Coil Flux Linkage	95
B2. Flux Linkage of Differential Elements	97
C1. Field Winding Pole Face Isometric	116
D1. Machine Shear Stress Versus Machine Rating	127
D2. Winding and Shield Configuration for Shield Thickness Determination	129
E1. Voltage-Current Relationship for Overexcited Compensated Machine	133

LIST OF TABLES

	<u>PAGE</u>
1. Data for Machines Plotted in Figure 13	42
2. Data for Machines Plotted in Figures 14 and 15	44
3. Data for a Feasible Torque-Compensated Machine	53
A1. Surface and Reflection Coefficients	69
A2. Substitutions for Field Expressions	93
B1. Machine Inductances	101
B2. Substitutions for Machine Inductances	112
D1. Current Machine Vehicle Application Parameters	125
D2. Minimum Armature Shaft Inner Radii for Indicated Naval Applications	125
E1. Effective Lengths	143
F1. Input/Output Data for THESIS I Program	145
F2. Arrangement of Input Data Deck	147

LIST OF SYMBOLS

$A_o, A_1, A_2, A_3, A_4, A_5$

$B_o, C_o, D_o, a_o, b_o, c_o$

d_o, A_k, B_k, C_k, D_k

coefficients arising
from analyses

$\underline{A}, \underline{B}$

\bar{B}_A armature field-vector

\bar{B}_C compensator field-vector

\bar{B}_F superconducting-main-
field field-vector

\bar{B}_N $\bar{B}_a + \bar{B}_c + \bar{B}_f$

\bar{B}_{FN} $\bar{B}_c + \bar{B}_f$

d_{sh} shield dissipation per
unit man of shield
material

\bar{E} electric field strength

E_C excitation voltage
generated by the
compensating field

E_f excitation voltage
generated by the super-
conducting field

E phasor sum of E_C and E_f

e_f	per unit excitation voltage generated by superconducting field
\bar{f}	force on moving charge, q
\bar{F}	force density, newtons/m ³
\bar{H}	magnetic field density (vector)
H_{rf}	radial component of the magnetic field density due to a current in the field winding in region $R_{fi} < r < R_{fo}$
$H_{\theta f}$	azimuthal component of magnetic field density due to a current in field winding in region $R_{fi} < r < R_{fo}$
$H_{r fi}$	radial component of magnetic field density due to a current in the field winding and in region $R_{ai} < r < R_{fi}$
$H_{\theta fi}$	azimuthal component of magnetic field density due to a current in the field winding in region $R_{ai} < r < R_{fi}$
$H_{r fo}$	radial component of magnetic field density due to a current in the field winding in region $R_{fo} < r < R_{si}$

$H_{\theta fo}$	azimuthal component of magnetic field density due to a current in field winding in region $R_{fo} < r < R_{si}$
H_{rc}	radial component of magnetic field density due to a current in compensator in region $R_{ci} < r < R_{co}$
H_{ra}	radial component of magnetic field density due to a current in phase a of armature in region $R_{ai} < r < R_{ao}$
i_a	per-unit phase current
I_z	polar moment of inertia
I_A	RMS phase current and line current
I_B	rated base current
J_a	armature current density
J_c	compensator current density
J_f	field current density
\bar{J}_F	free current density
k	index, separation constant

L_a	armature phase a self-inductance
L_c	compensator self-inductance
L_f	field self-inductance
L_{ab}	phase-to-phase mutual inductance
l	machine physical length
l_a	effective length for calculating armature winding self-inductance
l_c	effective length for calculating compensator self-inductance
l_f	effective length for calculating field self-inductance
l_m	effective length for calculating field-to-armature mutual inductance
l_{sh}	effective length in calculating shield losses
M_{af}	mutual inductance, field-to-phase-a of armature
M_{ac}	mutual inductance, compensator-to-phase-a of armature
M_{fc}	mutual inductance, field to compensator
M_t	moment

N_{ta}	number of phase-a turns per pole pair
N_{tc}	number of compensator turns per pole pair
N_{tf}	number of field turns per pole pair
n	index, harmonic
P	machine power in volt-amps
p	number pole pairs
\underline{p}	$\frac{2\pi}{p}$
PWR	real power in kw or hp
P_c	armature and compensator loss in hp
P_{ec}	eddy-current losses in armature
P_{sh}	shield losses in hp or kw
q	charge in coulombs
r	radial coordinate
R_{ai}	armature inner radius
R_{ao}	armature outer radius
R_{fi}	field inner radius

R_{fo}	field outer radius
R_{ci}	compensator inner radius
R_{co}	compensator outer radius
R_{si}	shield inner radius
R_{so}	shield outer radius
R	separation of variables parameter
\bar{T}	torque
\bar{T}_a	armature torque
\bar{T}_f	field torque
\bar{v}	charge linear velocity
V	volume
V_B	rated base phase voltage
V_T	machine phase terminal voltage
v_T	per-unit terminal phase voltage
w	R_{si}/R_{so} ; shield radius ratio
x	R_{ai}/R_{ao} ; armature radius ratio
x_a	internally normalized reactance
x_d	per-unit synchronous reactance

X_A	synchronous reactance in henrys
y	R_{fi}/R_{fo} ; field radius ratio
z	R_{si}/R_{so} ; compensator radius ratio
\bar{l}_r	unit normal vector in radial direction
\bar{l}_θ	unit normal vector in azimuthal direction
\bar{l}_z	unit normal vector in z direction
K_1, K_2, K_3, K_4, K_5	constants of convenience arising from analysis
α	angle between compensator and field direct axes
α_o	reflection coefficient
θ	separation of variables parameter
θ	azimuthal coordinate
θ_{wa}	armature winding included angle
θ_{wc}	compensator winding included angle
θ_{wf}	field winding included angle
μ_o	permeability of free space
μ_s	permeability of shield material

σ_m	magnetic shear stress
$\tau_{\theta z}$	shear stress
σ	conductivity of armature and compensator conductors
Φ	magnetic potential
λ	space winding factor, trigonometric coefficient defined in equation 51
ψ	magnetic flux function
ω_e	electrical angular frequency
ω_m	mechanical angular frequency
$\Gamma, \sigma_1, \sigma_2, \Omega_f, \Omega_c$	
$\Lambda_1, \Lambda_2, \bar{\Lambda}, \Delta_i (i=1,2,3), \eta, \zeta_1, \zeta_2$	constants of convenience arising from analysis

III. PHYSICAL DESCRIPTION OF MOTOR

Figures 1 and 5 depict the approximate physical configuration of the compensated motor. The illustrations used throughout this paper address only the two pole-pair (four pole) machine, but the analysis herein applies to configurations with any desired number of pole pairs.

The three-phase armature is wound on the rotor and supplied power through a high voltage slip ring assembly. The armature is to operate at ambient temperatures and is cooled by conventional non-cryogenic techniques. It is assumed that the upper constraint on armature current density is approximately 2.5×10^6 amps per square meter.

The superconducting field winding is positioned either outside of the compensator winding or between the armature and compensator windings. It is to operate at a temperature less than 5°C. As discussed earlier, the field winding may be fixed to the machine housing through an insulating medium which also functions as the supporting structure for the field. The field structure is assumed to contain little, if any, ferromagnetic material.

An idealized depiction of the field winding support structure is shown in Figure 6. This configuration is particularly applicable to a machine with the compensator within the field winding. Otherwise, the field could be supported radially and axially through the end housings of the machine. The optimum support structure could be depicted as some configuration of bicycle spoke supports made from an effective thermal insulator.

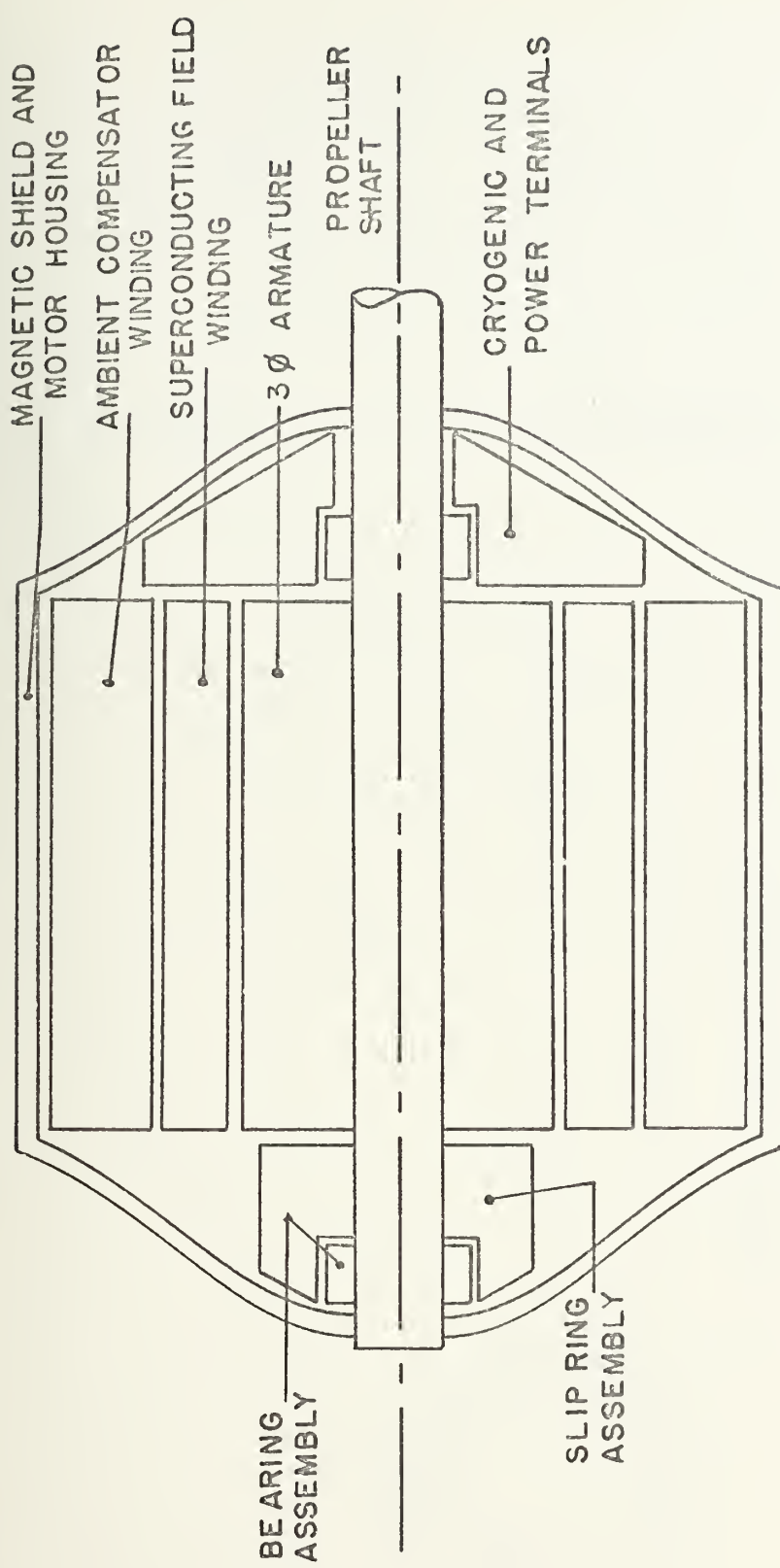


FIGURE 5. CROSS SECTION OF TORQUE-COMPENSATED SUPERCONDUCTING MOTOR, Y-Z PLANE.

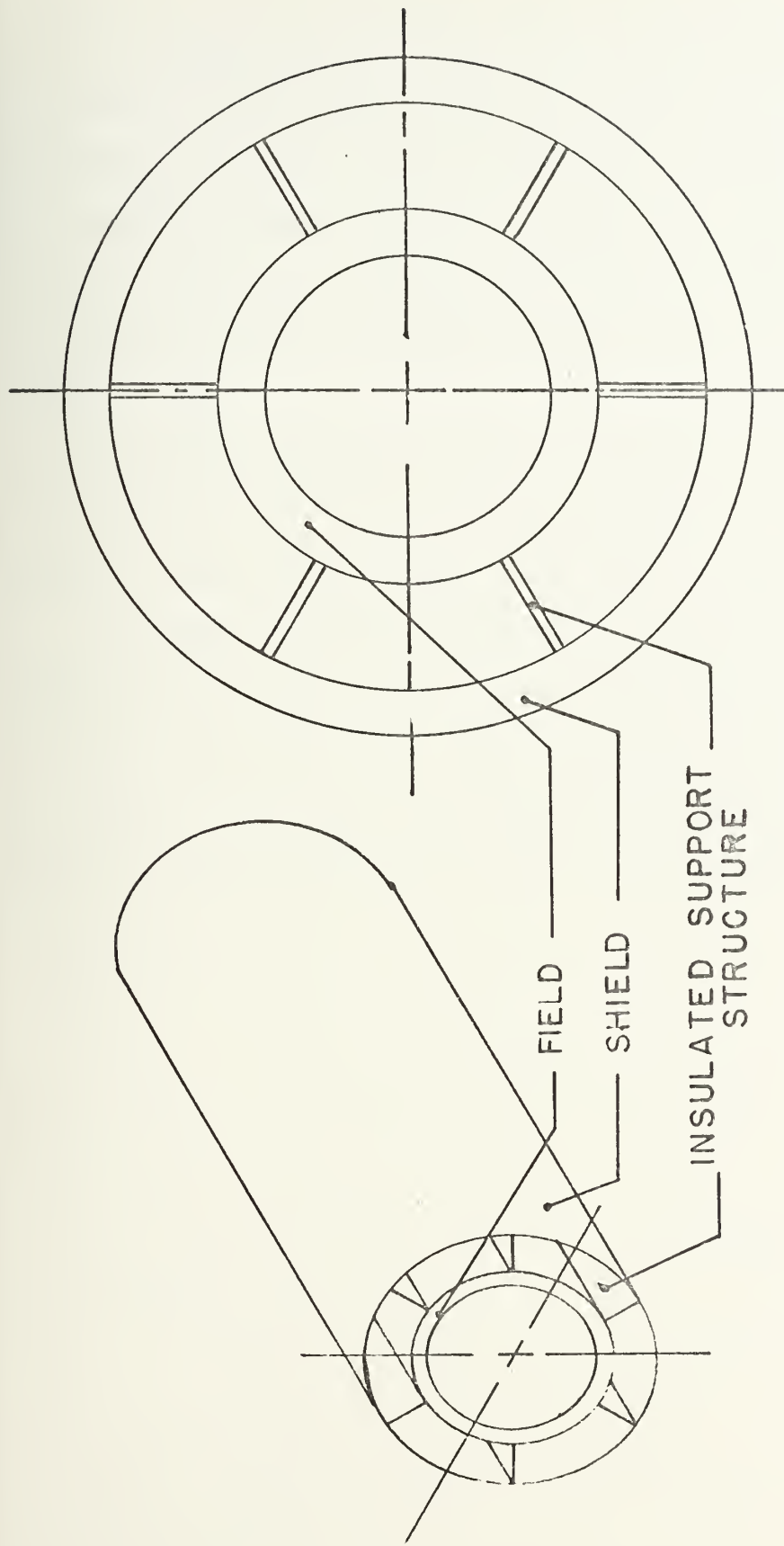


FIGURE 6. IDEALIZED SUPPORT STRUCTURE FOR SUPERCONDUCTING MAIN FIELD ELEMENT.

The compensating winding is physically located either outside of the field winding or between the field and the armature windings. It is to operate at ambient temperatures, to be cooled by non-cryogenic techniques, and to contain little, if any, ferromagnetic material. The current density is constrained at a maximum value of $2.5 \times 10^{+6}$ amps per square meter.

The motor examined herein is envisioned to be designed as a modular element in a propulsion system which must operate with a minimum down time after failure.

The motor will be fitted with easily disconnected fittings in order to facilitate rapid replacement upon failure at shore based facility. The cryogenic auxiliaries as shown in Figures 2, 3, and 4 are also to be modular packages which may be rapidly replaced by new or refurbished units.

III. THEORETICAL CHARACTERISTICS AND RATING EXPRESSIONS

An examination of Figure 7 reveals the requirement for zero torque on the superconducting field winding in terms of the machine's magnetic fields. The fields are referenced to the stator, and the resulting field vector at any location may be found as:

$$\bar{B}_N = \bar{B}_A + \bar{B}_{FN} \quad (1)$$

where the resultant of the compensator and superconducting field winding fields is expressed as an effective field flux density:

$$\bar{B}_{FN} = \bar{B}_F + \bar{B}_C \quad (2)$$

\bar{B}_A , \bar{B}_C , and \bar{B}_F are the field vectors of the armature, compensator and field respectively.

A requirement for zero torque on the superconducting field winding is that the vectors \bar{B}_N and \bar{B}_F be colinear as reflected in Figures 7 and 8.

The following constraints placed on machine design parameters are specified as:

1. Maximum field current limited to $1.25 \times 10^8 \text{ A/m}^2$
2. Maximum armature current limited to $2.5 \times 10^6 \text{ A/m}^2$
3. Maximum compensator current limited to $2.5 \times 10^6 \text{ A/m}^2$

- LOCUS OF ALL POSSIBLE VALUES OF \bar{B}_{FN} .
- LOCUS OF ALL POSSIBLE VALUES OF \bar{B}_A .
- LOCUS OF ALL POSSIBLE MACHINE OPERATING POINTS.

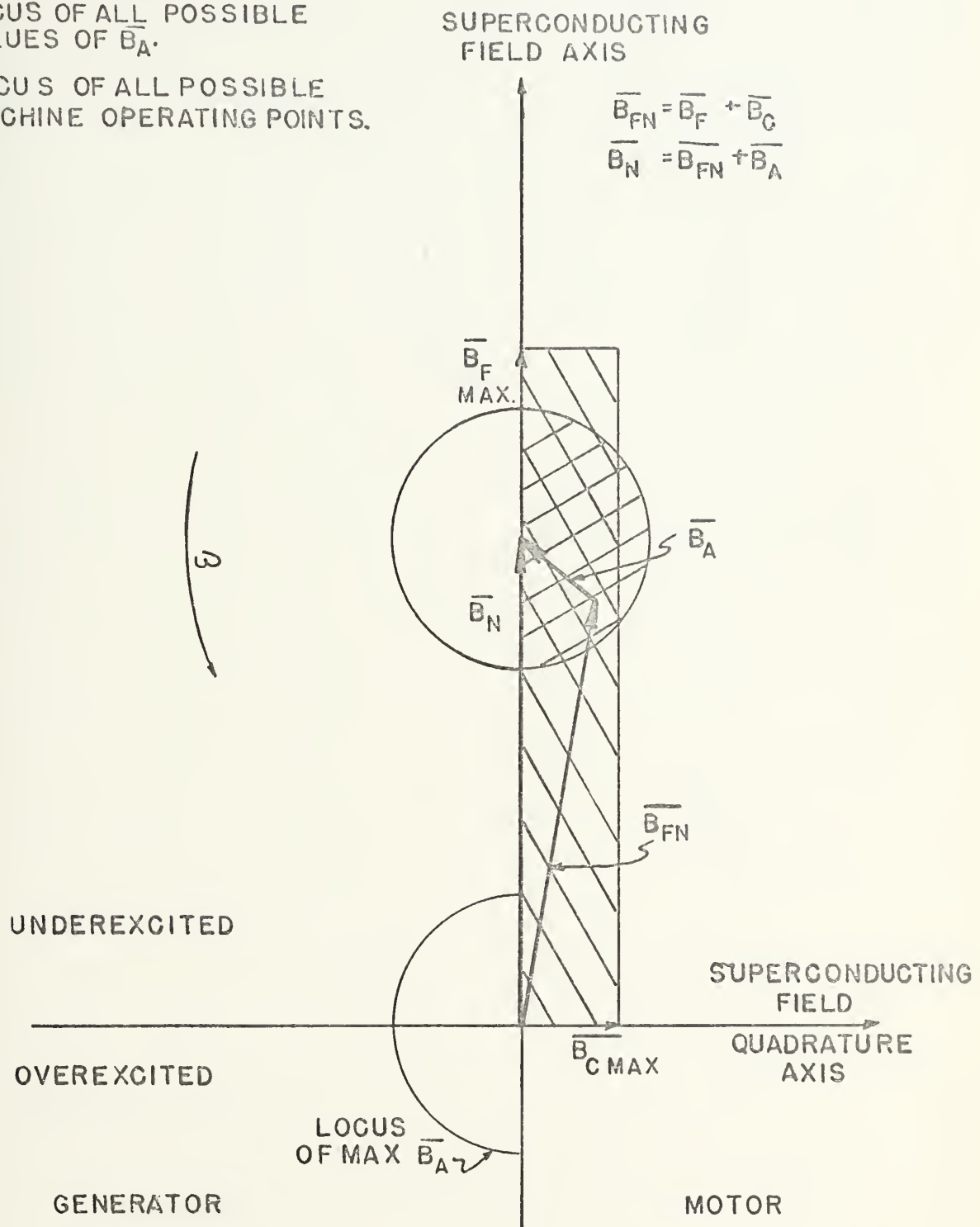


FIGURE 7. FIELD DENSITY CAPABILITY PLOT, $\alpha = 90^\circ$;
UNDEREXCITED MODE.

- LOCUS OF ALL POSSIBLE VALUES OF \bar{B}_{FN} .
- LOCUS OF ALL POSSIBLE VALUES OF \bar{B}_A .
- LOCUS OF ALL POSSIBLE MACHINE OPERATING POINTS.

SUPERCONDUCTING FIELD AXIS

$$\bar{B}_{FN} = \bar{B}_F + \bar{B}_C$$

$$\bar{B}_N = \bar{B}_{FN} + \bar{B}_A$$

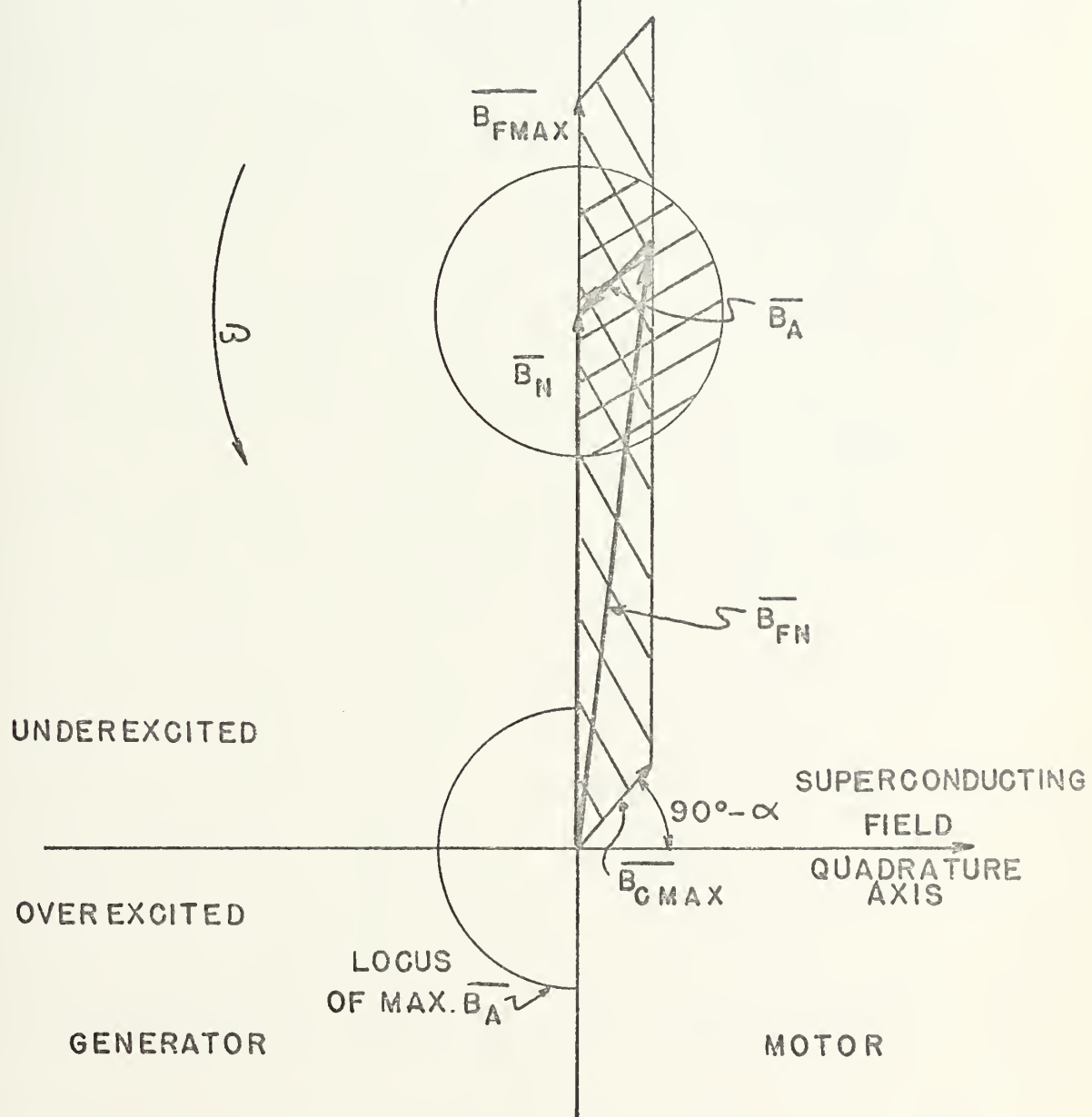


FIGURE 8. FIELD DENSITY CAPABILITY PLOT, $\alpha < 90^\circ$; OVEREXCITED MODE.

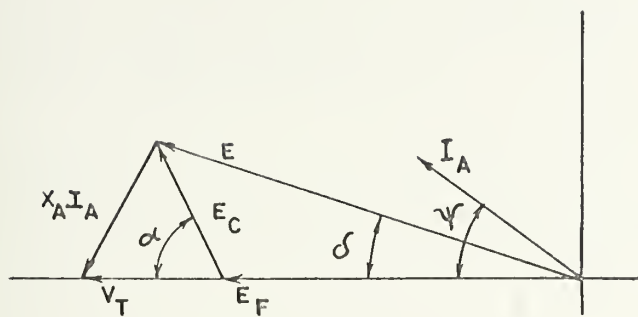
4. Machine magnetic shear stress is to be consistent with current design practices

Reference 6 presents a detailed discussion of constraints 1 through 3 above; and reference 7, Figure 11, shows magnetic shear stresses found in recent designs.

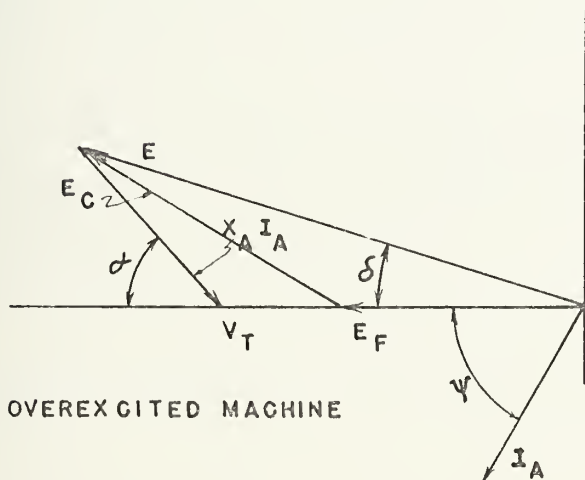
Referring to Figures 1, 7, and 8, the angle α represents the angle between the axis of the superconducting field and the compensator field. Figures 7 and 8 show all possible operating loci for the machine field vectors constrained as above and operating as a motor. If angle α is decreased from 90° electrically to some other fixed position, the domain of operation decreases also. A comparison of Figures 7 and 8 shows this clearly. If α is permitted to vary rather than fixing the relative position of the two fields, an additional degree of freedom is introduced into the analysis. Figures 9 and E1 represent the resulting voltage-current relationships for the compensated machine. As a result of the colinearity requirement imposed on the fields \bar{B}_N and \bar{B}_F , E_F and V_T must also be colinear as shown in Figures 9 and E1. This results in a somewhat simplified analysis as presented in Appendix E. The analysis in Appendix E treats α as a constant $\leq 90^\circ$ electrically.

Referring to Figures 9 or E1, the internal excitation voltage arising from the field vector \bar{B}_F is expressed as:

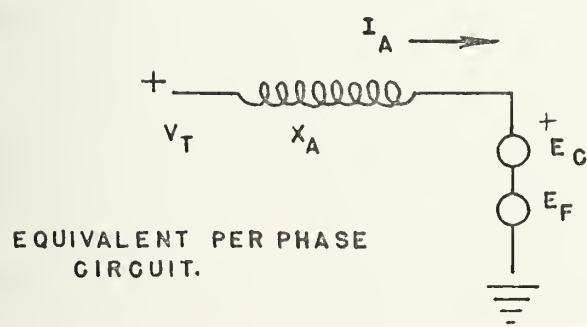
$$E_F = V_T + X_A I_A (\sin \psi - \cos \psi \cot \alpha) \quad (E1)$$



UNDEREXCITED MACHINE



OVEREXCITED MACHINE



EQUIVALENT PER PHASE CIRCUIT.

FIGURE 9. VOLTAGE-CURRENT RELATIONSHIPS FOR OVEREXCITED AND UNDEREXCITED COMPENSATED MOTORS.

Utilizing this relationship and the appropriate expressions for machine inductances, machine power in volt-amps is found to be (see Appendix E):

$$P = \frac{24}{\sqrt{2}\pi} \omega_e \mu_o J_a J_f \ell_m (1 - y^{2+p}) R_{fo}^4 C_{lpf} \sin\left(\frac{p\theta_{wa}}{2}\right) \sin\left(\frac{p\theta_{wf}}{2}\right) \left(\frac{V_T}{E_F}\right) \quad (E8)$$

when

$$\frac{V_T}{E_F} = 1 - x_a (\sin \psi - \cos \psi \cot \alpha) \quad (E14)$$

and, x_a , the internally normalized synchronous reactance is given by equation E16. Equation C38, the armature torque expression, may be written as

$$T_a = \Delta_1 [\Delta_2 \sin k \phi + \Delta_3 J_c \sin k(\phi - \alpha)] \quad (E20)$$

where Δ_1 , Δ_2 , and Δ_3 are defined in equations E17 through E19; and are functions of J_a , J_f , and machine geometry.

The armature torque, T_a , may also be expressed by equation E21 and the resolution of equations E20 and E21 results in a quadratic expression for the angle between the axis of phase a and the superconducting field (angle ϕ):

$$Q_A \sin^2(k\phi) + Q_B \sin(k\phi) + Q_C = 0 \quad (E22)$$

where Q_A , Q_B , and Q_C are defined in equations E23 through E25; and are functions of J_a , J_f , J_c , and machine geometry.

Utilizing the constraint expression for zero torque on the superconducting field winding given by equations C38, C33 or E26:

$$\cos(k\phi) = J_C \bar{A} \cos(k\alpha) \quad (E26)$$

A fourth order equation for the compensator current density is found in Appendix E to be

$$A_5 J_C^4 + A_4 J_C^3 + A_3 J_C^2 + A_2 J_C + A_1 = 0 \quad (E27)$$

where A_1 through A_5 are defined in equations E29 through E33. The coefficients are also given in equation E34 for the specialized machine with four poles ($p=2$).

Using the above expressions in light of the aforementioned constraints, a FORTRAN program, THESIS I, was developed as a design tool to facilitate the selection of a feasible machine. "Feasible" is defined here to indicate a machine that meets the size, shear stress, and current density constraints discussed earlier. Other machine operating characteristics such as per-unit synchronous reactance, terminal or phase voltage, line current, and power factor are also considered. Appendix F presents more detailed information for use of the program. The program allows an incremental adjustment of the angle α and determines the required compensator current density to maintain zero torque or the superconducting field.

As indicated in Appendix E it is also possible to approach the problem by incrementing J_c and determining the angle α required for zero torque (see equation E47).

Because the solution of equation E27 yields four roots, some complex, some real, the valid real root may be found by substituting back into equation E22 and then E26.

Figures 7 and 8 indicate that angle α set at 90° electrically allows the greatest possible range of machine operation. Of course, by setting α to any value requires an adjustment in the compensator current density in order to maintain a net zero torque on the superconducting field. This particular mode of operation permits the designer to use fixed, rigid interfaces between the compensator and superconducting field winding and the supporting environment.

An attractive alternative to this technique is to permit the angle α to seek its own natural value as power level changes and J_c is held constant. This requires a flexible interface for cryogenics and electrical power cables but eliminates the need for an external control loop. A third possible, but less attractive method, is to fix the compensator current J_c , and mechanically position the field or compensator through a feedback control loop.

Equation E40

$$P = K_3 J_a - K_4 J_a^2 (\sin \psi - \cos \psi \cot \alpha) \quad (E40)$$

K_3 and K_4 defined by equations E36, E38, and E41, indicates

the utility that angle α may offer in adjusting the machine power level. It is noted that if α is used to adjust power level, J_c must be varied to maintain the zero torque condition.

It is also possible to express the field current density, J_f , as:

$$J_f = K_5 + K_4 J_a (\sin \psi - \cos \psi \cot \alpha) \quad (E42)$$

where K_5 is defined by equation E43. If λ is defined as

$$\lambda \equiv \sin \psi - \cos \psi \cot \alpha, \quad (3)$$

E42 may be written as:

$$J_a = \left(\frac{1}{K_4 \lambda}\right) J_f - \left(\frac{K_5}{K_4 \lambda}\right) \quad (E44)$$

Figure 10 depicts λ as a function of the power factor angle ψ for various values of α . If the machine is overexcited (quadrants I and IV of Figure 10), λ may have either positive or negative values, depending upon the value of angle α . If the machine is underexcited (quadrants II and III of Figure 10), λ may only assume negative values. Figure 11 depicts plots of equation E44 for a fixed power factor angle with the machine underexcited. An examination of Figures 10 and 11 shows that the slope of equation E44 may have either positive or negative values depending on the angle α for the overexcited machine. Conversely, Figures 10 and 12 indicate

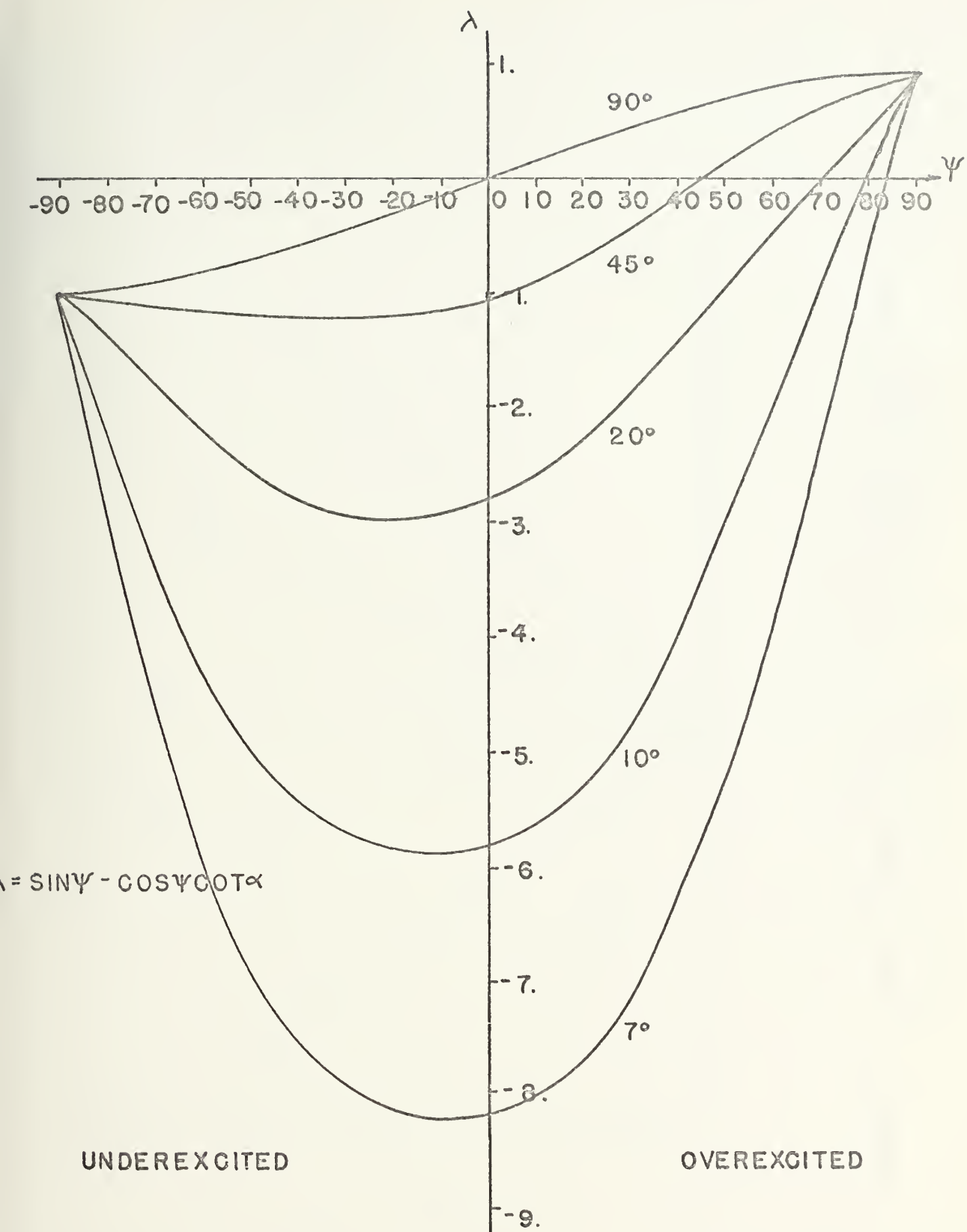


FIGURE 10. λ AS A FUNCTION OF POWER FACTOR ANGLE, ψ .

$\psi = \psi_i$

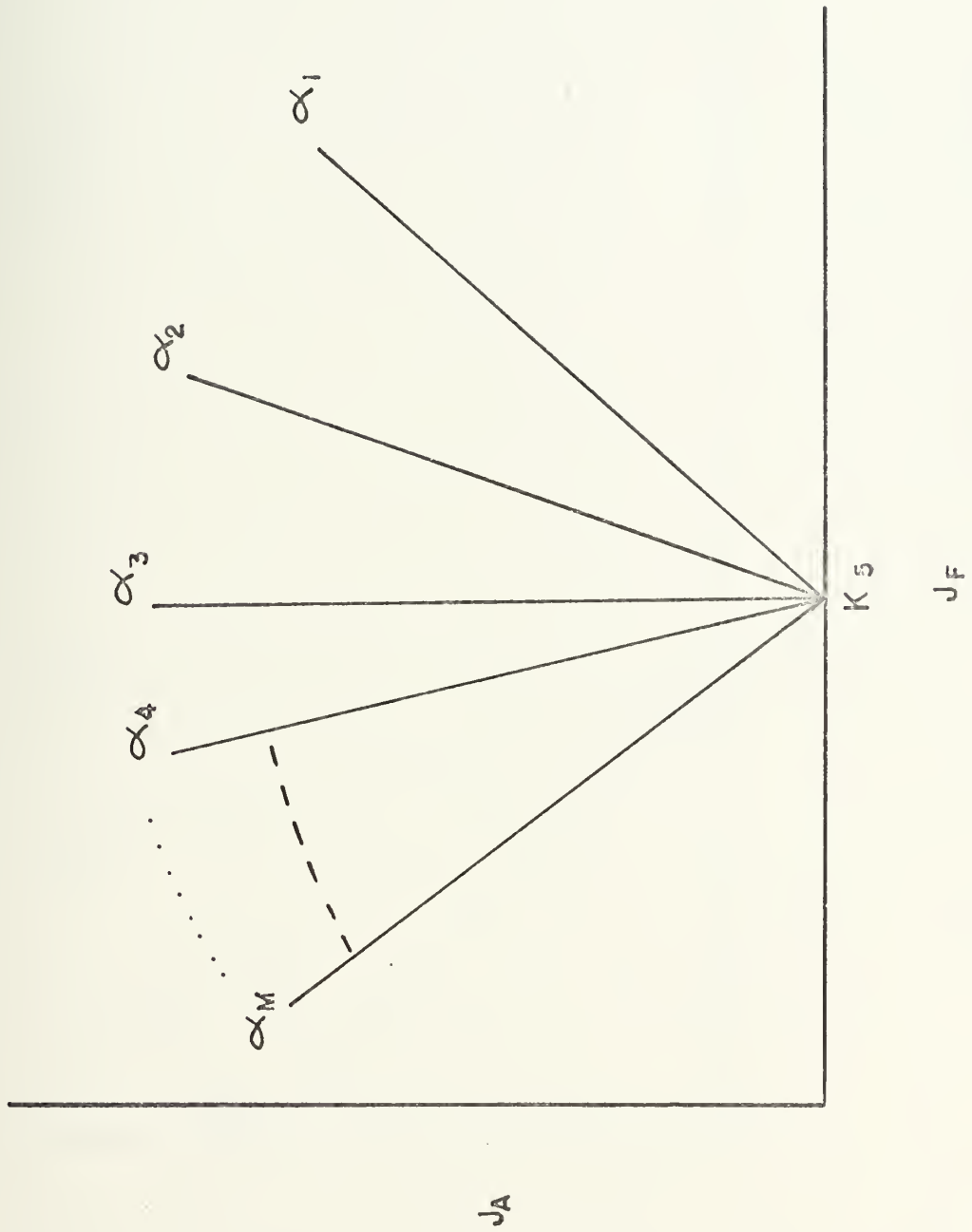
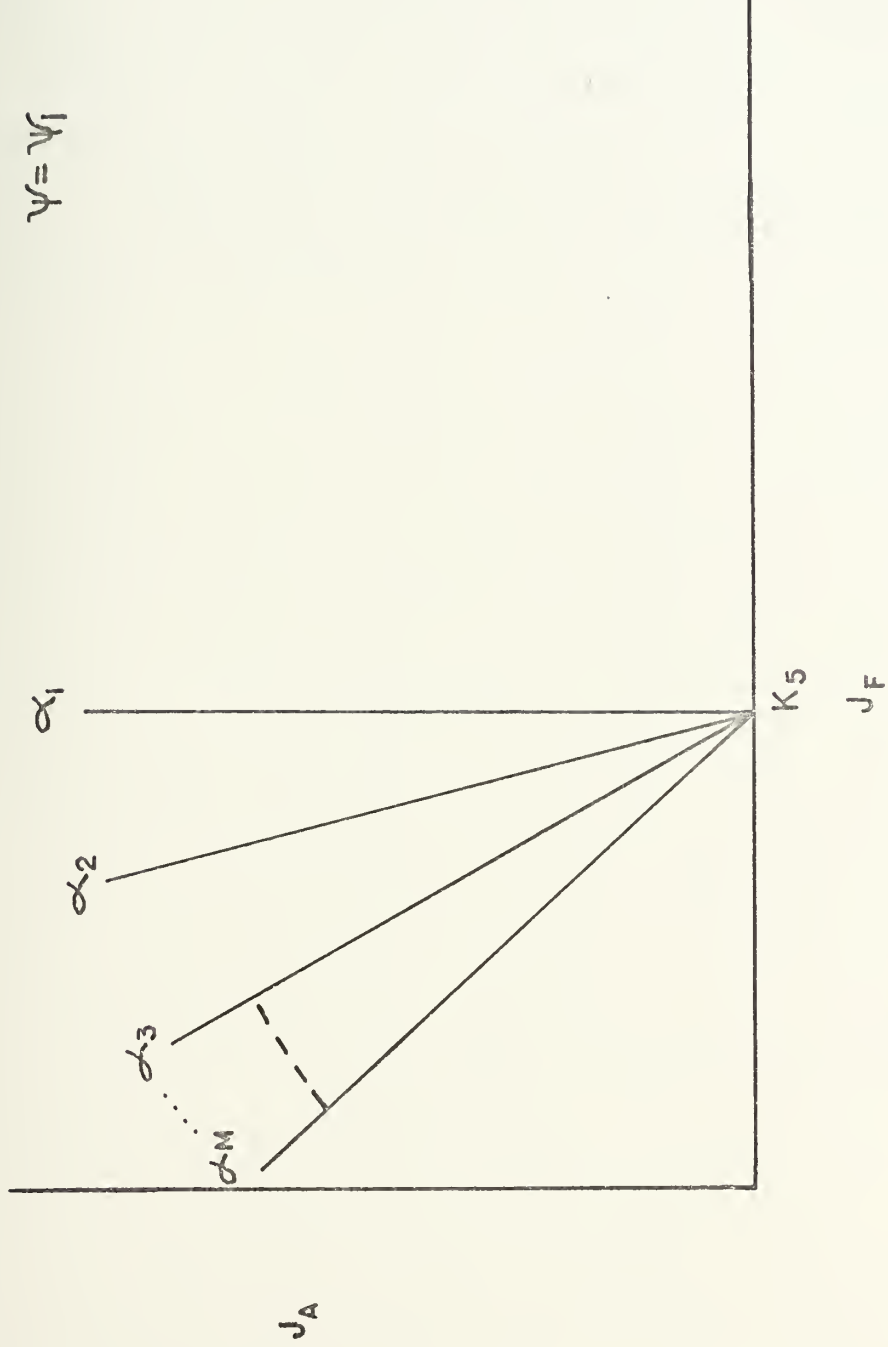


FIGURE II. J_A AS A FUNCTION OF J_F FOR A FIXED POWER FACTOR;
OVEREXCITED MODE.

FIGURE 12. J_A AS A FUNCTION OF J_F FOR A FIXED POWER FACTOR:
UNDEREXCITED MODE.



only positive slopes for equation E44 if the machine is under-excited. A classical "V-curve" for the synchronous motor can only be obtained if $\alpha = 90^\circ$. From Figure 10 this yields the same magnitude of λ regardless of the machine excitation, and a "V-curve" is obtained for each value of $\pm\psi$.

Otherwise, if $\alpha \neq 90^\circ$, from Figure 10, it is evident that the magnitude of λ is not the same for both $a + \psi$ and $a - \psi$. Therefore the "V-curve" will not be symmetric about a vertical line through $J_f = K_5$.

IV. RESULTS

Utilizing the program listed in Appendix E (THESIS I) a feasible machine, whose physical and operating parameters are listed in Table 3, was developed. This machine employs a compensator physically positioned concentric with and outside of the main superconducting field winding.

Figure 13 is a plot of some of the designs investigated during the course of the development of this thesis. All machines in Figure 13 have the compensator winding physically located between the armature and the main field windings. Adjacent to each data point is printed the per unit synchronous reactance at the power level indicated. Each machine plotted in both Figures 12 and 13 are designed at the upper limit of armature current density ($J_a = 2.5 \times 10^6 \text{ A/m}^2$). All machines plotted in Figure 13 were designed at the upper limit of field current ($1.25 \times 10^8 \text{ A/m}^2$). All machines were assumed to operate from a 60hz bus and configured for two pole-pairs.

Figure 15 is a plot of magnetic shear stress as a function of power for a number of machines with the compensator outside of the main field winding.

Tables 1 and 2 are provided to augment the data plotted in Figures 12, 13, and 14.

The machine presented herein is rated at 22,700 horsepower before losses, and is intended to operate as part of the main propulsion system for the aforementioned hydrofoil. This choice is purely arbitrary, and the SES or SWATH

PER-UNIT SYNCHRONOUS
REACTANCE PRINTED ABOVE
EACH DATA POINT.

.088

.033

.083

-.031

.005

D

.077

.027

A .072 .047

.048

E

.028

D

.028

E

.062

F

.096

G

.115

H

.062

I

.067

J

.076

K

.067

L

.082

M

.066

N

.069

O

.075

P

.059

Q

.078

R

.092

S

.074

T

.066

U

.066

V

.066

W

.066

X

.066

Y

.066

Z

.066

AA

.066

AB

.066

AC

.066

AD

.066

AE

.066

AF

.066

AG

.066

AH

.066

AI

.066

AJ

.066

AK

.066

AL

.066

AM

.066

AN

.066

AO

.066

AP

.066

AQ

.066

AR

.066

AS

.066

AT

.066

AU

.066

AV

.066

AW

.066

AX

.066

AY

.066

AZ

.066

AA

.066

AB

.066

AC

.066

AD

.066

AE

.066

AF

.066

AG

.066

AH

.066

AI

.066

AJ

.066

AK

.066

AL

.066

AM

.066

AN

.066

AO

.066

AP

.066

AQ

.066

AR

.066

AS

.066

AT

.066

AU

.066

AV

.066

AW

.066

AX

.066

AY

.066

AZ

.066

AA

.066

AB

.066

AC

.066

AD

.066

AE

.066

AF

.066

AG

.066

AH

.066

AI

.066

AJ

.066

AK

.066

AL

.066

AM

.066

AN

.066

AO

.066

AP

.066

AQ

.066

AR

.066

AS

.066

AT

.066

AU

.066

AV

.066

AW

.066

AX

.066

AY

.066

AZ

.066

AA

.066

AB

.066

AC

.066

AD

.066

AE

.066

AF

.066

AG

.066

AH

.066

AI

.066

AJ

.066

AK

.066

AL

.066

AM

.066

AN

.066

AO

.066

AP

.066

AQ

.066

AR

.066

AS

.066

AT

.066

AU

.066

AV

.066

AW

.066

AX

.066

AY

.066

AZ

.066

AA

.066

AB

.066

AC

.066

AD

.066

AE

.066

AF

.066

AG

.066

AH

.066

AI

.066

AJ

.066

AK

.066

AL

.066

AM

.066

AN

.066

AO

.066

AP

.066

AQ

.066

AR

.066

AS

.066

AT

.066

AU

.066

AV

.066

AW

.066

AX

.066

AY

.066

Machine Code (see Fig. 12)	R_{ai} (in)	R_{ao} (in)	R_{ci} (in)	R_{co} (in)	R_{fi} (in)	R_{fo} (in)	R_{si} (in)	R_{so} (in)	PF	$J_E^{10^{-8}}$ (a/m ²)	σ_m (psi)	x_d^2	Rated Power (hp) $\times 10^3$
A	7.	9.	9.5	10.5	11.	11.75	12.25	16.25	.8	1.25	30	58	.027 20.
B	7.	11.	11.5	12.75	12.75	13.25	13.75	17.75	.55	.8	25	42	.094 13.
C	7.	9.5	10.	10.5	11.	11.75	12.25	16.25	.8	1.25	10	50	.061 7.6
D	7.	9.	9.5	10.25	10.75	11.5	12.	16.	.8	1.25	35	42.5	.028 21.
E	6.	9.5	10.	11.	11.5	12.	12.5	16.5	.6	1.25	30	51	.048 19.5
F	6.	9.5	10.	11.	11.5	12.25	12.75	16.75	.55	1.25	30	75	.031 27.
G	6.	9.5	10.	11.	11.5	11.75	12.25	16.25	.8	.4	30	7.5	.255 4.5
H	6.	9.5	10.	11.	11.5	12.	12.5	16.5	.7	.4	30	13.8	.139 6.1

TABLE 1. Machine Data Extracted For Machines Plotted On Figure 13--Compensator Inside Field

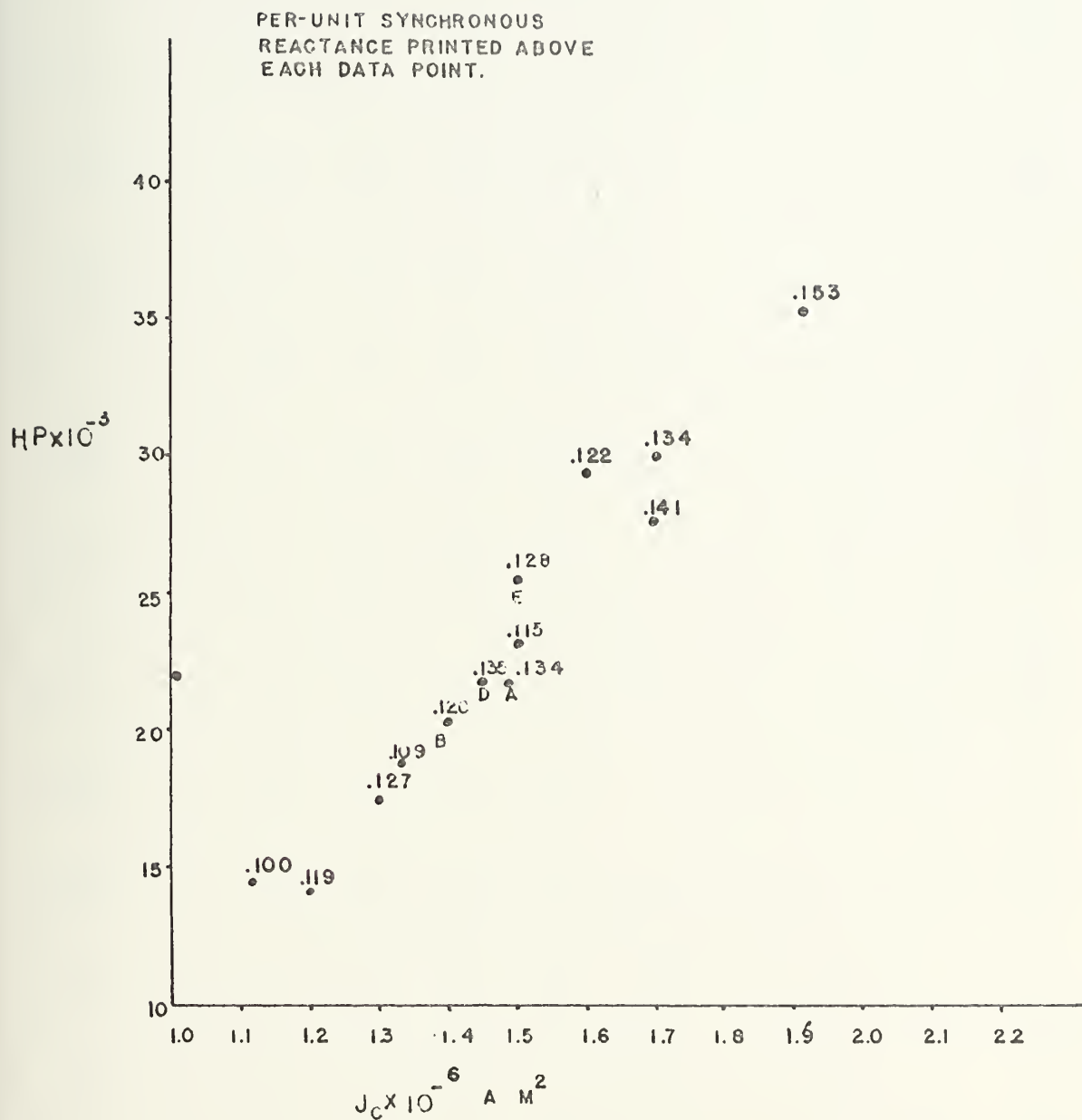


FIGURE 14. J_C AS A FUNCTION OF HORSEPOWER FOR MACHINES
WITH COMPENSATOR OUTSIDE OF FIELD.

Machine Code (see Figs. 13 & 14)	R_{ai} (in)	R_{ao} (in)	R_{fi} (in)	R_{fo} (in)	R_{ci} (in)	R_{co} (in)	R_{si} (in)	R_{so} (in)	P_F (in)	ℓ (in)	σ_m (psi)	x_d (pu)	Rated Power (hp) $\times 10^{-8}$	Rated J_f a/m ² $\times 10^{-8}$
A	7.	11.5	12.	13.	13.5	15.5	16.	20.	.85	30	30	.134	21.5	.4
B	7.	11.	11.5	12.5	13.	15.	15.5	19.5	.85	35	26.7	.12	21.	.4
C	7.	10.	10.5	11.5	12.	14.	14.5	18.5	.85	30	41.	.056	22.	.8
D	7.	11.	11.5	12.5	13.	15.	15.5	19.5	.85	30	30.	.135	22.5	.4
E	7.	11.5	12.	13.	13.5	15.5	16.	20.	.85	35	35.	.128	25.	.4

TABLE 2. Machine Data Extracted For Machines Plotted On Figures 14 and 15. Compensator Outside Field

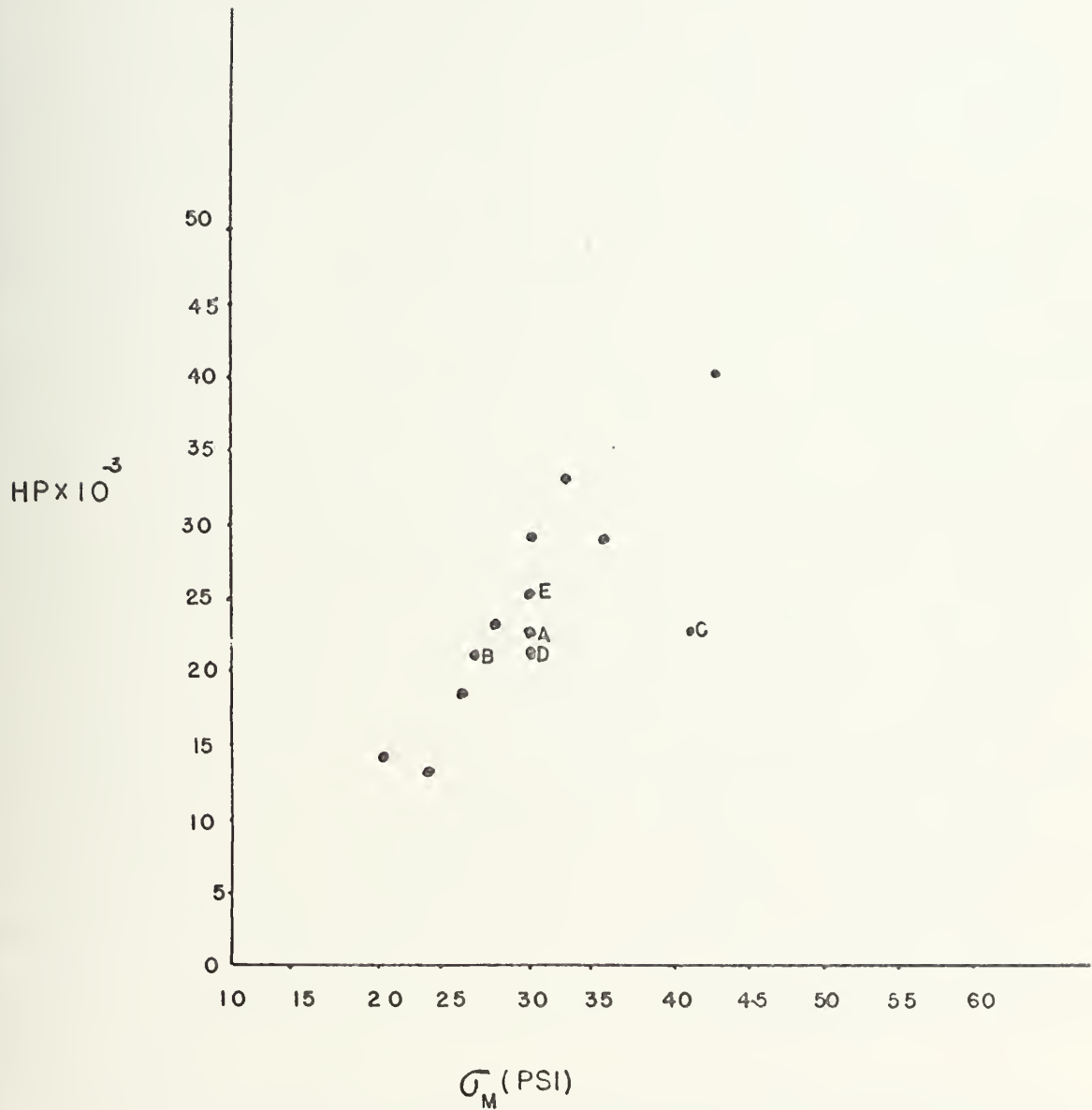


FIGURE 15. \bar{O}_M AS A FUNCTION OF HORSEPOWER FOR MACHINES WITH COMPENSATOR OUTSIDE OF FIELD.

application could have been chosen for illustration with correspondingly higher horsepower ratings.

Figure 16 shows J_c as a function of J_a for a fixed field current and a fixed value of the phase angle between the main superconducting field and the compensator field. The plots indicate a relatively simple control problem, without the need for mechanical components in the control loop.

As discussed earlier, another option available to control the torque on the main field winding is physical angular adjustment of the main field winding (angle α in Figure 1), with a constant value of the compensator current density, J_c . Figure 17 shows the effects of varying angle α and J_a on machine power output. The small circles on the $\alpha = 10^\circ$ and 20° plots indicate the operating point at which J_c exceeds the constraint of $2.5 \times 10^6 \text{ A/m}^2$. In the other plots, $\alpha \geq 30^\circ$, the constraint on J_c is not exceeded, but as shown, a similar constraint on J_a is reached prior to reaching the J_c constraint. Therefore, for the machine described in Table 3 the limiting value for the current density in the compensator is not exceeded for $\alpha \geq 30^\circ$.

Figure 18 depicts the variation required in angle α for constant values of J_c as J_a or power varies. It is again noted that the power level at any angle α and any armature current density, J_a , is also a function of the compensator current density, J_c . In the limiting case of $\alpha = 0^\circ$ electrically, the compensator would act as only as a power augmenting field element and in order to maintain zero torque on the

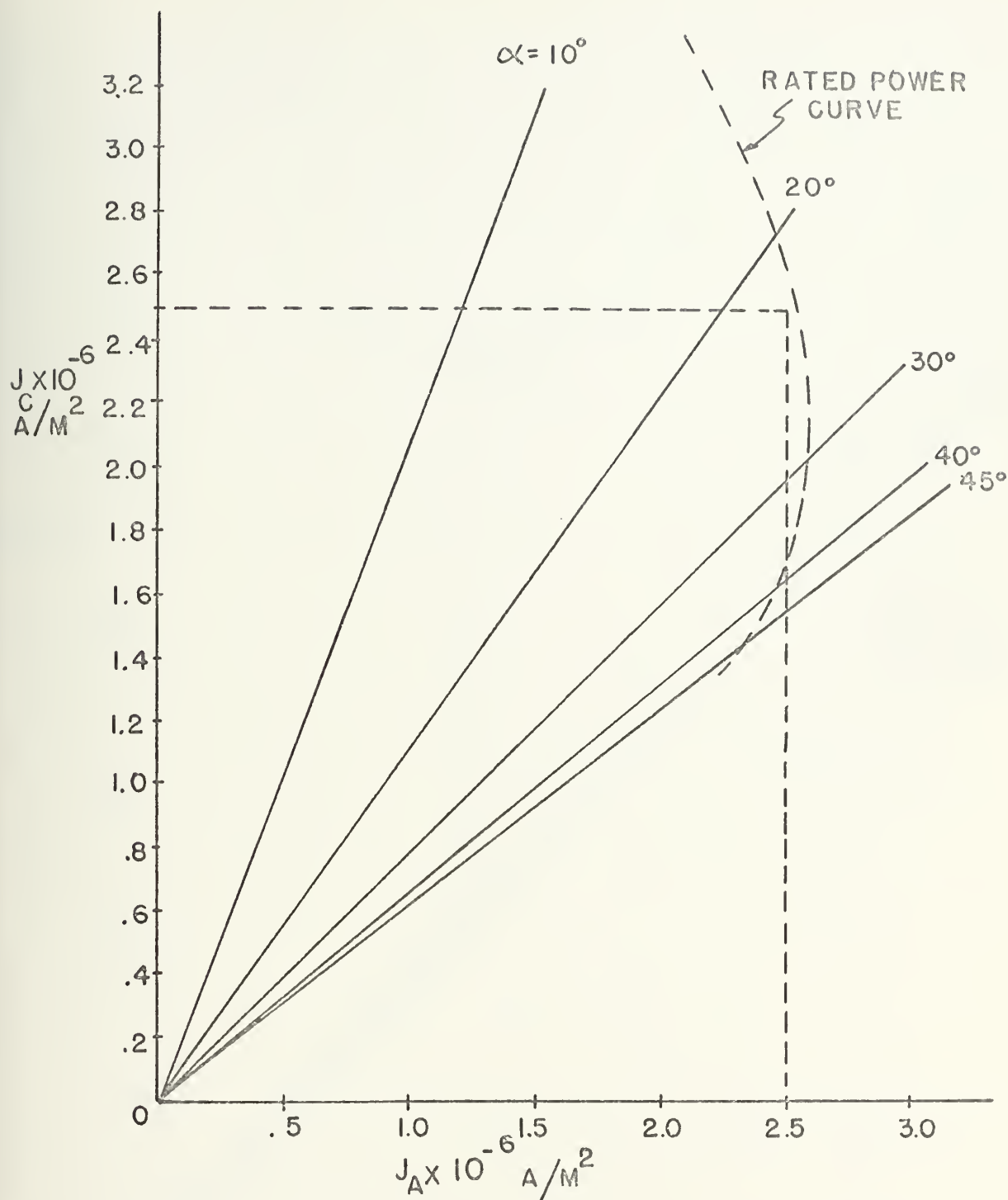


FIGURE 16. J_C AS A FUNCTION OF J_A FOR SELECTED MOTOR DESCRIBED IN TABLE 3.

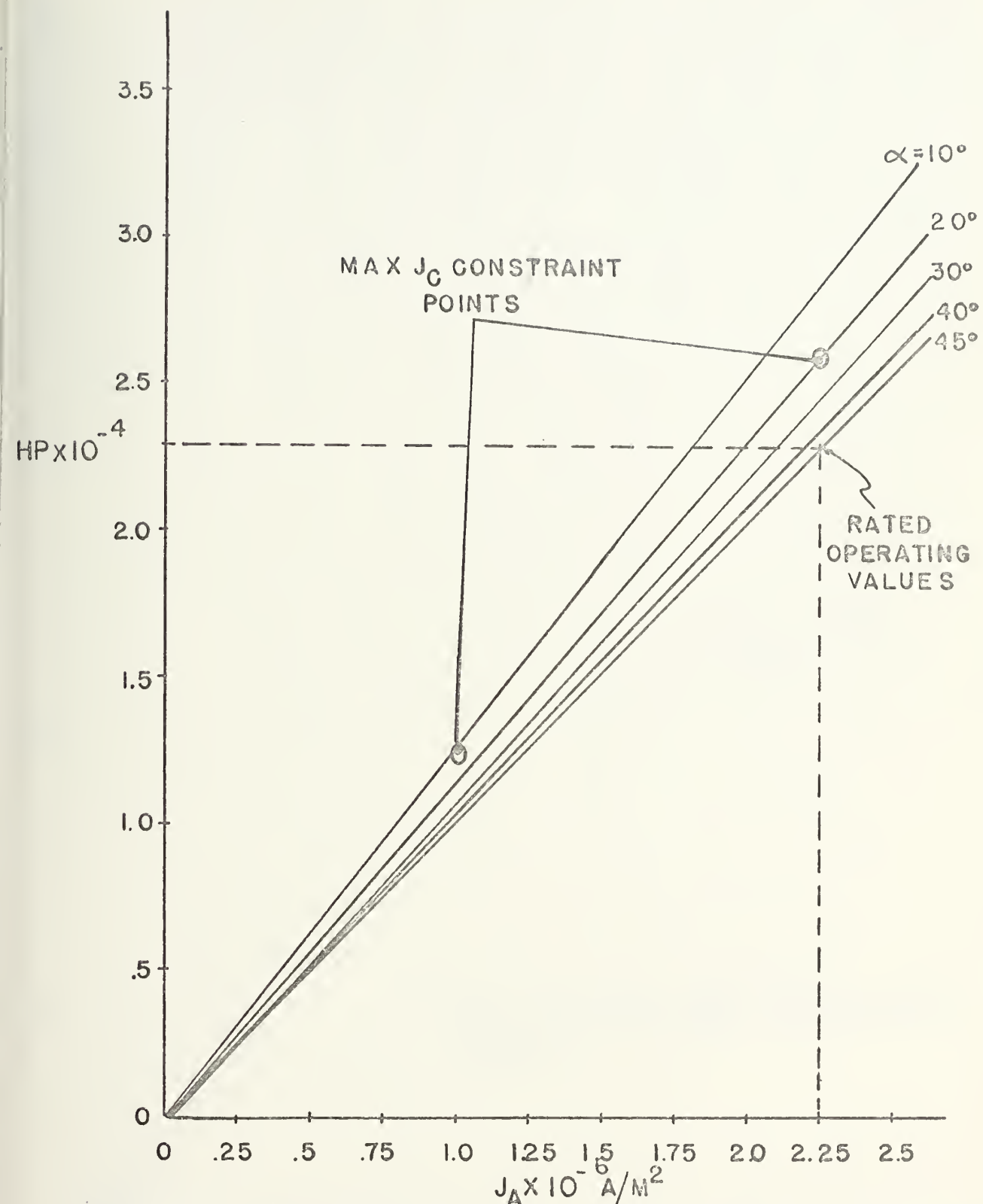
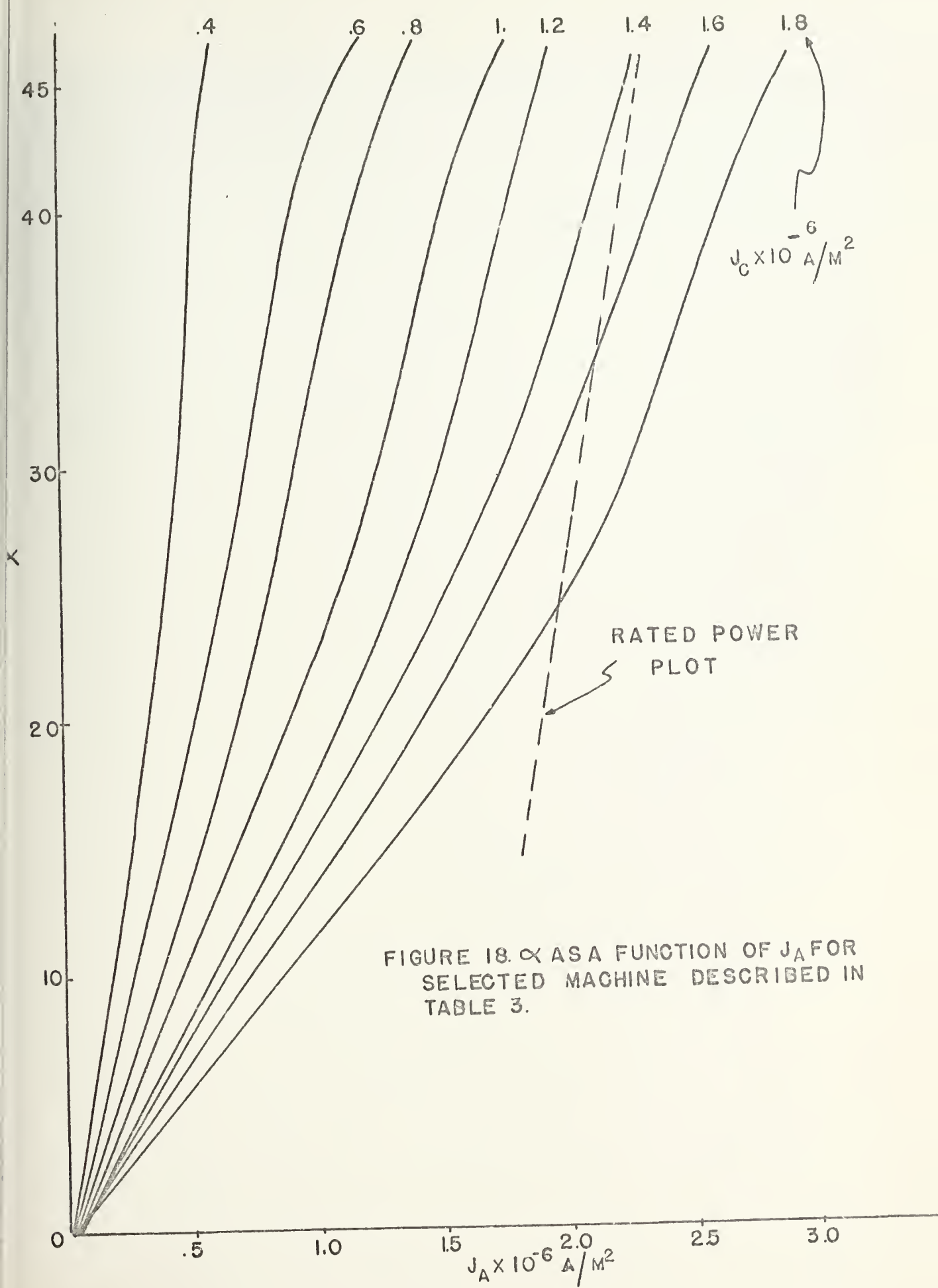


FIGURE 17. HORSEPOWER AS A FUNCTION OF J_A FOR SELECTED MACHINE DESCRIBED IN TABLE 3.



superconducting field, an infinite amount of current would be required in the compensator.

V. DISCUSSION OF RESULTS AND CONCLUSIONS

As indicated in Figures 13 and 14, a significant number of machine designs were investigated using the analysis developed and constraints specified herein. THESIS I, as listed in Appendix F, was employed extensively as a design tool.

No machine with the compensator located between the superconducting field and armature was found to be satisfactory either because of a firm constraint violation (high current densities or low shear stresses) a because of unacceptably low values of per-unit synchronous reactance. It is recognized that low values of per-unit synchronous reactance present problems primarily during machine transients and because of the extraordinary sequence of events that must occur to induce a major casualty to the motor, low values may not be meaningful either to the designer or operator. Figure 13, augmented by Table 1, does indicate some machines (such as machine A, D, E, or F) which are theoretically plausible but have either low per-unit synchronous reactances or poor power factors at designed power levels, or both. The inability to obtain satisfactory machines at high power levels ($\geq 20,000$ hp) is attributed to the pronounced decrease in field strength in the radial direction. Consequently, with the compensator located between the superconducting field and the armature, lower power must be expected than that produced from a machine with the compensator located outside of the

field winding, for the same superconductor, compensator, and armature winding areas.

In summary, the machine with the compensator located inside of the superconducting field presents many design problems because each machine investigated at rated power either exceeds or approaches the design constraints.

On the other hand, a motor with the compensator located between the superconducting field winding and the shield is less demanding in terms of the design constraints. Figure 14 depicts rated horsepower as a function of compensator current density for a number of designs investigated. The machine parameters used as constraints are not approached, and as indicated in Figures 14 and 15 and Table 2 acceptable values of per-unit synchronous reactance and power factor are easily realized. If Figures 15 and D1 are compared, the values of σ_m for those machines investigated are acceptable.

Table 3 presents data for a feasible machine to be employed as a main propulsor for a hydrofoil. The compensator, superconducting field, and armature current densities are all well within the constraints outlined in Section III of this paper. An optimum machine was not investigated, and possibly a machine of smaller dimensions could be synthesized.

Of the three options discussed earlier to control the torque on the superconductors, fixing the angle α at 90° electrically is, from the author's point of view, the better choice because such a mode of operation allows the widest possible locus of operation as depicted in Figure 7.

TABLE 3. DATA FOR A FEASIBLE TORQUE--COMPENSATED MACHINE

<u>Parameter</u>	<u>Value</u>
Design Horsepower	22,700 shp
Power Factor	.85
KVA Rating	35.8 KVA
Design RPM	1800
Rated Compensator Current Density, J_c	1.4×10^6
Rated Field Current Density, J_f	$4. \times 10^7$
Rated Armature Current Density, J_a	2.25×10^6
Rated Terminal Phase Voltage	6300 volts PMS
Rated Terminal Line Voltage, V_T	10,000 volts PMS
Phase Angle Between Main and Compensator Fields, α	45°
Armature Winding Angle, θ_{wa}	28°
Field Winding Angle, θ_{wf}	80°
Compensator Winding Angle, θ_{wc}	80°
Armature Space Factor, λ	.27
Armature Winding Inside Radius, R_{ai}	7."
Armature Winding Outside Radius, R_{ao}	11.5"
Field Winding Inside Radius, R_{fi}	12."
Field Winding Outside Radius, R_{fo}	13."
Compensator Winding Inside Radius, R_{ci}	13.5"
Compensator Winding Outside Radius, R_{co}	15.5"
Shield Inside Radius, R_{si}	16."
Shield Outside Radius, R_{so}	18"
Shield Permeability, μ_s	.009 hy/in

TABLE 3 continued

<u>Parameter</u>	<u>Value</u>
Total Machine Length, l_t	72"
Straight Section Length, l	35"
Synchronous Reactance (per unit), x_d	.1156
Armature Conductivity	$\sigma = 6 \times 10^7 \text{ mho/m}$
End Turn Length ($R_{ai} + R_{ao}$)	18."
Effective <u>Lengths</u> For:	
Self Inductance, Armature	53"
Self Inductance, Field	35"
Self Inductance, Compensator	35"
Mutual Inductance, Field-to-Armature	35"
Mutual Inductance, Compensator-to-Armature	35"
Conductor Loss	72"
Eddy-Current Loss	35"
Losses at Rated Conditions:	
Conductions (compensator and shield)	200 hp
Eddy-currents	15 hp
Total, percent of rating	.94%
Ratio of l_t/D (see Table D1)	1.8

Figure 8 indicates that for any other fixed value of α , a more limited locus is to be expected. Figure 16 shows that as angle α is reduced from 45° mechanically for a four pole machine, a higher value of compensator current is required at any particular value of J_A (or any particular power level since V_T is assumed constant). Such an arrangement also eliminates the need for moving interfaces between the superconducting field winding or the compensating winding. This means that rotating fluid cryogenic couplings and slip rings are not necessary; and consequently should both improve machine reliability and simplify the mechanical design.

The primary disadvantages of employing this technique is a slower compensator response to machine load changes and the added complexity of an external feedback loop required to control J_c .

Figure 17, plots of motor horsepower as a function of J_a for the machine described in Table 3, indicates an increase in horsepower due to the improved armature-to-compensator coupling as angle α is varied. As discussed earlier, if angle α is permitted to go to 0° , the compensator field aligns with the superconducting field and acts only as a power element, no longer capable of compensating the superconducting field without infinite currents in the compensating winding. Some compensation, of course, would be realized at $\alpha = 0^\circ$ because the compensator would absorb some torque, but its value would be insignificant compared to that carried by the superconducting field.

A viable alternative, as briefly addressed above, but not as advantageous from the standpoint of hardware reliability and mechanical design is to mount either the superconducting field winding or the compensating winding on bearings (possibly a self-aligning ball or cylindrical bearing) and allow the element to seek the proper value of angle α at some fixed J_c as power level changes. Figure 18 predicts the behavior of the element for various values of J_c as the power level varies. The machine depicted is that described in Table 3, and the terminal voltage is assumed constant. The advantages of such a mode of operation are rapid response of the compensator to changes in load, and the elimination of the external feedback control system necessitated in the system mentioned above.

Since either the superconducting field winding or the compensating winding can be gimbled, the designer has an additional choice of configurations; both of which require moving interfaces with the environment. If the superconducting field is fixed, the rotating cryogenic coupling is not required and only power slip rings are necessary to provide power to the compensator which, of course, would be gimbled. Otherwise, if the compensator is fixed, the main superconducting field requires both cryogenic and electrical interfaces. Because of the initial conclusion presented herein, which placed the compensator outside of the superconducting field, a fixed compensator and a gimbled main field would further complicate the machine's mechanical design.

As may be seen above strong cases for either mode of operation can be made; but because this machine is envisioned to be employed in naval or possibly marine vehicles, the author feels that machine reliability should play an important role in the design decision. Therefore, a fixed compensator and superconducting field with a variable compensator current is recommended.

VI. RECOMMENDATIONS

Additional areas that could be investigated using the material developed in this thesis are:

1. Develop field equations in terms of α_o and α_i and apply results to develop steady state and transient machine performance.
2. Construct, as an initial prototype, a small non-cryogenic machine and examine machine behavior.
3. On a systems level, develop alternative power trains based on system volume, weight, arrangements, efficiency, and complexity for various naval applications.
4. Synthesize a control system model for the motor operating at a constant value of α , varying J_c with power level.
5. Develop transient and steady-state behavior of machine with variable shield permeability by modeling the shield magnetization characteristics.

APPENDIX A

FIELD ANALYSIS

This Appendix addresses the derivation of the basic field equations for the machine under consideration. The technique employed is that discussed in references 2 and 3 which utilizes axially constant boundary conditions expressed as ratios of radial and azimuthal fields. The use of these ratios, referred to as surface coefficients, simplifies the arithmetic involved and permits a wide range of boundary conditions to be applied to the machine problem after the solutions are formalized.

In the most general form, Ampere's circutial law may be expressed as:

$$\bar{\nabla} \times \bar{H} = \bar{J} + \frac{\partial \bar{D}}{\partial t} \quad (A1)$$

The primary concern here is with the fields within the machine air-gaps which are current-free, where Ampere's Law may be expressed as follows:

$$\bar{\nabla} \times \bar{H} = \frac{\partial \bar{D}}{\partial t} \quad (A2)$$

Assuming that the \bar{E} fields do not vary with time, Ampere's Law becomes:

$$\bar{\nabla} \times \bar{H} = 0 \quad (A3)$$

The electromagnetic fields may be specified by a system of equipotentials which are cut at right angles by lines of magnetic force. This property of orthogonality between the lines of force and the equipotential surfaces leads to some relatively simple geometric conditions. Define:

ψ = magnetic flux function

ϕ = magnetic potential

The family of curves, ϕ = constant and ψ = constant, are orthogonal and this constraint may be expressed in polar coordinates as:

$$\frac{\partial \phi}{\partial r} \cdot \frac{\partial \psi}{\partial r} = - \frac{\partial \phi}{r \partial \theta} \frac{\partial \psi}{r \partial \theta} \quad (A4)$$

From the theory of functions of a complex variable⁽¹⁾, the functions ϕ and ψ are analytically related via the complex variable

$$z = x + jy \quad (A5)$$

Converting A5 into polar coordinates

$$x = r \cos \theta \text{ and } y = r \sin \theta$$

therefore

$$\Phi + j\psi = f[r(\cos\theta + j\sin\theta)] \quad (A6)$$

Differentiating A6 partially with respect to r and θ successively, a comparison of the results indicates

$$\frac{\partial \Phi}{\partial r} = \frac{\partial \psi}{r \partial \theta} \quad (A7)$$

$$\frac{\partial \Phi}{r \partial \theta} = -\frac{\partial \psi}{\partial r} \quad (A8)$$

Differentiating A7 with respect to r yields

$$\frac{\partial^2 \Phi}{\partial r^2} = \frac{1}{r} \frac{\partial^2 \psi}{\partial r \partial \theta} - \frac{1}{r^2} \frac{\partial \psi}{\partial \theta} \quad (A9)$$

Differentiation of A8 with respect to θ yields

$$\frac{\partial^2 \Phi}{r \partial \theta^2} = -\frac{\partial^2 \psi}{\partial r \partial \theta} \quad (A10)$$

The elimination of derivations of ψ using A9 and A10 shows

$$\frac{\partial^2 \Phi}{\partial r^2} + \frac{\partial \Phi}{r \partial r} + \frac{\partial^2 \Phi}{r^2 \partial \theta^2} = 0 \quad (A11)$$

All is recognized as Laplace's equation in two dimensions
 (r, θ)

$$\bar{\nabla}^2 \Phi = 0 \quad (A12)$$

From the principles of vector calculus it is known that in a conservative magnetic field region in space where $\nabla \times \bar{H} = 0$, there exists a scalar potential such that

$$\bar{H} = -\nabla\Phi \quad (A13)$$

A13 in cylindrical coordinates may be written as

$$H_r = -\frac{\partial\Phi}{\partial r}; \quad H_\theta = -\frac{\partial\Phi}{r\partial\theta} \quad (A14)$$

Notice that the machine is modeled in two dimensions only and therefore $H_z \equiv 0$. Equations A11 or A12 may now be solved with the appropriate boundary conditions and using A14, the components of \bar{H} may be found in cylindrical components.

Using separation of variables (see reference 1, pages 434-435) equation A11 may be solved by first assuming a solution of the form

$$\Phi(r, \theta) = R(r) \Theta(\theta) \quad (A15)$$

Differentiating A15 appropriately,

$$\frac{\partial\Phi}{\partial r} = \Theta R'; \quad \frac{\partial^2\Phi}{\partial r^2} = \Theta R'' \quad (A16)$$

$$\frac{\partial\Phi}{\partial\theta} = R\Theta; \quad \frac{\partial^2\Phi}{\partial\theta^2} = R\Theta''$$

Substituting A16 into A11

$$R'' \theta + \frac{1}{r} R' \theta + \frac{1}{r^2} R \theta'' = 0 \quad (A16a)$$

And, upon separating variables

$$\frac{1}{R} (r^2 R'' + r R') = - \frac{\theta''}{\theta} = k^2 \quad (A17)$$

Where k^2 \equiv separation constant

Because the left hand member of A17 is by hypothesis independent of θ and the right hand member is independent of r , it follows that both sides must be independent of both r and θ and equal to a separation constant, k^2 . With some insight as to the form of solution expected, designate k^2 as the constant. Equation A17 implies the following set of second order ordinary differential equations.

$$r^2 R'' + r R' - k^2 R = 0 \quad (A18)$$

$$\theta'' + k^2 \theta = 0 \quad (A19)$$

The sign of k^2 is chosen at the stage of the analysis so that periodic functions which are continuous will appear in the solution of A18 rather than exponentials (sinh) in the θ direction. Equation A18 is an equidimensional linear second order equation and may be solved as follows:

$$\text{assume } R = r^\lambda, \quad k > 0 \quad (\text{A20})$$

Differentiating and substituting A20 into A18

$$\lambda(\lambda-1)r^\lambda + \lambda r^\lambda - k^2 r^\lambda = 0$$

$$\lambda = \pm k \quad (\text{A21})$$

and,

$$R = a_k r^k + b_k r^{-k} \quad (\text{A22})$$

$$\text{assume } R = r^\lambda, \quad k = 0 \quad (\text{A23})$$

Differentiating A23 and substituting into A18

$$r^2 R'' + r R' = 0$$

$$\frac{R''}{R'} = -\frac{1}{r}$$

$$\ln R' = -(\ln r)'$$

$$\ln R' = -\ln r + \ln b_o$$

$$R' = \frac{b_o}{r}$$

$$R = a_o + b_o \ln r, \quad k = 0 \quad (\text{A24})$$

Equation A19 is an ordinary second order linear equation with constant coefficients, and yields the general solution:

$$\theta = c_k \cos k\theta + d_k \sin k\theta, \quad k > 0 \quad (A25)$$

$$\theta = c_o + d_o \theta, \quad k = 0 \quad (A26)$$

Substituting A23 through A26 into A15 the general solution of A11 is found to be

$$\begin{aligned} \Phi(r, \theta) = & A_o + B_o \ln r + (C_o + D_o \ln r) \theta + \\ & \sum_k [(A_k r^k + B_k r^{-k}) \cos k\theta + (C_k r^k + D_k r^{-k}) \sin k\theta] \end{aligned} \quad (A27)$$

The following constant equalities are applicable to A27:

$$A_o = a_o c_o \quad A_k = a_k c_k$$

$$B_o = b_o c_o \quad B_k = b_k c_k$$

$$C_o = a_o d_o \quad C_k = a_k d_k$$

$$D_o = b_o d_o \quad D_k = b_k d_k$$

In order that $\Phi(r, \theta)$ be single valued set $a_o = c_o = d_o = 0$.

For the same reason, the periodic part of A27 must possess

a period of 2π . This requirement leads to the permissible values of the separation constant k .

$$k = np; n = 1, 2, 3, \dots; p = 1, 2, 3, \dots$$

It will be later shown in this analysis that n may assume only odd positive non-zero integer values. p is also later defined as pole pairs in our analysis. If it is required that $\Phi(r, \theta)$ to be defined at $r = 0$, b_0 must be 0, and A27 becomes

$$\Phi(r, \theta) = \sum_k [(A_k r^k + B_k r^{-k}) \cos k\theta + (C_k r^k + D_k r^{-k}) \sin k\theta] \quad (A29)$$

The solution of A29, subject to appropriate boundary conditions, must meet the following additional requirements:

1. Be finite.
2. Be a solution of A11.
3. Satisfy the circuital or curl condition imposed by electromagnetic considerations.
4. As will be shown later, $\Phi(r, \theta)$ must be an odd periodic function of θ with a period of 2π .

Considering only one particular harmonic solution of A11, A29 may be rewritten as

$$\Phi(r, \theta) = (Ar^k + Br^{-k}) \cos k\theta + (Cr^k + Dr^{-k}) \sin k\theta \quad (A30)$$

realizing A, B, C, and D are functions of k .

Utilizing the technique developed in references 2 and 3, A30 may be written in complex form, and the general expressions for the magnetic fields and inductances (see Appendix B) may be developed. The machine will be characterized in terms of surface coefficients defined as functions of machine boundary conditions. These surface coefficients are then substituted into the general expressions for magnetic fields and inductances to find the specific solution desired. This approach allows the designer more flexibility in the machine analysis than the more classic approach of fixing the boundary conditions and then solving the magnetic field problem.

Writing A30 in complex notation:

$$\Phi = \operatorname{Re} [\underline{A} r^k e^{-jk\theta} + \underline{B} r^{-k} e^{-jk\theta}] \quad (A31)$$

It may be shown that

$$\underline{A} = A + jC$$

$$\underline{B} = B + jD$$

Allowing Φ to vary both in space and time, A31 becomes:

$$\Phi = \operatorname{Re} [(\underline{A} r^k + \underline{B} r^{-k}) e^{j(\omega t - k\theta)}] \quad (A32)$$

It is now possible to examine the definitions of the surface coefficients, s , and the reflection coefficients, α . A more detailed derivation may be found in references 1 and 2.

Using A14 and A32

$$\bar{H} = H_r \bar{i}_r + H_\theta \bar{i}_\theta \quad (A33)$$

when

$$H_r = -\operatorname{Re} [(\underline{A}r^{k-1} - \underline{B}r^{-k-1})_k e^{j(wt-k\theta)}] \quad (A34)$$

$$H_\theta = -\operatorname{Re} [-j(\underline{A}r^{k-1} + \underline{B}r^{-k-1})_k e^{j(wt-k\theta)}] \quad (A35)$$

A parameter referred to earlier as the surface coefficient which is the ratio of the radial to azimuthal component of the field is defined as

$$s \equiv \frac{H_r}{H_\theta} \quad (A36)$$

The complex surface coefficient is defined as

$$\underline{s} \equiv \frac{H_r}{H_\theta} = j \left[\frac{\underline{A}r^{k-1} - \underline{B}r^{-k-1}}{\underline{A}r^{k-1} + \underline{B}r^{-k-1}} \right] \quad (A37)$$

and the complex reflection coefficient is defined as

$$\underline{\alpha} \equiv \frac{1 + j \underline{s}(R)}{1 - j \underline{s}(R)} \quad (A38)$$

and it may be shown that

$$\underline{s}(r) = j \left[\frac{1 - \underline{\alpha} \left(\frac{R}{r} \right)^{2k}}{1 + \underline{\alpha} \left(\frac{R}{r} \right)^{2k}} \right] \quad (A39)$$

A39 allows $\underline{s}(r)$ to be transferred from one boundary to another in the radial direction. The development of this expression is addressed in more detail in reference 2.

Table A1 below reflects the values of $\underline{\alpha}$ and \underline{s} for the boundary conditions indicated.

BOUNDARY CONDITIONS	\underline{s}	$\underline{\alpha}$
Nothing Inside	$+j$	0
Nothing Outside	$-j$	∞
$\sigma \rightarrow \infty$	0	+1
$\mu \rightarrow \infty$	∞	-1

TABLE A1. SURFACE AND REFLECTION COEFFICIENTS

Referring to Figure 1, field equations for the machine may now be developed assuming no magnetic material inside the driving shaft and no material outside the shield. At this point in the analysis no particular value of the shield permeability will be specified but will carry as the variable μ_s . The air gap fields both inside and then outside of the field winding will now be developed followed by a development

of the fields within the field winding. The results are then extended to the armature and compensator windings.

Based on the two dimensional schematic representation of the machine in Figure 1 a harmonic expression for the field current density may be developed. Figure A1 depicts $J_f(\theta)$ vs. θ and is used as a basis for the following Fourier analysis.

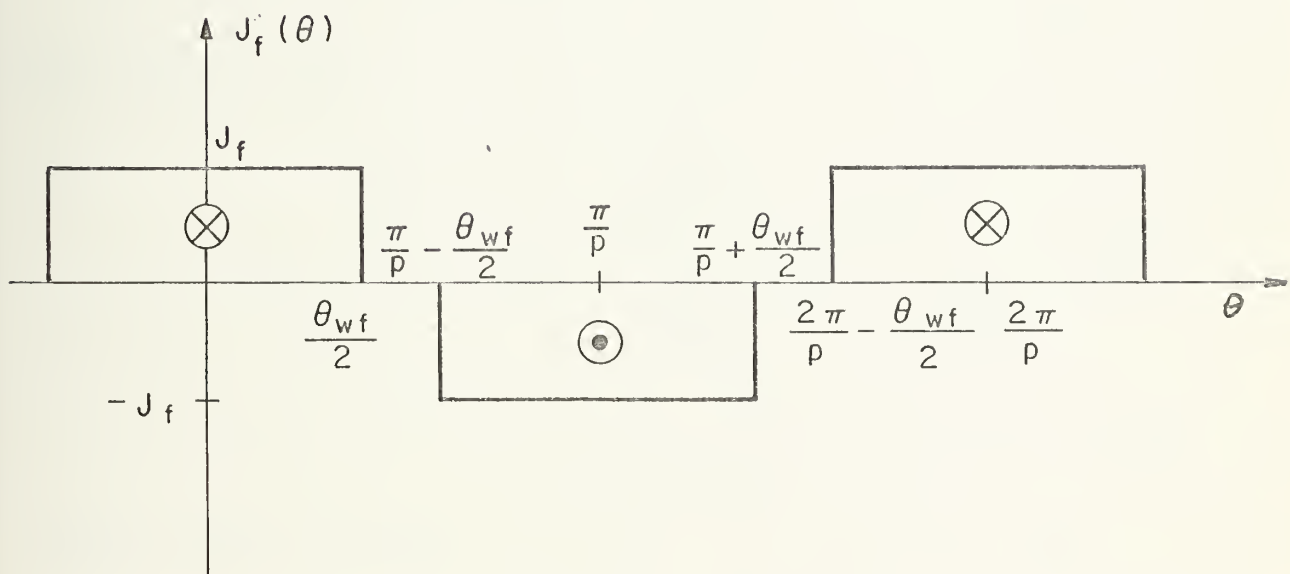


Figure A-1 Field Winding Angular Dependence of Current Density

$J_f(\theta)$ may be represented in a complete Fourier series as developed below:

$$J_f(\theta) = J_0 + \sum_{n=1}^{\infty} (J_{fn} \cos \frac{2n\pi\theta}{p} + K_{fn} \sin \frac{2n\pi\theta}{p}) \quad (A40)$$

where p is the period and equal to $\frac{2\pi}{\omega}$.

$$J_{fo} = \frac{1}{p} \int_0^p F(\theta) d\theta = \frac{p}{2\pi} \int_0^{\frac{2\pi}{\omega}} F(\theta) d\theta = 0 \quad (A41)$$

$$J_{fn} = \frac{2}{p} \int_0^p F(\theta) \cos \frac{2n\pi\theta}{p} d\theta = \frac{p}{\pi} \int_0^{\frac{2\pi}{\omega}} F(\theta) \cos np\theta d\theta \quad (A42)$$

where $F(\theta) = J_f(\theta)$

$$J_{fn} = \frac{p J_f}{\pi} \left[\int_0^{\frac{\theta wf}{2}} \cos np\theta d\theta - \int_{\frac{\pi}{p} - \frac{\theta wf}{2}}^{\frac{\pi}{p} + \frac{\theta wf}{2}} \cos np\theta d\theta + \int_{\frac{2\pi}{p} - \frac{\theta wf}{2}}^{\frac{2\pi}{p}} \cos np\theta d\theta \right] \quad (A43)$$

Integrating A43 yields

$$J_{fn} = \frac{J_f}{n\pi} \left[\sin \left(\frac{np\theta wf}{2} \right) - \sin \left(n\pi + \frac{np\theta wf}{2} \right) + \sin \left(n\pi - \frac{np\theta wf}{2} \right) - \sin \left(2n\pi - \frac{np\theta wf}{2} \right) \right] \quad (A44)$$

Using a trigonometric identity it can be shown that

$$J_{fn} = \begin{cases} \frac{4J_f}{n\pi} \sin \frac{np\theta wf}{2} & n \text{ odd} \\ 0 & n \text{ even} \end{cases} \quad (A45)$$

We can show that

$$K_{fn} = \frac{2}{p} \int_0^{\frac{p}{2}} F(\theta) \sin \frac{2n\pi\theta}{p} d\theta = 0 \quad (A46)$$

If we allow J_f to be a function of both time and space, A40 becomes after substituting A41, A44 and A46

$$J_f(\theta, t) = \sum_{n=1}^{\infty} J_{fn} \cos(\omega t - np\theta) \quad (A47)$$

where J_{fn} are described by equation A45.

The harmonic components of $J_f(\theta, t)$ may be written in a complex form as

$$\underline{J}_{fn}(\theta, t) = \operatorname{Re} [J_{fn} e^{j(\omega t - np\theta)}] \quad (A48)$$

Where $\underline{J}_{fn} = J_{fn} + j0$, n odd, J_{fn} defined in A45.

The effective field current density may be related to the terminal current as

$$J_f = \frac{N_{tf} I_f}{A_f} = \frac{2N_{tf} I_f}{\theta_{wf} (R_{fo}^2 - R_{fi}^2)}$$

Define

$$y \equiv \frac{R_{fi}}{R_{fo}}$$

$$J_f = \frac{2N_{tf} I_f}{\theta_{wf} (1-y^2) R_{fo}^2} \quad (A49)$$

and J_{fn} becomes

$$J_{fn} = \begin{cases} \frac{8N_{tf} I_f}{n\pi\theta_{wf} (1-y^2) R_{fo}^2} \sin \frac{n\pi\theta_{wf}}{2} & n \text{ odd} \\ 0 & n \text{ even} \end{cases} \quad (A50)$$

Referring to Figure 1 and references 1 and 2, the field components, H_{rf} and $H_{r\theta}$, in each region of concern ($R_{ai} < r < R_{fi}$; $R_{fi} < r < R_{fo}$; $R_{fo} < r < R_{si}$) may now be derived. The field equations will be treated as complex expressions, and the detailed derivation of these expressions may be founded in reference 2.

Again referring to Figure 1 and reference 2, the field component in the radial direction inside the field winding is:

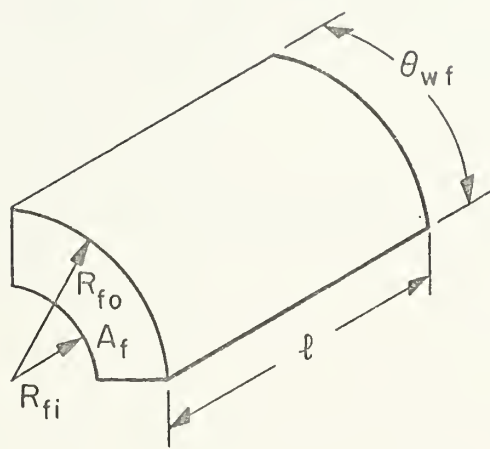


Figure A-2 Field Winding Pole Face

$$\underline{H}_{rfi} = j \frac{J_{fn}}{2} \left[\frac{\frac{r^{k-1} - \underline{\alpha}_{fi} R_{ai}^{2k} \cdot r^{-k-1}}{\underline{\alpha}_{fo} R_{si}^{2k} - \underline{\alpha}_{fi} R_{ai}^{2k}} \cdot \left[\frac{R_{fo}^{2+k} - R_{fi}^{2+k}}{2+k} - \right. \right. \\
 \left. \left. \frac{\underline{\alpha}_{fo} R_{si}^{2k} (R_{fo}^{2-k} - R_{fi}^{2-k})}{2-k} \right] \right] \quad (A51)$$

The separation constant initially introduced in equation A17 is now defined as

$$k = np \quad (A52)$$

It is assumed at this point in the analysis that the permeability of the shaft material approaches that of free space, therefore $\underline{\alpha}_i$ now equals 0. This is done as a matter of problem simplification realizing that $\underline{\alpha}_i$ could be carried throughout the analysis. A 51 becomes

$$\underline{H}_{rfi} = j \frac{J_{fn}}{2} \left(\frac{r^{k-1}}{\underline{\alpha}_{fo} R_{si}^{2k}} \right) \left[\frac{R_{fo}^{2+k} - R_{fi}^{2+k}}{2+k} - \right. \\
 \left. \frac{\underline{\alpha}_{fo} R_{si}^{2k} (R_{fo}^{2-k} - R_{fi}^{2-k})}{2-k} \right] \quad (A53)$$

In general,

$$H = \operatorname{Re} [H e^{j(\omega t - k\theta)}] \quad (A54)$$

therefore

$$H_{r_{fi}} = \operatorname{Re} \left\{ j \frac{J_{fn}}{2} \left(\frac{r^{k-1}}{\alpha_{fo} R_{si}^{2k}} \right) \left[\frac{R_{fo}^{2+k} - R_{fi}^{2+k}}{2+k} - \frac{\alpha_{fo} R_{si}^{2k} (R_{fo}^{2-k} - R_{fi}^{2-k})}{2-k} \right] e^{j(\omega t - k\theta)} \right\} \quad (A55)$$

In order to simplify A55, define

$$\Omega = \frac{R_{fo}^{2+k} - R_{fi}^{2+k}}{2+k} - \frac{\alpha_{fo} R_{si}^{2k} (R_{fo}^{2-k} - R_{fi}^{2-k})}{2-k} \quad (A56)$$

and A55 becomes

$$H_{r_{fi}} = \operatorname{Re} \left\{ j \frac{J_{fn}}{2} \left(\frac{r^{k-1}}{\alpha_{fo} R_{si}^{2k}} \right) \Omega e^{j(\omega t - k\theta)} \right\} \quad (A57)$$

Substituting $J_{fn} = J_{fn} + j0$ into A57 and reducing to the real part only $H_{r_{fi}}$ becomes

$$H_{r_{fi}} = -\frac{J_{fn}}{2} \left(\frac{r^{k-1}}{\alpha_{fo} R_{si}^{2k}} \right) \Omega \sin(\omega t - k\theta) \quad (A58)$$

Substituting A50 into A58,

$$H_{rfi} = -\frac{4N_{tf} I_f}{n\pi\theta_{wf}(1-y^2)R_{fo}^2} \left(\frac{r^{k-1}}{\alpha_{fo} R_{si}} \right) \Omega \sin \frac{n\pi\theta_{wf}}{2} \sin(\omega t - k\theta) \quad (A59)$$

A59 is an expression for only one harmonic component of H_{rfi} , and the total field must be represented as

$$H_{rfi} = -\sum_{\substack{n=1 \\ n \text{ odd}}}^{\infty} \frac{4N_{tf} I_f}{n\pi\theta_{wf}(1-y^2)R_{fo}^2} \left(\frac{r^{k-1}}{\alpha_{fo} R_{si}} \right) \Omega \sin \frac{k\theta_{wf}}{2} \sin(\omega t - k\theta) \quad (A60)$$

Relieving A60 of the requirement for time variation it becomes ($\omega = 2\pi f = 0$)

$$H_{rfi} = \sum_{\substack{n=1 \\ n \text{ odd}}}^{\infty} \frac{4N_{tf} I_f}{n\pi\theta_{wf}(1-y^2)R_{fo}^2} \left(\frac{r^{k-1}}{\alpha_{fo} R_{si}} \right) \Omega \sin \frac{k\theta_{wf}}{2} \sin k\theta \quad (A61)$$

Before proceeding with the field analysis an examination of α_o is in order. This derivation is patterned after that of reference 3 and utilizes Figure A-3.

At the outer boundary, R_{so} ; $\underline{s}(R_{so})^+ = -j$, and at the outer surface;

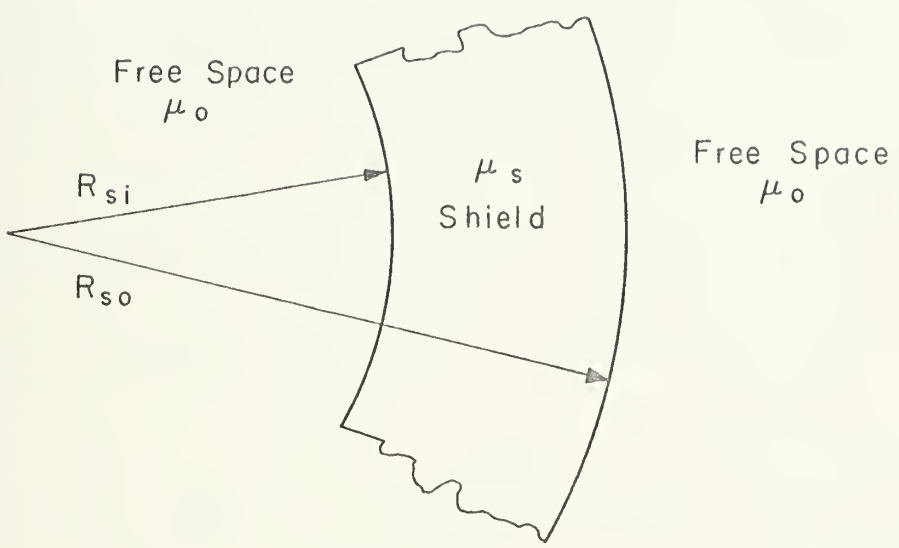


Figure A-3 Schematic of Machine Shield Showing Parameters used to derive $\underline{\alpha}_0$.

$$\underline{H_{f0}}(R_{SO}^-) = \underline{H_{f0}}(R_{SO}^+)$$

$$\underline{H_{fr}}(R_{SO}^-) = \frac{\mu_o}{\mu_s} \underline{H_{fr}}(R_{SO}^+)$$

where R_{SO}^+ and R_{SO}^- represent incremental positions adjacent to R_{SO} . It may therefore show that

$$\underline{s}(R_{SO}^-) = \frac{\underline{H_{fr}}(R_{SO}^-)}{\underline{H_{f0}}(R_{SO}^-)} = \frac{\mu_o}{\mu_s} \frac{\underline{H_{fr}}(R_{SO}^+)}{\underline{H_{f0}}(R_{SO}^+)}$$

$$\underline{s}(R_{SO}^-) = \frac{\mu_o}{\mu_s} \underline{s}(R_{SO}^+)$$

$$\text{and } \underline{s}(R_{SO}^-) = -j \frac{\mu_o}{\mu_s} \quad (A62)$$

To transfer $\underline{s}(R)$ across a radial increment use the equation A63 below⁽²⁾

$$\underline{s}(r) = j \left[\frac{r^{k-1} - \underline{\alpha} R^{2k} r^{-k-1}}{r^{k-1} + \underline{\alpha} R^{2k} r^{-k-1}} \right] \quad (A63)$$

Substituting A58 into A63 and simplifying yields

$$\underline{s}(r) = j \left[\frac{1 - \left(\frac{R}{r}\right)^{2k} - j \underline{s}(R) \left[1 + \left(\frac{R}{r}\right)^{2k} \right]}{1 + \left(\frac{R}{r}\right)^{2k} - j \underline{s}(R) \left[1 - \left(\frac{R}{r}\right)^{2k} \right]} \right] \quad (A64)$$

At the inner surface ($r = R_{si}^-$) of the shield, the boundary conditions require

$$\underline{s}(R_{si}^-) = \frac{\mu_s}{\mu_o} \underline{s}(R_{si}^+) \quad (A65)$$

Equation A64 is used to transfer the known boundary condition at $r = R_{so}^-$ (equation A62) across to R_{si}^+ . Using equation A65 the desired boundary condition at $r = R_{si}^-$ may be found as

$$\underline{s}(R_{si}^-) = -j \frac{\mu_s}{\mu_o} \left(\frac{1 - \left(\frac{R_{si}}{R_{so}}\right)^{2k} + \frac{\mu_o}{\mu_s} [1 + \left(\frac{R_{si}}{R_{so}}\right)^{2k}]}{1 + \left(\frac{R_{si}}{R_{so}}\right)^{2k} + \frac{\mu_o}{\mu_s} [1 - \left(\frac{R_{si}}{R_{so}}\right)^{2k}]} \right) \quad (A66)$$

Because $\underline{s}(R_{si}^-) = \underline{s}_{fo}(R_{si})$, using equation A38 it can be shown that

$$\underline{\alpha}_{fo} = \left[\frac{1 + j \underline{s}_{fo}(R_{si})}{1 - j \underline{s}_{fo}(R_{si})} \right] \quad (A67)$$

A general expression for $\underline{\alpha}_{fo}$ can be developed by substituting A66 into A67:

$$\frac{\alpha_{fo}}{1+\frac{\mu_s}{\mu_o}} = \frac{\alpha_{fo}}{1-\frac{\mu_s}{\mu_o}} = \left| \begin{array}{c} \left\{ 1 - \left(\frac{R_{si}}{R_{so}} \right)^{2k} + \frac{\mu_o}{\mu_s} [1 + \left(\frac{R_{si}}{R_{so}} \right)^{2k}] \right\} \\ \hline \left\{ 1 + \left(\frac{R_{si}}{R_{so}} \right)^{2k} + \frac{\mu_o}{\mu_s} [1 + \left(\frac{R_{si}}{R_{so}} \right)^{2k}] \right\} \end{array} \right| \quad (A68)$$

Note that $\underline{\alpha}_{fo}$ is real, and in future analysis the complex notation will be dropped. Also note that for all windings α_o is equivalent and the first subscript may be dropped.

In summary, the magnetic field density for the three particular regimes of interest may be written as:

$r < R_{fi}$; $k = np$ not constrained; the most generalized form:

$$H_{rfi} = \sum_{\substack{n=1 \\ n \text{ odd}}}^{\infty} \frac{4N_{tf} I_f}{n\pi(1-y^2)\theta_{wf}^2 R_{fo}^2} \left(\frac{r^{k-1}}{\alpha_o R_{si}} \right) \Omega \sin k\theta \sin \frac{k\theta_{wf}}{2} \quad (A61)$$

$$\Omega = \frac{R_{fo}^{2+k} - R_{fi}^{2+k}}{2+k} - \frac{\alpha_o R_{si}^{2k}}{2-k} (R_{fo}^{2-k} - R_{fi}^{2-k}) \quad (A56)$$

α_o defined by equation A68.

$r < R_{fi}$; $k = 2$, $n = 1$, $p = 2$

$$H_{rfi} = \frac{4N_{tf} I_f}{\pi (1-y^2) \theta_{wf} R_{fo}^2} \left(\frac{r}{\alpha_o R_{si}^4} \right) (\Omega) \sin 2\theta \sin \theta_{wf} \quad (A69)$$

$$\Omega = \frac{R_{fo}^4 - R_{fi}^4}{4} - \alpha_o R_{si}^4 \ln \left(\frac{R_{fo}}{R_{fi}} \right) \quad (A70)$$

$$\alpha_o = \frac{\frac{1 + \frac{\mu_s}{\mu_o}}{\frac{1 + (\frac{R_{si}}{R_{so}})^4 + \frac{\mu_o}{\mu_s} [1 + (\frac{R_{si}}{R_{so}})^4]}{1 + (\frac{R_{si}}{R_{so}})^4 + \frac{\mu_o}{\mu_s} [1 + (\frac{R_{si}}{R_{so}})^4]}}}{\frac{1 - \frac{\mu_s}{\mu_o}}{\frac{1 - (\frac{R_{si}}{R_{so}})^4 + \frac{\mu_o}{\mu_s} [1 + (\frac{R_{si}}{R_{so}})^4]}{1 + (\frac{R_{si}}{R_{so}})^4 + \frac{\mu_o}{\mu_s} [1 + (\frac{R_{si}}{R_{so}})^4]}}} \quad (A71)$$

allowing μ_s to approach ∞ reduces A68 to

$$\alpha_o = -1$$

$r < R_{fi}$; $\mu_s \rightarrow \infty$; k not constrained

$$H_{rfi} = - \sum_{\substack{n=1 \\ n \text{ odd}}}^{\infty} \frac{4N_{tf} I_f}{\theta_{wf} n \pi (1-y^2) R_{fo}^2} \left(\frac{r^{k-1}}{R_{si}^{2k}} \right) \Omega \sin k\theta \sin \frac{k\theta_{wf}}{2} \quad (A72)$$

$$\Omega = \frac{R_{fo}^{2+k} - R_{fi}^{2+k}}{2+k} + \frac{R_{si}^{2k}}{2-k} (R_{fo}^{2-k} - R_{fi}^{2-k}) \quad (A73)$$

$r < R_{fi}$; $\mu_s \rightarrow \infty$; $k = 2$, $n = 1$, $p = 2$

$$\alpha_o = -1$$

$$H_{rfi} = -\frac{4N_{tf} I_f}{\theta_{wf} \pi (1-y^2) R_{fo}^2} \left(\frac{r}{R_{si}}\right)^4 \Omega \sin \theta_{wf} \sin 2\theta \quad (A74)$$

$$\Omega = \frac{R_{fo}^4 - R_{fi}^4}{4} + R_{si}^4 \ln \left(\frac{R_{fo}}{R_{fi}}\right) \quad (A75)$$

Again, using results from reference 2 the azimuthal component of magnetic field density may be found as

$$H_{\theta fi} = \frac{J_{fn}}{2} \left[\frac{r^{k-1} + \alpha_{fi} R_{ai}^{2k} r^{-k-1}}{\alpha_o R_{si}^{2k} - \alpha_{fi} R_{ai}^{2k}} \right] \cdot \left[\frac{R_{fo}^{2+k} - R_{fi}^{2+k}}{2+k} \right. \\ \left. - \alpha_o \frac{R_{si}^{2k} (R_{fo}^{2-k} - R_{fi}^{2-k})}{2-k} \right] \quad (A76)$$

again $\alpha_{fi} = 0$, and taking real part of A76 yields:

$$H_{\theta fi} = \frac{J_{fn}}{2} \left(\frac{r^{k-1}}{\alpha_o R_{si}^{2k}} \right) \Omega \cos(\omega t - k\theta) \quad (A77)$$

Using A45 and realizing $\omega = 0$ it can be shown that

$$H_{\theta fi} = \frac{2J_f}{n\pi} \left(\frac{r^{k-1}}{\alpha_o R_{si}^{2k}} \right) \Omega \cos k\theta \sin \frac{k\theta_{wf}}{2} \quad (A78)$$

Ω defined by equation A56 and α_o by A68

$r < R_{fi}$; $k = 2$, $n = 1$, $p = 2$; μ_s not constrained

α_o defined by equation A71 and Ω by A70

$$H_{\theta fi} = \frac{2J_f}{\pi} \left(\frac{r}{\alpha_o R_{si}^4} \right) \Omega \cos 2\theta \sin \theta_{wf} \quad (A79)$$

$r < R_{fi}$; $\mu_s \rightarrow \infty$; k not constrained

$\alpha_o = -1$; Ω defined by equation A56

$$H_{\theta fi} = - \sum_{\substack{n=1 \\ n \text{ odd}}}^{\infty} \frac{2J_f}{n\pi} \left(\frac{r^{k-1}}{R_{si}^{2k}} \right) \Omega \cos k\theta \sin \frac{k\theta_{wf}}{2} \quad (A80)$$

$r < R_{fi}$; $\mu_s \rightarrow \infty$; $k = 2$, $n = 1$, $p = 2$

$\alpha_{fo} = -1$; Ω defined by equation A70

$$H_{\theta fi} = \frac{-2J_f}{\pi} \left(\frac{r}{R_{si}^4} \right) \Omega \cos 2\theta \sin \theta_{wf} \quad (A81)$$

The fields generated by currents in the field winding in the region $R_{fo} < r < R_{si}$ will now be examined. From reference 2

$$\begin{aligned}
 H_{rfo} = & j \frac{J_{fn}}{2} \left[\frac{r^{k-1} - \alpha_o R_{si}^{2k} r^{-k-1}}{\alpha_o R_{si}^{2k} - \alpha_{fi} R_{ai}^{2k}} \right] \left[\frac{R_{fo}^{2+k} - R_{fi}^{2+k}}{2+k} - \alpha_{fi} R_{ai}^{2k} \right. \\
 & \left. \frac{(R_{fo}^{2-k} - R_{fi}^{2-k})}{2-k} \right] \quad (A82)
 \end{aligned}$$

Assuming nothing inside the driving shaft and $\underline{\alpha_{fi}} = 0$, taking the real part of A54 and considering all harmonics yields

$$\begin{aligned}
 H_{rfo} = & + \sum_{n=1}^{\infty} \frac{J_f}{n\pi} \left[\frac{r^{k-1} - \alpha_o R_{si}^{2k} r^{-k-1}}{\alpha_o R_{si}^{2k}} \right] \left(\frac{R_{fo}^{2+k} - R_{fi}^{2+k}}{2+k} \right) \\
 & n \text{ odd} \\
 & \sin k \theta \sin \frac{k\theta_{wf}}{2} \quad (A83)
 \end{aligned}$$

α_o defined by equation A68.

$$\underline{R_{fo} < r < R_{si}; k=2, n=1, p=2; \mu_s \text{ not constrained}}$$

$$H_{rfo} = -\frac{2J_f}{n\pi} \left(\frac{r - \alpha_o R_{si}^4 r^{-3}}{\alpha_o R_{si}^4} \right) \left(\frac{R_{fo}^4 - R_{fi}^4}{4} \right) \sin \theta_{wf} \sin 2 \theta \quad (A84)$$

α_o defined by equation A71

$R_{fo} < r < R_{si}$; k not constrained; $\mu_s \rightarrow \infty$

$$H_{rfo} = + \sum_{\substack{n=1 \\ n \text{ odd}}}^{\infty} \frac{2J_f}{n\pi} \left(\frac{r^{k-1} + R_{si}^{2k} r^{-k-1}}{R_{si}^{2k}} \right) \left(\frac{R_{fo}^{2+k} - R_{fi}^{2+k}}{2+k} \right) \sin k \theta \sin \frac{k\theta_{wf}}{2} \quad (A85)$$

$$\alpha_o = -1$$

$R_{fo} < r < R_{si}$; $k = 2$, $n = 1$, $p = 2$; $\mu_s \rightarrow \infty$

$$H_{rfo} = + \frac{2J_f}{n\pi} \left(\frac{r + R_{si}^4 r^{-3}}{R_{si}^4} \right) \left(\frac{R_{fo}^4 - R_{fi}^4}{4} \right) \sin 2\theta \sin \theta_{wf} \quad (A86)$$

$$\alpha_o = -1$$

The azimuthal component of the field outside the field winding is now found from reference 2:

$$H_{\theta fo} = \frac{J_{fn}}{2} \left(\frac{r^{k-1} + \alpha_o R_{si}^{2k} r^{-k-1}}{\alpha_o R_{si}^{2k} - \alpha_{fi} R_{ai}^{2k}} \right) \left[\frac{R_{fo}^{2+k} - R_{fi}^{2+k}}{2+k} \right. \\ \left. - \alpha_{fi} \frac{R_{ai}^{2k} (R_{fo}^{2-k} - R_{fi}^{2-k})}{2-k} \right] \quad (A87)$$

$\alpha_{fi} = 0$, taking the real part of A54, and considering all harmonics yields:

$$H_{\theta fo} = \sum_{\substack{n=1 \\ n \text{ odd}}}^{\infty} \frac{2J_f}{n\pi} \left(\frac{r^{k-1} + \alpha_o R_{si}^{2k} r^{-k-1}}{\alpha_o R_{si}^{2k}} \right) \left(\frac{R_{fo}^{2+k} - R_{fi}^{2+k}}{2+k} \right) \sin \frac{k\theta}{2} \cos k \theta \quad (A88)$$

α_o defined by equation A68

$R_{fo} < r < R_{si}; k=2, n=1, p=2, \mu_s$ not constrained

$$H_{\theta fo} = \frac{2J_f}{\pi} \left(\frac{r + \alpha_o R_{si}^4 r^{-3}}{\alpha_o R_{si}^4} \right) \left(\frac{R_{fo}^4 - R_{fi}^4}{4} \right) \cos 2\theta \sin \theta_{wf} \quad (A89)$$

α_o defined by equation A71

$R_{fo} < r < R_{si}; k$ not constrained, $\mu_s \rightarrow \infty$

$$\alpha_o = -1$$

$$H_{\theta fo} = - \sum_{\substack{n=1 \\ n \text{ odd}}}^{\infty} \frac{2J_f}{n\pi} \left(\frac{r^{k-1} - R_{si}^{2k} r^{-k-1}}{R_{si}^{2k}} \right) \left(\frac{R_{fo}^{2+k} - R_{fi}^{2+k}}{2+k} \right) \cos k \theta \sin \frac{k\theta}{2} \quad (A90)$$

$$R_{fo} < r < R_{si}; k=2, n=1, p=2; \mu_s \rightarrow \infty$$

$$\alpha_o = -1$$

$$H_{\theta fo} = - \frac{2J_f}{n\pi} \left(\frac{r - R_{si}^4 r^{-3}}{R_{si}^4} \right) \left(\frac{R_{fo}^4 - R_{fi}^4}{4} \right) \cos 2\theta \sin \theta_{wf} \quad (A91)$$

The field expressions within the field winding are now developed. ($R_{fi} < r < R_{fo}$). From reference 2:

$$H_{rf} = j \frac{J_{fn}}{2} \left(\frac{r^{k-1} - \alpha_o R_{si}^{2k} r^{-k-1}}{\alpha_o R_{si}^{2k} - \alpha_{fi} R_{ai}^{2k}} \right) \left[\frac{r^{k+2} - R_{fi}^{2+k}}{2+k} - \frac{\alpha_{fi} R_{ai}^{2k}}{\alpha_{fi} R_{ai}^{2k}} \right] \\ + j \frac{J_{fn}}{2} \left(\frac{r^{k-1} - \alpha_{fi} R_{ai}^{2k} r^{-k-1}}{\alpha_o R_{si}^{2k} - \alpha_{fi} R_{ai}^{2k}} \right) \\ \left[\frac{R_{fo}^{2+k} - r^{2+k}}{2+k} - \frac{\alpha_o R_{si}^{2k} (R_{fo}^{2-k} - r^{2-k})}{2-k} \right] \quad (A92)$$

$\underline{\alpha_{fi}} = 0$, taking real part of A54 and considering all harmonics yields:

$$H_{rf} = \sum_{n=1}^{\infty} \frac{2J_f}{n} \left\{ \left(\frac{r^{k-1} - \alpha_o R_{si}^{2k} r^{-k-1}}{\alpha_o R_{si}^{2k}} \right) \left(\frac{r^{2+k} - R_{fi}^{2+k}}{2+k} \right) \right. \\ \left. + \left(\frac{r^{k-1}}{\alpha_o R_{si}^{2k}} \right) \left[\frac{R_{fo}^{2+k} - r^{2+k}}{2+k} - \frac{\alpha_o R_{si}^{2k} (R_{fo}^{2-k} - R_{fi}^{2-k})}{2-k} \right] \right\} \\ \sin \frac{\theta_{wf}}{2} \sin k \theta \quad (A93)$$

α_o defined by equation A68

$R_{fi} < r < k_{fo}$; $R=2$, $n=1$, $p=2$; μ_s not constrained

$$H_{rf} = \frac{2J_f}{n\pi} \left[\left(\frac{r - \alpha_o R_{si}^4 r^{-3}}{\alpha_o R_{si}^4} \right) \left(\frac{r^4 - R_{fi}^4}{4} \right) + \left(\frac{r}{\alpha_o R_{si}^4} \right) \left(\frac{R_{fo}^4 - r^4}{4} - \alpha_o R_{si}^4 \ln \frac{R_{fo}}{r} \right) \right] \sin \theta_{wf} \sin 2\theta \quad (A94)$$

α_o defined by equation A71

$R_{fi} < r < R_{fo}$; $\mu_s \rightarrow \infty$; k not constrained

$$H_{rf} = - \sum_{\substack{n=1 \\ n \text{ odd}}}^{\infty} \frac{2J_f}{n\pi} \left[\left(\frac{r^{k-1} + R_{si}^{2k} r^{-k-1}}{R_{si}^{2k}} \right) \left(\frac{r^{2+k} - R_{fi}^{2+k}}{2+k} \right) + \left(\frac{r^{k-1}}{R_{si}^{2k}} \right) \left[\frac{R_{fo}^{2+k} - r^{2+k}}{2+k} + \frac{R_{si}^{2k} (R_{fo}^{2-k} + r^{2-k})}{2-k} \right] \right] \sin \frac{k\theta_{wf}}{2} \sin k\theta \quad (A95)$$

$$R_{fi} < r < R_{fo}; \quad k=2, \quad n=1, \quad p=2; \quad \mu_s \rightarrow \infty$$

$$H_{rf} = -\frac{2J_f}{n\pi} \left[\left(\frac{r+R_{si}^4 r^{-3}}{R_{si}^4} \right) \left(\frac{r^4 - R_{fi}^4}{4} \right) + \left(\frac{r}{R_{si}^4} \right) \left(\frac{R_{fo}^4 - r^4}{4} \right) \right. \\ \left. + R_{si}^4 \ln \frac{R_{fo}}{r} \right] \sin \theta_{wf} \sin 2\theta \quad (A96)$$

Again, from reference 2:

$$H_{\theta f} = \frac{J_{fn}}{2} \left(\frac{r^{k-1} + \alpha_{fi} R_{si}^{2k} r^{-k-1}}{\alpha_o R_{si}^{2k} - \alpha_{fi} R_{ai}^{2k}} \right) \left(\frac{r^{2+k} - R_{fi}^{2+k}}{2+k} \right) \\ - \frac{\alpha_{fi}}{2} \frac{R_{ai}^{2k} (r^{2-k} - R_{fi}^{2-k})}{2-k} + \frac{J_{fn}}{2} \left(\frac{r^{k-1} + \alpha_{fi} R_{ai}^{2k} r^{-k-1}}{\alpha_o R_{si}^{2k} - \alpha_{fi} R_{ai}^{2k}} \right) \\ \left[\frac{R_{fo}^{2+k} - r^{2+k}}{2+k} - \alpha_o R_{si}^{2k} \frac{(R_{fo}^{2-k} - r^{2-k})}{2-k} \right] \quad (A97)$$

$\underline{\alpha_{fi}} = 0$, taking real part of A54, and considering all harmonics yields:

$$H_{\theta f} = \sum_{\substack{n=1 \\ n \text{ odd}}}^{\infty} \frac{2J_f}{n\pi} \left\{ \left(\frac{r^{k-1}}{\alpha_o R_{si}^{2k}} \right) \left(\frac{r^{2+k} - R_{fi}^{2+k}}{2+k} \right) + \left(\frac{r^{2-k}}{\alpha_o R_{si}^{2k}} \right) \right. \\ \left. \left[\frac{R_{fo}^{2+k} - r^{2+k}}{2+k} - \alpha_o \frac{R_{si}^{2k} (R_{fo}^{2-k} - r^{2-k})}{2-k} \right] \right\} \\ \sin \frac{k\theta_{wf}}{2} \cos k\theta \quad (A98)$$

α_o defined by equation A68.

$R_{fi} < r < R_{fo}$; $R=2$, $n=1$, $p=2$; μ_s not constrained

$$H_{\theta f} = \frac{2J_f}{\pi} \left[\left(\frac{r}{\alpha_o R_{si}^4} \right) \left(\frac{r^4 - R_{fi}^4}{4} \right) + \left(\frac{1}{\alpha_o R_{si}^4} \right) \left(\frac{R_{fo}^4 - r^4}{4} \right) \right]$$

$$- \alpha_o R_{si}^4 \ln \frac{R_{fo}}{r} \sin \theta_{wf} \cos 2\theta \quad (A99)$$

α_o defined by equation A71.

$R_{fi} < r < R_{fo}$; R not constrained, $\mu_s \rightarrow \infty$

$$H_{\theta f} = - \sum_{\substack{n=1 \\ n \text{ odd}}}^{\infty} \frac{2J_f}{n\pi} \left\{ \left(\frac{r^{k-1}}{R_{si}^{2k}} \right) \left(\frac{r^{2+k} - R_{fi}^{2+k}}{2+k} \right) + \left(\frac{r^{2-k}}{R_{si}^{2k}} \right) \left[\frac{R_{fo}^{2+k} - r^{2+k}}{2+k} + \frac{R_{si}^{2k} (R_{fo}^{2-k} - r^{2-k})}{2-k} \right] \right\}$$

$$\sin \frac{k\theta_{wf}}{2} \cos k\theta \quad (A100)$$

$$\underline{R_{fi} < r < R_{fo}; \ k=2, \ n=1, \ p=2; \ \mu_s \rightarrow \infty}$$

$$H_{\theta f} = -\frac{2J_f}{\pi} \left[\left(\frac{r}{R_{si}^4} \right) \left(\frac{r^4 - R_{fi}^4}{4} \right) + \left(\frac{1}{R_{si}^4} \right) \left(\frac{R_{fo}^4 - r^4}{4} \right) + R_{si}^4 \ln \frac{R_{fo}}{r} \right]$$

$$\sin \theta_{wf} \sin 2 \theta \quad (A101)$$

Referring to Figure 1, the field equations as developed above are valid for the fields generated by the current in the compensator if we replace θ with $\theta-\alpha$. α is defined as the angle between the direct axis field component of the field winding and the direct axis field component of the compensator winding. We may also find the field expressions for the armature by making the appropriate substitutions as outlined in Table A3.

Substitute term in column B for column C to find fields due to currents in column A.

A	B	C
Compensator	θ_{wc}	θ_{wf}
	J_c	J_f
	N_{tc}	N_{tf}
	I_c	I_f
	R_{ci}	R_{fi}
	R_{co}	R_{fo}
	z	y
	$\theta - \alpha$	θ
Phase A or Armature	$\theta + \phi$	θ
	θ_{wa}	θ_{wf}
	J_a	J_f
	N_{ta}	N_{tf}
	I_a	I_f
	R_{ai}	R_{fi}
	R_{ao}	R_{fo}
	x	y
Phase B of Armature	$\theta + \phi + \frac{2\pi}{3}$	θ
Phase C of Armature	$\theta + \phi + \frac{4\pi}{3}$	θ

TABLE A2. Substitutions for Field Expressions

APPENDIX B

MACHINE INDUCTANCES

The flux-current relationships for the machine may be expressed in a matrix format as

$$\begin{vmatrix} \lambda_1 \\ \lambda_2 \\ \lambda_3 \\ \lambda_c \\ \lambda_f \end{vmatrix} = \begin{vmatrix} L_1 & L_{12} & L_{13} & M_{1c} & M_{1f} \\ L_{12} & L_2 & L_{23} & M_{2c} & M_{2f} \\ L_{13} & L_{23} & L_3 & M_{3c} & M_{3f} \\ M_{1c} & M_{2c} & M_{3c} & L_c & M_{cf} \\ M_{1f} & M_{2f} & M_{3f} & M_{fc} & L_f \end{vmatrix} \begin{vmatrix} I_1 \\ I_2 \\ I_3 \\ I_c \\ I_f \end{vmatrix}$$

In the above expression, for clarification a, b, and c (armature phase subscripts) have been replaced with 1, 2, and 3 respectfully.

In general, the self-inductance of the field may be found as

$$L_f = \frac{\lambda_f}{I_f} \quad \left| \begin{matrix} I_1 = I_2 = I_3 = I_c = 0 \end{matrix} \right.$$

Referring to Figure B1 the flux linkage may be interpreted as that flux, Φ passing through the coil. More exactly

$$\lambda = N_t \Phi \quad (B1)$$

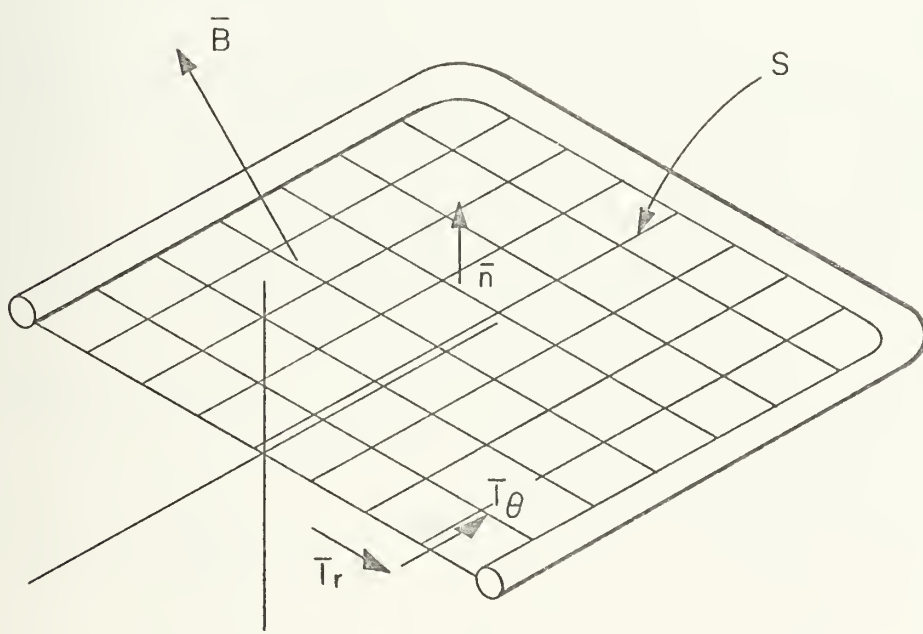


Figure B-1 Single Turn Coil Flux Linkage

where for a single turn coil $N_t = 1$ and

$$\Phi = \int_S \bar{B} \cdot \bar{n} \, da \quad (B2)$$

equation B1 becomes

$$\lambda = N_t \int_S \bar{B} \cdot \bar{n} \, da \quad (B3)$$

By referring to Figure B-2 this concept may be extended to determine the flux linked by a thick winding composed of many turns. The differential number of turns in the differential element $rd\psi dr$ may be expressed as

$$d^2N_t = \frac{N_t}{A} dA \quad (B4)$$

$$d^2N_t = \frac{2N_t}{\theta_w (R_{wo}^2 - R_{wi}^2)} dA \quad (B5)$$

where $dA = r dr d\psi$

The flux linked by this element is given by

$$d^2\lambda = \Phi d^2N_t \quad (B6)$$

$$d^2\lambda = \frac{2N_t \Phi}{\theta_w (R_{wo}^2 - R_{wi}^2)} dA \quad (B7)$$

where Φ is expressed in equation B2. If we are determining the self-inductance of the winding, Φ is generated by currents flowing in the winding in question. Otherwise (mutual) Φ is

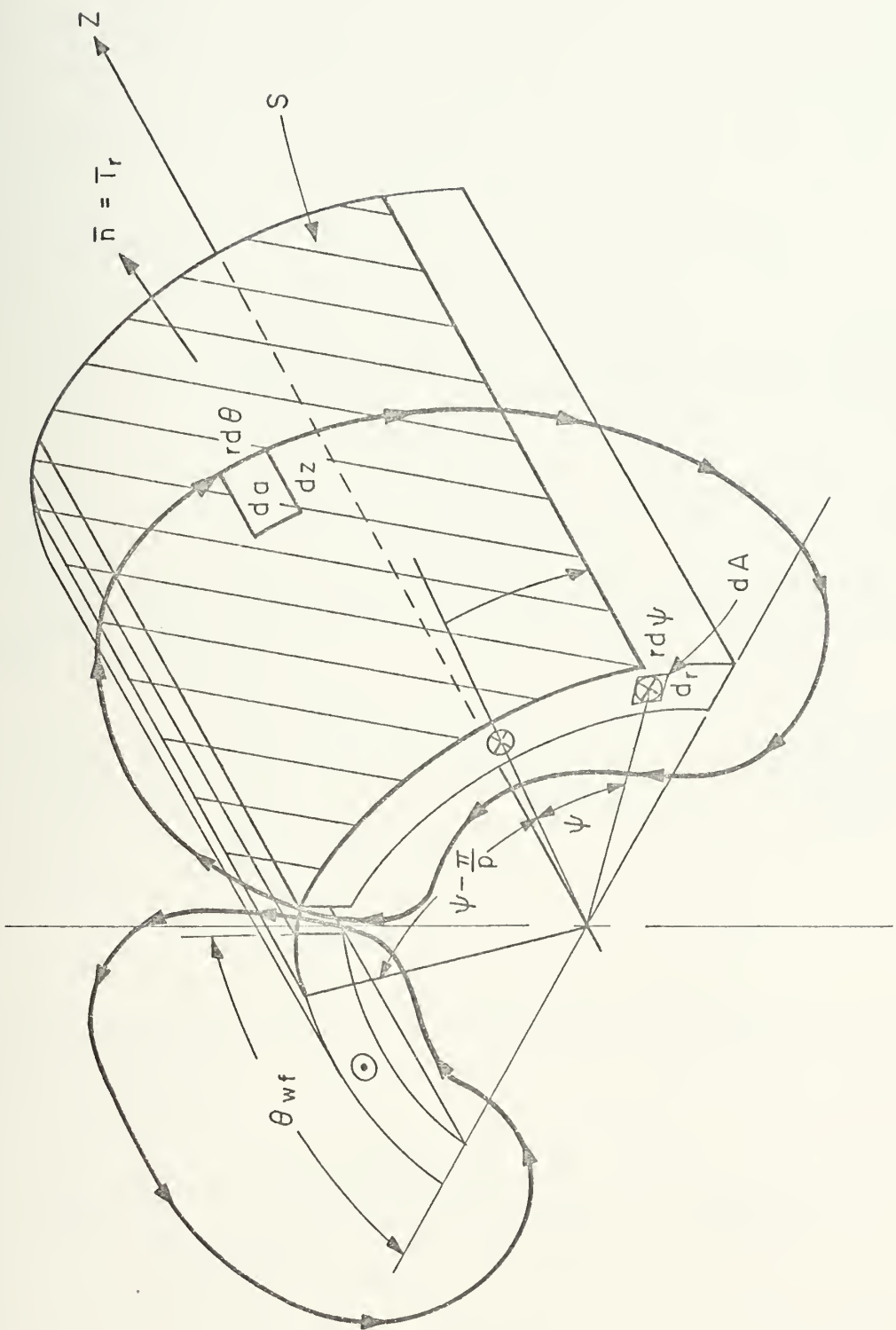


Figure B-2 Flux Linkage of Differential Elements

generated by some other current within the machine. Within the air-gap we assume the fields are conservative and may express \bar{B} as:

$$\bar{B} = \mu_o \bar{H} \quad (B8)$$

and, B7 becomes

$$d^2\lambda = [\int_S \mu_o \bar{H} \cdot \bar{n} da] d^2N_t = [\int_S \mu_o \bar{H} \cdot \bar{n} da] \frac{2N_t dA}{\theta_w (R_{so}^2 - R_{wi}^2)} \quad (B7)$$

Treating the field winding self inductance, equation B7 may be written as

$$L_f = \frac{P}{I_f} \left[\int_{-\frac{\theta_{wf}}{2}}^{\frac{\theta_{wf}}{2}} \int_{R_{fi}}^{R_{fo}} \int_{\psi - \frac{\pi}{p}}^{\psi} \mu_o H_{rf}(r, \theta) r dr d\theta dz \right] \frac{2N_t f \cdot r dr d\psi}{\theta_{wf} (R_{fo}^2 - R_{fi}^2)} \quad (B7)$$

Using equation A93 we may integrate B7 and obtain the field self inductance:

$$L_f = \sum_{\substack{n=1 \\ n \text{ odd}}}^{\infty} \frac{16 \sin^2 \left(\frac{k\theta_{wf}}{2} \right) N_t f^2 \ell_f \mu_o}{\alpha_o n^3 p \pi \theta_{wf}^2 (k^2 - 4) (1 - y^2)^2} \left\{ 2 \left(\frac{2-k}{2+k} \right) (1 - y^{2+k})^2 \left(\frac{R_{fo}}{R_{si}} \right)^{2k} + \alpha_o [(k-2) + 4y^{2+k} - y^4 (2+k)] \right\} \quad (B9)$$

when α_o is given by equation A68.

Let $\mu_s \rightarrow \infty$, k not constrained

$$\alpha_o = -1$$

$$L_f = \sum_{\substack{n=1 \\ n \text{ odd}}}^{\infty} \frac{16 \sin^2(\frac{k\theta_{wf}}{2}) N_{tf}^2 \ell_f \mu_o}{n^3 p \pi \theta_{wf}^2 (k^2 - 4) (1 - y^2)^2} [2(\frac{k-2}{k+2}) (1 - y^{2+k})^2$$

$$(\frac{R_{fo}}{R_{si}})^{2k} + (k-2) + 4y^{2+k} - y^4(2+k)] \quad (B10)$$

This result agrees with the tabulated value for L_f in reference 6, and can be obtained directly from equation 60 of reference 2.

$k=2, n=1, p=2, \mu_s$ not constrained

$$L_f = \frac{8 \sin^2(\theta_{wf}) N_{tf}^2 \ell_f \mu_o}{\alpha_o \pi \theta_{wf}^2 (1 - y^2)^2} \left[-\frac{(1 - y^4)^2}{8} (\frac{R_{fo}}{R_{si}})^4 + \alpha_o [y^4 \ln y + \frac{1 - y^4}{4} + \frac{(1 - y^4)^2}{8} (\frac{R_{fo}}{R_{si}})^4] \right] \quad (B11)$$

α_o defined by equation A71

$$k=2, n=1, p=2, \mu_s \rightarrow \infty \quad \alpha_o = -1$$

$$L_f = \frac{8 \sin^2(\theta_{wf}) N_{tf}^2 \ell_{fo}^2}{\pi \theta_{wf}^2 (1-y^2)^2} \left[\frac{(1-y^4)^2}{8} \left(\frac{R_{fo}}{R_{si}} \right)^4 + y^4 \ln y + \frac{1-y^4}{4} \right]$$

(B12)

Using the same technique discussed above, we may find all machine self and mutual inductances, allowing for the angles between various windings when developing the expressions for mutual inductances. The results of this analysis are listed in Table B-1.

TABLE B-1

MACHINE INDUCTANCES

See Appendix B for expressions for L_f .

$k = np$ not constrained, μ_s not constrained

$$L_a = \sum_{\substack{n=1 \\ n \text{ odd}}}^{\infty} \frac{16 \sin^2(\frac{k\theta_{wa}}{2}) N_{ta}^2 \ell_a \mu_o}{\alpha_o n^3 p \theta_{wa}^2 (k^2 - 4) (1-x^2)^2} \left[2 \left(\frac{2-k}{k+2} \right) (1-x^{2+k})^2 \left(\frac{R_{ao}}{R_{si}} \right)^{2k} + \alpha_o [(k-2) + 4x^{2+k} - x^4 (2+k)] \right] \quad (B13)$$

α_o given by equation A68

$k = np$ not constrained, $\mu_s \rightarrow \infty$

$$L_a = \sum_{\substack{n=1 \\ n \text{ odd}}}^{\infty} \frac{16 \sin^2(\frac{k\theta_{wa}}{2}) N_{ta}^2 \ell_a \mu_o}{n^3 p \pi \theta_{wa}^2 (k^2 - 4) (1-x^2)^2} [2 \left(\frac{k-2}{k+2} \right) (1-x^{2+k})^2 \left(\frac{R_{ao}}{R_{ai}} \right)^2 + (k-2) + 4x^{2+k} - x^4 (2+k)] \quad (B14)$$

$$\alpha_o = -1$$

$k=2, n=1, p=2, \mu_s \rightarrow \infty$

$$\alpha_o = -1$$

$$L_a = \frac{8 \sin^2(\theta_{wa}) N_{ta}^2 \ell_a \mu_o}{\pi \theta_{wa}^2 (1-x^2)^2} \left[\frac{(1-x^4)^2}{8} \left(\frac{R_{ao}}{R_{si}} \right)^4 + x^4 \ln x + \frac{1-x^4}{4} \right] \quad (B15)$$

TABLE B-1 continued

k=2, n=1, p=2, μ_s not constrained

$$L_a = \frac{8 \sin^2(\theta_{wa}) N_{ta}^2 \ell_a \mu_o}{\alpha_o \pi \theta_{wa}^2 (1-x^2)^2} \left\{ -\frac{(1-x^4)^2}{(R_{ao})^4} \left(\frac{R_{ao}}{R_{si}} \right)^4 \right. \\ \left. + \alpha_o [x^4 \ln x + \frac{(1-x^4)}{4} + \frac{(1-x^4)^2}{8} \left(\frac{R_{ao}}{R_{si}} \right)^4] \right\} \quad (B16)$$

 α_o given by equation A71k = np not constrained, μ_s not constrained

$$L_c = \sum_{\substack{n=1 \\ n \text{ odd}}}^{\infty} \frac{16 \sin^2(\frac{k\theta_{wc}}{2}) N_{tc}^2 \ell_c \mu_o}{\alpha_o n^3 \pi p \theta_{wc} (k^2-4) (1-z^2)^2} \left\{ 2 \left(\frac{2-k}{k+2} \right) (1-z^{2+k})^2 \right. \\ \left. \left(\frac{R_{co}}{R_{si}} \right)^{2k} + \alpha_o [(k-2)+4z^{2+k} - z^4(2+k)] \right\} \quad (B17)$$

 α_o given by equation A68k = np not constrained, $\mu_s \rightarrow \infty$

$$L_c = \sum_{\substack{n=1 \\ n \text{ odd}}}^{\infty} \frac{\alpha_o = -1}{n^3 \pi p \theta_{wc} (k^2-4) (1-z^2)^2} \left[2 \left(\frac{k-2}{k+2} \right) (1-z^{2+k})^2 \right. \\ \left. \left(\frac{R_{co}}{R_{si}} \right)^2 + (k-2) + 4z^{2+k} + z^4(2+k) \right] \quad (B18)$$

TABLE B-1 continued

k=2, n=1, p=2, μ_s not constrained

$$L_C = \frac{8 \sin^2(\theta_{WC}) N_{TC}^2 \ell_C \mu_O}{\alpha_O \pi \theta_{WC}^2 (1-z^2)^2} \left\{ -\frac{(1-z^4)^2}{8} \left(\frac{R_{CO}}{R_{Si}} \right)^4 + \alpha_O \left[z^4 \ln z + \frac{(1-z^4)}{4} + \frac{(1-z^4)}{8} \left(\frac{R_{CO}}{R_{Si}} \right)^4 \right] \right\} \quad (B19)$$

 α_O given by equation A71.k=2, n=1, p=2, $\mu_s \rightarrow \infty$

$$L_C = \frac{8 \sin^2(\theta_{WC}) N_{TC}^2 \ell_C \mu_O}{\pi \theta_{WC}^2 (1-z^2)^2} \left[\frac{(1-z^4)^2}{8} \left(\frac{R_{CO}}{R_{Si}} \right)^4 + z^4 \ln z + \frac{1-z^4}{4} \right] \quad (B20)$$

 $\alpha_O = -1$ k=np not constrained, μ_s not constrained

$$L_{ab} = \sum_{\substack{n=1 \\ n \text{ odd}}}^{\infty} \frac{16 \sin^2(\frac{k\theta_{wa}}{2}) N_{ta}^2 \ell_a \mu_O \cos(\frac{2n\pi}{3})}{\alpha_O n^3 p \theta_{wa}^2 (k^2-4) (1-x^2)^2} \left\{ 2 \left(\frac{2-k}{k+2} \right) (1-x^{2+k})^2 \left(\frac{R_{ao}}{R_{si}} \right)^{2k} + \alpha_O [(k-2)+4x^{2+k}-x^4(2+k)] \right\} \quad (B21)$$

 α_O given by equation A68.

TABLE B-1 continued

k=np not constrained, $\mu_s \rightarrow \infty$

$$L_{ab} = \sum_{\substack{n=1 \\ n \text{ odd}}}^{\infty} \frac{16 \sin^2(\frac{k\theta}{2}) N_{ta}^2 \ell_a \mu_o \cos(\frac{2n\pi}{3})}{n^3 p \pi \theta_{wa}^2 (k^2 - 4) (1-x^2)^2} [2(\frac{k-2}{k+2}) (1-x^{2+k})^2 \\ (\frac{R_{ao}}{R_{si}})^2 + (k-2) + 4x^{2+k} - x^4 (2+k)] \quad (B22)$$

$$\alpha_o = -1$$

k=2, n=1, p=2, μ_s not constrained

$$L_{ab} = \frac{8 \sin^2(\theta_{wa}) N_{ta}^2 \ell_a \mu_o \cos(\frac{2\pi}{3})}{\alpha_o \pi \theta_{wa}^2 (1-x^2)^2} \left\{ -\frac{(1-x^4)^2}{8} (\frac{R_{ao}}{R_{si}})^4 \right. \\ \left. + \alpha_o [x^4 \ln x + \frac{(1-x^4)}{4} + \frac{(1-x^4)^2}{8} (\frac{R_{ao}}{R_{si}})^4] \right\} \quad (B23)$$

 α_o given by equation A71.k=2, n=1, p=2, $\mu_s \rightarrow \infty$

$$\alpha_o = -1 \\ L_{ab} = \frac{8 \sin^2(\theta_{wa}) N_{ta}^2 \ell_a \mu_o \cos(\frac{2\pi}{3})}{\pi \theta_{wa}^2 (1-x^2)^2} [\frac{(1-x^4)^2}{8} (\frac{R_{ao}}{R_{si}})^4 \\ + x^4 \ln x + \frac{1-x^4}{4}] \quad (B24)$$

TABLE B-1 continued

k=np not constrained, μ_s not constrained

$$L_a - L_{ab} = \frac{16 \ell_a \mu_o N_{ta}^2}{\alpha_o \pi \theta_{wa}^2 (1-x^2)^2} \sum_{\substack{n=1 \\ n \text{ odd}}}^{\infty} \frac{\sin^2(\frac{k\theta_{wa}}{2}) (1-\cos\frac{2n\pi}{3})}{n^3} C_{snp} \quad (B25)$$

$$C_{snp} = 2 \left(\frac{2-k}{k+2} \right) (1-x^{2+k})^2 \left(\frac{R_{ao}}{R_{si}} \right)^2 + \alpha_o [(k-2) + 4x^{2+k} - x^4 (2+k)] \quad (B26)$$

 α_o defined by equation A68.k=np not constrained, $\mu_s \rightarrow \infty$

$$L_a - L_{ab} = \frac{16 \ell_a \mu_o N_{ta}^2}{\pi \theta_{wa}^2 (1-x^2)^2} \sum_{\substack{n=1 \\ n \text{ odd}}}^{\infty} \frac{\sin^2(\frac{k\theta_{wa}}{2}) (1-\cos\frac{2n\pi}{3})}{n^3} C_{snp} \quad (B27)$$

$$C_{snp} = 2 \left(\frac{k-2}{k+2} \right) (1-x^{2+k})^2 \left(\frac{R_{ao}}{R_{si}} \right)^2 + (k-2) + 4x^{2+k} - x^4 (2+k) \quad (B28)$$

$$\alpha_o = -1$$

TABLE B-1 continued

 $k=1, p=2, n=1, \mu_s$ not constrained

$$L_a - L_{ab} = \frac{8 \ell_a \mu_o N_{ta}^2}{\alpha_o \pi \theta_{wa}^2 (1-x^2)^2} \sin^2(\theta_{wa}) (1-\cos \frac{2\pi}{3}) C_{s2} \quad (B29)$$

$$C_{s2} = -\frac{(1-x^4)^2}{8} \left(\frac{R_{ao}}{R_{si}} \right)^4 + \alpha_o [x^4 \ln x + \frac{(1-x^4)}{4} + \frac{(1-x^4)^2}{8} \left(\frac{R_{ao}}{R_{si}} \right)^4] \quad (B30)$$

 α_o given by equation A71. $k=1, p=2, n=1, \mu_s \rightarrow \infty$

$$\alpha_o = -1$$

$$L_a - L_{ab} = \frac{8 \ell_a \mu_o N_{ta}^2}{\pi \theta_{wa}^2 (1-x^2)^2} \sin^2(\theta_{wa}) (1-\cos \frac{2\pi}{3}) C_{s2} \quad (B31)$$

$$C_{s2} = \frac{(1-x^4)^2}{8} \left(\frac{R_{ao}}{R_{si}} \right)^4 + x^4 \ln x + \frac{1-x^4}{4} \quad (B32)$$

 $k=np$ not constrained, μ_s not constrained

$$M_{af} = \sum_{\substack{n=1 \\ n \text{ odd}}}^{\infty} M_{nf} \cos k \phi \quad (B33)$$

TABLE B-1 continued

where

$$M_{nf} = -\frac{32(l-y^{2+k}) \operatorname{Im} N_{ta}^N \operatorname{tf} \mu_o \sin(\frac{k\theta_{wa}}{2}) \sin(\frac{k\theta_{wf}}{2}) (\frac{R_{fo}}{R_{ao}})^k C_{npf}}{\alpha_o \pi n^2 \theta_{wa} \theta_{wf} (l-y^2) (l-x^2)} \quad (B34)$$

$$C_{npf} = \frac{[l-x^{2-k} - \alpha_o (\frac{2-k}{2+k}) (l-x^{2+k}) (\frac{R_{ao}}{R_{si}})^{2k}]}{k(4 - k^2)} \quad (B35)$$

α_o given by equation A68.

$k=np$ not constrained, $\mu_s \rightarrow \infty$

$$M_{af} = \sum_{\substack{n=1 \\ n \text{ odd}}}^{\infty} M_{nf} \cos k \phi, \quad \alpha_o = -1 \quad (B33)$$

$$M_{nf} = \frac{32(l-y^{2+k}) \operatorname{Im} \mu_o N_{ta}^N \operatorname{tf} \sin(\frac{k\theta_{wa}}{2}) \sin(\frac{k\theta_{wf}}{2}) (\frac{R_{fo}}{R_{ao}})^k C_{npf}}{\pi n^2 \theta_{wa} \theta_{wf} (l-y^2) (l-x^2)} \quad (B36)$$

$$C_{npf} = \frac{[l-x^{2-k} + (\frac{2-k}{2+k}) (l-x^{2+k}) (\frac{R_{ao}}{R_{si}})^{2k}]}{k(4 - k^2)} \quad (B37)$$

$k=2, n=1, p=2, \mu_s$ not constrained

$$M_{2f} = \frac{-32 \operatorname{Im} \mu_o N_{ta}^N \operatorname{tf} \sin(\theta_{wa}) \sin(\theta_{wf})}{\alpha_o \pi \theta_{wa} \theta_{wf} (l-y^2) (l-x^2)} \left(\frac{R_{fo}}{R_{ao}} \right)^2 (l-y^4) C_{2f} \quad (B38)$$

$$C_{2f} = -\frac{1}{8} \ln x - \alpha_o \frac{(l-x^4)}{32} \left(\frac{R_{ao}}{R_{si}} \right)^4 \quad (B39)$$

TABLE B-1 continued

 α_o given by equation A71 $k=2, n=1, p=2, \mu_s \rightarrow \infty$

$$M_{2f} = \frac{32lm\mu_o N_{ta} N_{tf} \sin(\theta_{wa}) \sin(\theta_{wf})}{\pi \theta_{wa} \theta_{wf} (1-y^2) (1-x^2)} \left(\frac{R_{fo}}{R_{ao}} \right)^2 (1-y^4) C_{2f} \quad (B40)$$

$$C_{2f} = -\frac{1}{8} \ln x + \frac{(1-x^4)}{32} \left(\frac{R_{ao}}{R_{si}} \right)^4 \quad (B41)$$

 $k=np$ not constrained, μ_s not constrained

$$M_{ac} = \sum_{\substack{n=1 \\ n \text{ odd}}}^{\infty} M_{nc} \cos k(\phi+\alpha) \quad (B42)$$

where,

$$M_{nc} = \frac{-32lmN_{ta} N_{tc} \mu_o \sin\left(\frac{k\theta_{wa}}{2}\right) \sin\left(\frac{k\theta_{wc}}{2}\right)}{\alpha_o \pi n^2 \theta_{wa} \theta_{wc} (1-x^2) (1-z^2)} \left(\frac{R_{co}}{R_{ao}} \right)^k C_{npc} \quad (B43)$$

$$C_{npc} = \frac{[1-x^{2-k} - \alpha_o \left(\frac{2-k}{2+k} \right) (1-x^{2+k}) \left(\frac{R_{ao}}{R_{si}} \right)^{2k}]}{k(4 - k^2)} \quad (B44)$$

 α_o given by equation A68. $k=np$ not constrained, $\mu_s \rightarrow \infty$

$$\alpha_o = -1$$

TABLE B-1 continued

$$M_{nc} = \frac{32l\mu_o N_{ta} N_{tf} \sin(\frac{k\theta_{wa}}{2}) \sin(\frac{k\theta_{wc}}{2})}{\pi n^2 \theta_{wa} \theta_{wc} (1-x^2) (1-z^2)} \left(\frac{R_{co}}{R_{ao}}\right)^k C_{npc} \quad (B45)$$

$$C_{npc} = \frac{[1-x^{2-k} + (\frac{2-k}{2+k}) (1-x^{2+k}) (\frac{R_{ao}}{R_{si}})^{2k}]}{k(4 - k^2)} \quad (B46)$$

$k=2, n=1, p=2, \mu_s$ not constrained

$$M_{2c} = \frac{-32l\mu_o N_{ta} N_{tc} \sin(\theta_{wa}) \sin(\theta_{wc})}{\alpha_o \pi \theta_{wa} \theta_{wc} (1-x^2) (1-z^2)} \left(\frac{R_{co}}{R_{ao}}\right)^2 C_{2c} \quad (B47)$$

$$C_{2c} = -\frac{1}{8} \ln x - \alpha_o \frac{(1-x^4)}{32} \left(\frac{R_{ao}}{R_{si}}\right)^4 \quad (B48)$$

α_o given by equation A71.

$k=2, n=1, p=2, \mu_s \rightarrow \infty$

$$\alpha_o = -1$$

$$M_{2c} = \frac{32l\mu_o N_{ta} N_{tc} \sin(\theta_{wa}) \sin(\theta_{wc})}{\pi \theta_{wa} \theta_{wc} (1-x^2) (1-z^2)} \left(\frac{R_{co}}{R_{ao}}\right)^2 C_{2c} \quad (B49)$$

$$C_{2c} = -\frac{1}{8} \ln x + \frac{(1-x^4)}{32} \left(\frac{R_{ao}}{R_{si}}\right)^4 \quad (B50)$$

TABLE B-1 continued

k=np not constrained, μ_s not constrained

$$M_{fc} = \sum_{\substack{n=1 \\ n \text{ odd}}}^{\infty} M_{nfc} \cos k \alpha \quad (B51)$$

where,

$$M_{nfc} = \frac{-32(1-y^{2+k}) \operatorname{Im} N_{tc} N_{tf} \mu_o \sin(\frac{k\theta_{wf}}{2}) \sin(\frac{k\theta_{wc}}{2})}{\alpha_o \pi n^2 \theta_{wc} \theta_{wf} (1-y^2) (1-z^2)} \left(\frac{R_{co}}{R_{fo}} \right)^{2k} C_{npfc} \quad (B52)$$

$$C_{npfc} = \frac{[1-z^{2-k} - \alpha_o (\frac{2-k}{2+k}) (1-z^{2+k}) (\frac{R_{co}}{R_{si}})^{2k}]}{k(4-k)^2} \quad (B53)$$

 α_o given by equation A68.k=np not constrained, $\mu_s \rightarrow \infty$

$$M_{fc} = \sum_{\substack{n=1 \\ n \text{ odd}}}^{\infty} M_{nfc} \cos k \alpha, \quad \alpha_o = -1 \quad (B54)$$

$$M_{nfc} = \frac{32(1+y^{2+k}) \operatorname{Im} N_{tc} N_{tf} \mu_o \sin(\frac{k\theta_{wf}}{2}) \sin(\frac{k\theta_{wc}}{2})}{\pi n^2 \theta_{wc} \theta_{wf} (1-y^2) (1-z^2)} \left(\frac{R_{co}}{R_{fo}} \right)^k C_{npfc} \quad (B55)$$

$$C_{npfc} = \frac{[1-z^{2-k} + (\frac{2-k}{2+k}) (1-z^{2+k}) (\frac{R_{co}}{R_{si}})^{2k}]}{k(4-k)^2} \quad (B56)$$

TABLE B-1 continued

k=2, n=1, p=2, μ_s not constrained

$$M_{2fc} = \frac{-32lm\mu_o (1-y^4)lmN_{tc}N_{tf}\sin\theta_{wc}\sin\theta_{wf}}{\alpha_o \pi \theta_{wc} \theta_{wf} (1-y^2)(1-z^2)} \left(\frac{R_{co}}{R_{fo}}\right)^2 C_{2fc} \quad (B57)$$

$$C_{2fc} = -\frac{1}{8} \ln z - \alpha_o \frac{(1-z^4)}{32} \left(\frac{R_{co}}{R_{si}}\right)^4 \quad (B58)$$

 α_o given by equation A71.k=2, n=1, p=2, $\mu_s \rightarrow \infty$

$$M_{2fc} = \frac{32lm\mu_o N_{tc} N_{tf} \sin\theta_{wc} \sin\theta_{wf}}{\left(\frac{R_{fo}}{R_{ao}}\right)^2 (1-y^4)} C_{2fc} \quad (B59)$$

$$C_{2fc} = -\frac{1}{8} \ln z + \frac{(1-z^4)}{32} \left(\frac{R_{co}}{R_{si}}\right)^4 \quad (B60)$$

We may determine all additional machine self and mutual inductances by making the substitutions listed below in Table B-2.

To Obtain For	Use Formula For	Equation Nos.	Replace ϕ	With
M_{bf}	M_{af}	B33 through B41	ϕ	$\phi - \frac{2\pi}{3}$
M_{cf}	M_{af}	B33 through B41	ϕ	$\phi + \frac{2\pi}{3}$
M_{bc}	M_{ac}	B42 through B50	$\phi + \alpha$	$\phi + \alpha - \frac{2\pi}{3}$
M_{cc}	M_{ac}	B42 through B50	$\phi + \alpha$	$\phi + \alpha + \frac{2\pi}{3}$

TABLE B-2. Substitutions for Machine Inductances

APPENDIX C

MACHINE INTERNAL TORQUE EXPRESSIONS

Using the basic concepts developed in reference 7 and other sources, expressions for machine internal torque are developed. Specifically, expressions for torque on the armature and for null torque on the field with a compensating winding either within or outside of the field are presented.

In general, the Lorentz force is representative of the total magnetic force on a charge of moving with a velocity \bar{V} and may be expressed as:

$$\bar{F} = q\bar{V} \times \bar{B} \quad (C1)$$

The force density, \bar{F} , in newtons per cubic meter can be obtained from C1 as:

$$\bar{F} = \lim_{\delta v \rightarrow 0} \frac{\sum \bar{F}_i}{\delta v} = \lim_{\delta v \rightarrow 0} \sum_i \frac{q_i \bar{V}_i \times \bar{B}_i}{\delta v} \quad (C2)$$

\bar{F}_i , q_i , and \bar{V}_i refer to all particles in δv and \bar{B}_i is the flux density experienced by q_i . Assuming all particles in δv experience the same flux density \bar{B} , the definition of free current density and equation C2 yields:

$$\bar{F} = \bar{J}_f \times \bar{B} \quad (C3)$$

Equation C3 may be used to express the average of forces on the charges flowing in the winding. This is equivalent to the force on the winding if there is some mechanism by which each charge transmits the Lorentz force to the material. Assuming that the charges in the winding conductors behave as particles moving through a viscous material, the force acting on each charge is transmitted to the medium by the viscous retarding force, and equation C3 represents the force density experienced by the medium (7).

It is also assumed that the windings have a constant permeability approximating that of free space and that

$$\bar{B} = \mu_0 \bar{H} \text{ is valid within the winding volume.} \quad (C4)$$

Substituting for \bar{B} , equation C3 becomes

$$\bar{F} = \mu_0 (\bar{J}_f \times \bar{H}) \quad (C5)$$

Expressions for radial and azimuthal components of \bar{H} are developed for various boundary conditions at the shield inner radius in Appendix A.

Equation C5 may be expressed in a matrix form as:

$$\bar{F} = \mu_0 \begin{vmatrix} \bar{I}_r & \bar{I}_\theta & \bar{I}_z \\ 0 & 0 & J \\ H_r & H_\theta & 0 \end{vmatrix} \quad (C6)$$

or

$$\bar{F} = \mu_0 J (H_r \bar{I}_\theta - H_0 \bar{I}_r) \quad (C7)$$

Field Winding Null Torque Expression:

Referring to Figure C-1, the torque on the field winding may be expressed as

$$\bar{T} = \int_V (\bar{r} \times \bar{F}) \, dv = \int_V (\bar{r} \times \bar{F}) \, r dr d\theta dz \quad (C8)$$

$$\frac{\bar{T}}{\bar{I}_f} = \int_{\theta} \int_r (\bar{r} \times \bar{F}) \, r dr d\theta \quad (C9)$$

$$\bar{r} \times \bar{F} = \begin{vmatrix} \bar{I}_r & \bar{I}_\theta & \bar{I}_z \\ r & 0 & 0 \\ F_r & F_\theta & 0 \end{vmatrix} = r F_\theta \bar{I}_z \quad (C10)$$

Using C10, equation C9 becomes:

$$\frac{\bar{T}}{\bar{I}_f} = \int_{\theta} \int_{R_{fi}}^{R_{fo}} r^2 F_\theta dr d\theta \bar{I}_z \quad (C11)$$

Equation C11 represents torque only on one pole face, and for the entire machine,

$$\frac{\bar{T}}{\bar{I}_f} = 2p \int_{\theta} \int_{R_{fi}}^{R_{fo}} \mu_0 J_f H_r r^2 dr d\theta \bar{I}_z \quad (C12)$$

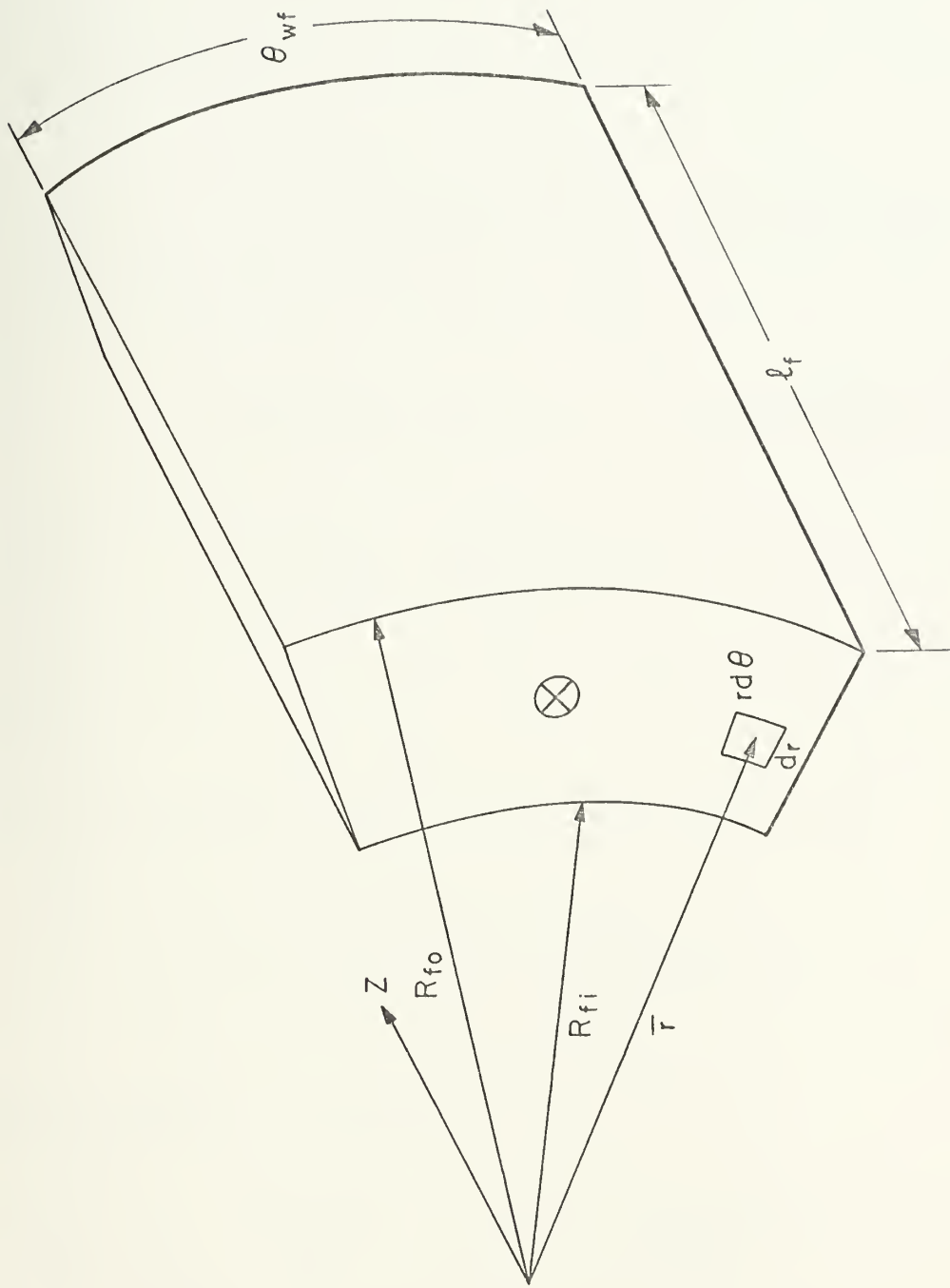


Figure C-1 Field Winding Pole Face Isometric

Consider the machine configured as in Figure 1 with the compensator located between the armature and the field. Using equation A83, H_r may be expressed as

$$H_r = \frac{3}{2} \cos k(\theta + \phi) H_{rao} + H_{rco} \quad (C13)$$

or,

$$H_r = \sum_{\substack{n=1 \\ n \text{ odd}}}^{\infty} \frac{2}{n\pi} \left(\frac{r^{k-1} - \alpha_o R_{si}^{2k} r^{-k-1}}{\alpha_o R_{si}^{2k}} \right) \left[\frac{3J_a}{2} \left(\frac{R_{ao}^{2+k} - R_{ai}^{2+k}}{2+k} \right) \right.$$

$$\left. \sin \left(\frac{k\theta_{wa}}{2} \right) \cos k(\theta + \phi) + J_c \left(\frac{R_{co}^{2+k} - R_{ci}^{2+k}}{2+k} \right) \right.$$

$$\left. \sin \left(\frac{k\theta_{wc}}{2} \right) \sin k(\theta - \alpha) \right] \quad (C14)$$

Define

$$\Gamma = \frac{3J_a}{2} \left(\frac{R_{ao}^{2+k} - R_{ai}^{2+k}}{2+k} \right) \sin \left(\frac{k\theta_{wa}}{2} \right) \cos k(\theta - \phi) + J_c \left(\frac{R_{co}^{2+k} - R_{ci}^{2+k}}{2+k} \right) \sin \left(\frac{k\theta_{wc}}{2} \right) \sin k(\theta - \alpha) \quad (C15)$$

Whereas, equation C12 becomes

$$\frac{\bar{T}}{\bar{\chi}_f} = \sum_{\substack{n=1 \\ n \text{ odd}}}^{\infty} \frac{4p\mu_o J_f}{n\pi} \int_0^{\chi_{fo}} \int_{\chi_{fi}}^{\chi_{fo}} \left(\frac{r^{k-1} - \alpha_o R_{si}^{2k} r^{-k-1}}{\alpha_o R_{si}^{2k}} \right) \Gamma r^2 dr d\theta \quad (C16)$$

Integrating Cl6 and dropping the vector notation, Cl6 becomes

$$\frac{T}{\ell_f} = \sum_{\substack{n=1 \\ n \text{ odd}}}^{\infty} \frac{4\mu_o J_f}{n\pi} \left[\frac{R_{fo}^{2+k} - R_{fi}^{2+k}}{2+k} - \frac{\alpha_o R_{si}^{2k} (R_{fo}^{2-k} - R_{fi}^{2-k})}{2-k} \right] \int_0^{\frac{\pi}{2k}} \frac{\Gamma}{\alpha_o R_{si}} d\theta \quad (C17)$$

Define

$$\eta \equiv \left[\frac{R_{fo}^{2+k} - R_{fi}^{2+k}}{2+k} - \alpha_o R_{si}^{2k} \frac{(R_{fo}^{2-k} - R_{fi}^{2-k})}{2-k} \right] \frac{4\mu_o J_f}{n\pi \alpha_o R_{si}^{2k}} \quad (C18)$$

and integrating equation Cl6 across the pole face

$$\frac{T}{\ell_f} = \sum_{\substack{n=1 \\ n \text{ odd}}}^{\infty} \eta \frac{\frac{\theta_{wf}}{2}}{\int_0^{\theta_{wf}}} [\zeta_1 \cos k(\theta+\phi) + \zeta_2 \sin k(\theta-\alpha)] d\theta \quad (C19)$$

where

$$\zeta_1 = \frac{3J_a}{2} \left(\frac{R_{ao}^{2+k} - R_{ai}^{2+k}}{2+k} \right) \sin \left(\frac{k\theta_{wa}}{2} \right) \quad (C20)$$

$$\zeta_2 = J_c \left(\frac{R_{co}^{2+k} - R_{ci}^{2+k}}{2+k} \right) \sin \left(\frac{k\theta_{wc}}{2} \right) \quad (C21)$$

The integration of Cl9 yields:

$$\frac{T}{\ell_f} = \sum_{\substack{n=1 \\ n \text{ odd}}}^{\infty} \frac{\eta}{k} \left\{ \zeta_1 \left[\sin k \left(\frac{\theta_{wf}}{2} + \phi \right) - \sin k \left(\phi - \frac{\theta_{wf}}{2} \right) \right] - \zeta_2 \left[\cos k \left(\frac{\theta_{wf}}{2} - \alpha \right) - \cos k \left(\frac{\theta_{wf}}{2} + \alpha \right) \right] \right\} \quad (C22)$$

Which reduces to:

$$\frac{T}{\ell} = \sum_{\substack{n=1 \\ n \text{ odd}}}^{\infty} \frac{2\eta}{k} [\zeta_1 \sin\left(\frac{k\theta_{wf}}{2}\right) \cos k\phi - \zeta_2 \sin\left(\frac{k\theta_{wf}}{2}\right) \cos k\alpha] \quad (C23)$$

In equation C23 the current in the armature winding is specified to vary as $\cos \omega_e t$. Equation C23 may be expressed as

$$\frac{T}{\ell} = \sum_{\substack{n=1 \\ n \text{ odd}}}^{\infty} \sigma_1 \cos k\phi - \sigma_2 \cos k\alpha \quad (C24)$$

when

$$\begin{aligned} \sigma_1 &= \frac{2\eta}{k} \zeta_1 \sin\left(\frac{k\theta_{wf}}{2}\right) \\ \sigma_2 &= \frac{2\eta}{k} \zeta_2 \sin\left(\frac{k\theta_{wc}}{2}\right) \end{aligned} \quad (C25)$$

The condition for null torque on the field winding becomes

$$\sum_{\substack{n=1 \\ n \text{ odd}}}^{\infty} \sigma_1 \cos k\phi - \sigma_2 \cos k\alpha = 0 \quad (C26)$$

Which leads to a set of null torque requirements encompassing all odd harmonics.

Considering only the first harmonic, equation C26 yields as the condition for null field torque.

$$\sigma_1 \cos k\phi = \sigma_2 \cos k\alpha \quad (C27)$$

$$\text{or } \cos k\phi = J_C \Lambda_1 \cos k\alpha \quad (C28)$$

where,

$$\Lambda_1 = \frac{2}{3J_a} \left(\frac{R_{co}^{2+k} - R_{ci}^{2+k}}{R_{ao}^{2+k} - R_{ai}^{2+k}} \right) \frac{\sin(\frac{k\theta_{wc}}{2})}{\sin(\frac{k\theta_{wa}}{2})} \quad (C29)$$

For a four pole machine, considering the first harmonic only, equations C28 and C29 may be expressed as:

$$\cos 2\phi = J_c \Lambda_1 \cos 2\alpha \quad (C30)$$

$$\Lambda_1 = \frac{2}{3J_a} \left(\frac{R_{co}^4 - R_{ci}^4}{R_{ao}^4 - R_{ai}^4} \right) \frac{\sin\theta_{wc}}{\sin\theta_{wa}}$$

Consider the machine configured as in Figure 1 with the compensator located between the main field winding and the shield. Using equation A33, H_r may be expressed as:

$$H_r = \frac{3}{2} \cos k(\theta + \phi) H_{rao} + H_{rci} \quad (C31)$$

$$H_r = \sum_{\substack{n=1 \\ n \text{ odd}}}^{\infty} \frac{2}{n\pi} \left[\frac{3J_a}{2} \left(\frac{r^{k-1} - \alpha_o R_{si}^{2k} r^{-k-1}}{\alpha_o R_{si}^{2k}} \right) \left(\frac{R_{ao}^{2+k} - R_{ai}^{2+k}}{2+k} \right) \right. \\ \left. \sin\left(\frac{k\theta_{wa}}{2}\right) \cos k(\theta + \phi) + J_c \left(\frac{r^{k-1}}{2k} \right) \Omega_c \sin\left(\frac{k\theta_{wc}}{2}\right) \sin k(\theta - \alpha) \right] \quad (C32)$$

where Ω_c is expressed in equation A3, modified by Table A3.

Substituting C32 into C11 and integrating yields:

$$\cos k\phi = J_c \Lambda_2 \cos k\alpha \quad (C33)$$

where

$$\Lambda_2 = \frac{2}{3J_a} \frac{\sin(\frac{k\theta_{wc}}{2})}{\sin(\frac{k\theta_{wa}}{2})} \frac{(R_{fo}^{2+k} - R_{fi}^{2+k})}{(R_{ao}^{2+k} - R_{ai}^{2+k})} \left[\frac{(2-k)(R_{co}^{2+k} - R_{ci}^{2+k})}{(2-k)(R_{fo}^{2+k} - R_{fi}^{2+k})} \right. \\ \left. \frac{-\alpha_o(2+k)R_{si}^{2k}(R_{co}^{2-k} - R_{ci}^{2-k})}{-\alpha_o(2+k)R_{si}^{2k}(R_{fo}^{2-k} - R_{fi}^{2-k})} \right] \quad (C34)$$

For a four pole machine, considering only the first harmonic C33 and C34 become:

$$\cos 2\phi = J_c \Lambda_2 \sin 2\alpha \quad (C35)$$

$$\Lambda_2 = \frac{2 \sin \theta_{wc}}{3J_a \sin \theta_{wa}} \frac{(R_{fo}^4 - R_{fi}^4)}{(R_{ao}^4 - R_{ai}^4)} \left[\frac{R_{co}^4 - R_{ci}^4 - 4\alpha_o R_{si}^4 \ln}{R_{fo}^4 - R_{fi}^4 - 4\alpha_o R_{si}^4 \ln} \right. \\ \left. \frac{\left(\frac{R_{co}}{R_{ci}} \right)}{\left(\frac{R_{fo}}{R_{fi}} \right)} \right] \quad (C36)$$

Note that for most windings where z and y are greater than .9, Λ_2 reduces for the four pole first harmonic case to approximately the same value as Λ_1 , if we consider a laminated iron shell.

Armature Torque Expression

The expression for H_r in the region $R_{ai} < r < R_{ao}$ is

$$H_r = H_{rfi} + H_{rci} \quad (C36)$$

Using equations A61 and A61, as modified by Table A3, equation C36 may be expressed as

$$H_r = \sum_{\substack{n=1 \\ n \text{ odd}}}^{\infty} \frac{2}{n\pi} \left(\frac{r^{k-1}}{\alpha_o R_{si}} \right) [J_f \Omega_f \sin \frac{k\theta_{wf}}{2} \sin k \theta \\ + J_c \Omega_c \sin \frac{k\theta_{wc}}{2} \sin k(\theta - \alpha)] \quad (C37)$$

where α_o , Ω_c , and Ω_f are expressed by equations A68, A56, and A56 modified by Table A3 respectfully.

Using equation C11 and integrating through the armature winding, the armature torque per unit length is

$$\frac{T_a}{l_a} = \frac{24\mu_o J_a}{n^2\pi} \left(\frac{1}{\alpha_o R_{si}} \right) \left(\frac{R_{ao}^{2+k} - R_{ai}^{2+k}}{2^{2+k}} \right) \sin \frac{k\theta_{wa}}{2} \\ [J_f \Omega_f \sin \frac{k\theta_{wf}}{2} \sin k \phi + J_c \Omega_c \sin \frac{k\theta_{wc}}{2} \sin k(\phi - \alpha)] \quad (C38)$$

When $k=2$, $n=1$, $p=2$; equation 38 becomes

$$\frac{T_a}{l_a} = \frac{6\mu_o J_a \sin \theta_{wa}}{\pi \alpha_o R_{si}^4} (R_{ao}^4 - R_{ai}^4) [J_f \Omega_f \sin \theta_{wf} \sin 2\phi \\ + J_c \Omega_c \sin \theta_{wc} \sin 2(\phi - \alpha)] \quad (C39)$$

When Ω_f and Ω_c are expressed by equations A56 and A56 modified by Table A3 respectfully.

APPENDIX D

MACHINE SIZING AND LOSSES

As discussed in preceding sections, this thesis addresses machines which may find applications in SWATH, hydrofoil, and SES vehicles. Current designs indicate machine dimensions and power requirements as indicated in Table D-1. Note the relatively large l/D required for hydrofoil applications.

Using the shaft horsepower requirements for various applications as listed in Table D-1, an estimate of minimum shaft radius may be made. This is equivalent to estimating the machine armature inner radius, R_{ai} .

Shaft shear stress $\tau_{\theta z}$ may be expressed as (see reference 8)

$$\tau_{\theta z} = \frac{M_t R_{ai}}{I_z} \quad (D1)$$

where $M_t = \frac{PWR}{\omega_m}$, $I_z = \frac{\pi R_{ai}^4}{2}$, assuming a solid machine shaft. (D2, D3)

Substituting D2 and D3 into D1 and solving for R_{ai} ,

$$R_{ai} = \left[\frac{PWR(60)}{\pi^2 \tau_{\theta z} N} \right]^{1/3} \quad (D3)$$

Where N = machine RPM. Table D-2 is a summary of machine minimum R_{ai} for a $\tau_{\theta z}$ of 30,000 psi.

NAVAL APPLICATION	NUMBER OF MACHINES REQUIRED	APPROX. MACHINE DIAMETER ALLOWED (in)	APPROX. MACHINE LENGTH ALLOWED (in)	$\frac{\ell}{D}$	APPROX. MACHINE SHAFT HORSE-POWER RATING (each)
SWATH (see Fig. 2)	2	96	120	1.25	40,000
HYDROFOIL (see Fig. 4)	2	54	100	1.85	20,000
SES (see Fig. 3)	2	72	90	1.25	30,000

TABLE D-1 Current Machine Vehicle Application Parameters

PWR (hp)	N (RPM)	Minimum R_{ai} (in)	Possible Application
20,000	1800	2.5	HYDROFOIL
30,000	900	3.6	SES
40,000	180	6.7	SWATH

TABLE D-2 Minimum Armature Shaft Inner Radial for Indicated Naval Applications

The machine RPM is a function of the drive train characteristics between the motor and the propeller and propeller characteristics in general. Machine RPM may be adjusted by varying either the number of machine poles or frequency of armature current. The shaft radius actually employed is increased to account for some margin of safety.

An examination of Figure 11, reference 7 (approximately reproduced herein as Figure D-1), indicates the approximate domain of magnetic shear stress to be expected for machines of various power ratings. As a design guide the machine in this presentation should fall within the cross-hatched area indicated in Figure D-1.

The magnetic shear stress may be expressed as

$$\sigma_m = \frac{(PWR)P}{(2\pi R_{ao})^2 \ell f} \quad (D4)$$

Figure D-1 and equation D4 together may be used to select a "reasonable" value of σ_m for any particular design. Equation D3, D4 and machine power as expressed by equation 12 are used to formulate the machine physical size exclusive of the shield.

Assuming an iron shield is employed, its thickness may be found by integrating the magnetic field density across the pole face of each winding at R_{si} , summing the resulting values, and determining the thickness from an assumed maximum magnetic flux density in the shield. As a design constraint, a value of 1.5 Teslas is assumed to be the maximum value.

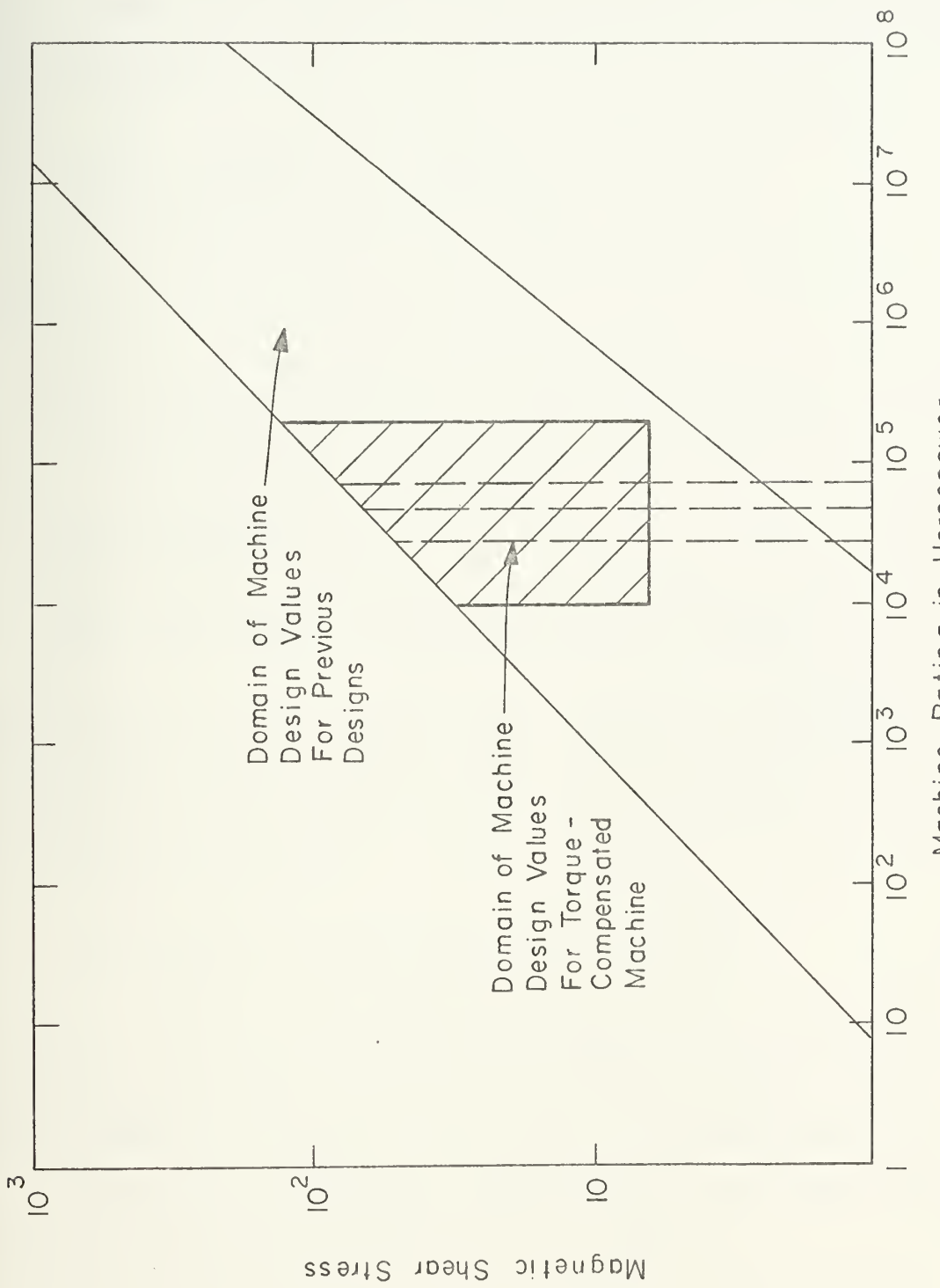


Figure D-1 Machine Shear Stress Versus Machine Rating (7)

Referring to Figure D2 and assuming that all flux from each winding generated in the radial direction enters the shield material, the total radial flux and iron shield flux is found from

$$\Phi_s = \int_A \bar{B}_o \cdot d\bar{A} = \mu_o \int_A \bar{H}_o \cdot d\bar{A} \quad (D5)$$

where

$$\bar{H}_o = (H_{rfo} + H_{rco} + \hat{H}_{rao}) \bar{I}_r + (H_{\theta fo} + H_{\theta co} + \hat{H}_{\theta ao}) \bar{I}_\theta \quad (D6)$$

$$d\bar{A} = rd\theta dz \bar{I}_r$$

$$\bar{H}_{ao} = \frac{3}{2} (H_{rao} \bar{I}_r + H_{\theta ao} \bar{I}_\theta); \quad \hat{H}_{rao} = \frac{3}{2} H_{rao} \quad (D7)$$

The limits of integration in the θ direction will vary according to each element's included winding angle. Equation D5 may be written as

$$\Phi_s = R_{si} \ell_t \mu_o \int_0^{\theta} (H_{rfo} + H_{rco} + \hat{H}_{rao}) d\theta \quad (D8)$$

Treating only the $k=2$, $n=1$, $p=2$ machine, the field strengths may be found from equation A86 with the appropriate substitution.

Once Φ_s is determined, constrained as mentioned above, the shield minimum thickness may be found as

$$(R_{so} - R_{si}) = \frac{\Phi_s}{B_{max} \ell_t} \quad (D9)$$

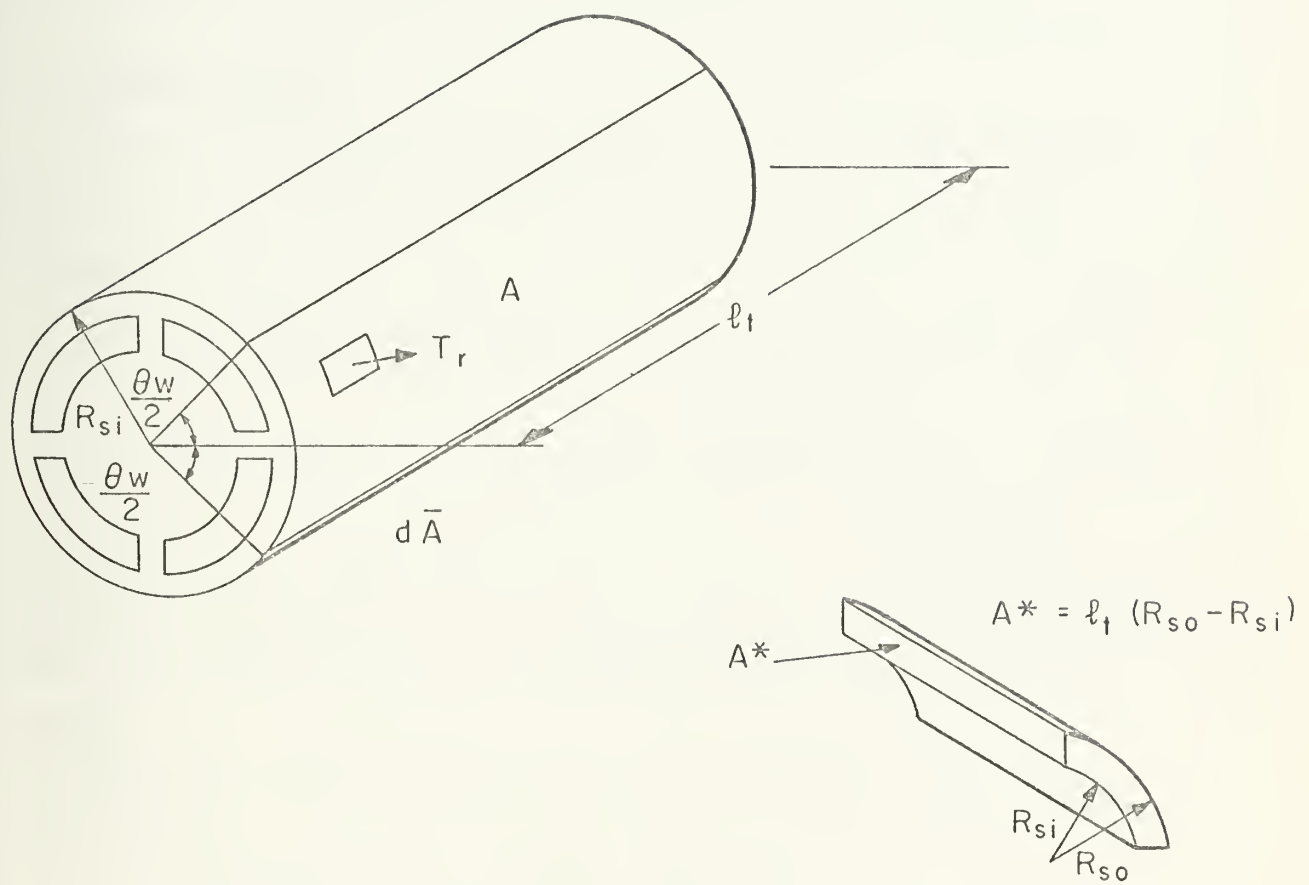


Figure D-2 Winding and Shield Configuration for Shield Thickness Determination

B_{max} is chosen from Figure 15a, reference 9, to be 1.5 Tesla. The philosophy of shield design is based on the need to protect personnel in an operating space or prevent undue electromagnetic radiation from the vessel.

Machine Losses

Machine losses may be attributed to two primary sources. Sources such as bearing friction, windage, etc., are not addressed.

a) Conductor losses due to current flow, J_a and J_c :

$$p_c = \frac{3p\lambda}{\sigma\lambda} [J_a^2 R_{ao}^2 (1-x^2) + J_c^2 R_{co}^2 (1-z^2)] \quad (D10)$$

In equation D10, the space winding factor, λ , is assumed to be essentially the same for both armature and compensator windings.

b) Eddy - current losses in the armature:

$$p_{ec} = \frac{3p\theta_{wa} R_{ao}^2 (1-x^2) \omega_e^2 \sigma \lambda \ell_{ed} d_w^2 B_{av}^2}{32} \quad (D11)$$

where B_{av}^2 is the mean-square magnetic field seen by the armature conductors:

$$B_{av}^2 = \frac{1}{R_{ao} - R_{ai}} \int_{R_{ao}}^{R_{ai}} B_{rfi}^2 dr \quad (D12)$$

B_{rfi} given by equations A56, A61, or A68 as applicable.

c) Losses due to eddy currents and hysteresis losses in the shield is considered to be negligible because of the large armature-shield separation ($R_{ai} \ll R_{si}$). Losses in the shaft material and armature winding support structure are recognized but not addressed in this analysis.

APPENDIX E

DERIVATION OF MACHINE CHARACTERISTICS AND RATING EXPRESSIONS

Referring to Figure E1, through trigonometric manipulation it may be shown that:

$$E_F = V_T + X_A I_A (\sin \psi - \cos \psi \cot \alpha) \quad (E1)$$

The internal excitation voltage, E_F , may be expressed as:

$$E_F = \frac{\omega e M_{1f} I_f}{\sqrt{2}} \quad (E2)$$

Where, from equation B34

$$M_{1f} = \frac{-32(1-y^{2+p})\ell_m N_{ta} N_{tf} \mu_o \sin(\frac{p\theta_{wa}}{2}) \sin(\frac{p\theta_{wf}}{2}) (\frac{R_{fo}}{R_{ao}})^p}{\alpha_o \pi \theta_{wa} \theta_{wf} (1-y^2) (1-x^2)} C_{1pf} \quad (E3)$$

and

$$C_{1pf} = \frac{[1-x^{2-p} - \alpha_o (\frac{2-p}{2+p}) (1-x^{2+p}) (\frac{R_{ao}}{R_{si}})^{2p}]}{p(4-p^2)} \quad (E4)$$

As a matter of convenience define

$$MIFA = \frac{-32 \ell_m C_{1pf} \mu_o \sin(\frac{p\theta_{wa}}{2}) \sin(\frac{p\theta_{wf}}{2}) (1-y^{2+p}) (\frac{R_{fo}}{R_{ao}})^p}{\alpha_o \pi \theta_{wa} \theta_{wf} (1-y^2) (1-x^2)} \quad (E5)$$

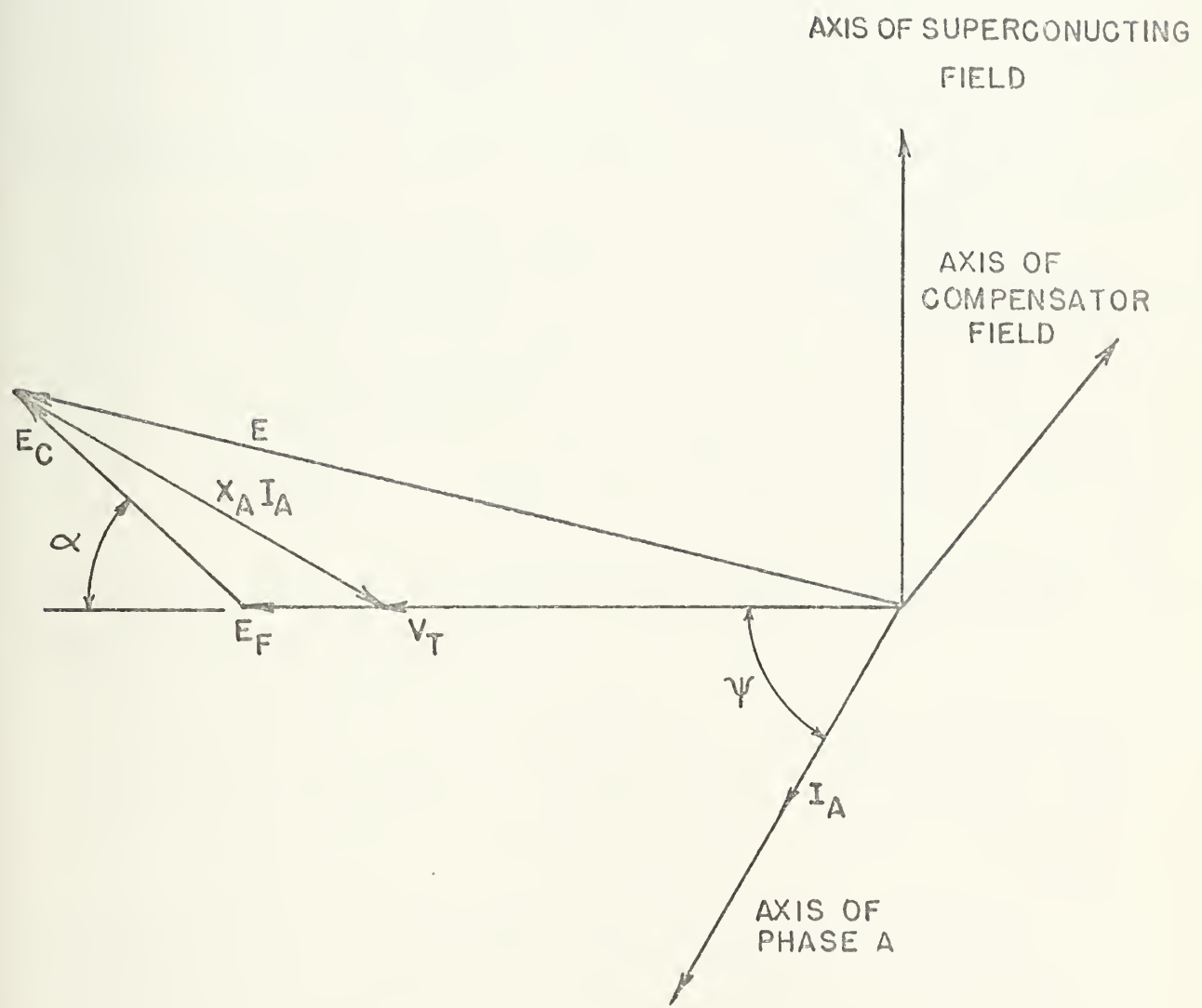


FIGURE EI. VOLTAGE-CURRENT RELATIONSHIP FOR OVEREXCITED COMPENSATED MACHINE.

Using equation E5, equation E3 may be reduced to:

$$M_{1f} = MIFA N_{ta} N_{tf} \quad (E6)$$

The volt-ampere rating of the machine may be expressed as

$$P = 3V_T I_A = 3E_F I_A \left(\frac{V_T}{E_F}\right) \quad (E7)$$

From Appendix A,

$$I_A = \frac{J_a \theta_{wa} R_{ao}^2 (1-x^2)}{2N_{ta}} \quad (A49) \text{ modified}$$

$$I_f = \frac{J_f \theta_{wf} R_{fo}^2 (1-y^2)}{2N_{tf}} \quad (A49)$$

Substituting equations E2, E3, and A49 into E7, the machine rating may be expressed as:

$$P = \frac{24}{\sqrt{2} \pi} \omega_e \mu_o J_a J_f \ell_m (1-y^2+p) R_{fo}^4 C_{1pf} \sin\left(\frac{p\theta_{wa}}{2}\right) \sin\left(\frac{p\theta_{wf}}{2}\right) \left(\frac{V_T}{E_F}\right) \quad (E8)$$

In order to solve for machine power from equation E8, an expression for (V_T/E_F) must be found. Define V_B and I_B as rated machine base voltage and current ($V_B = V_T$, $I_B = I_A$). Also, define the per-unit variables

$$v_t = \frac{V_T}{V_B}; \quad i_a = \frac{I_A}{I_B}; \quad e_f = \frac{E_F}{V_B} \quad (E9)$$

Dividing equation E1 by V_B and the substitution of equations E9 yields:

$$e_f = v_t + \frac{x_A I_B}{V_B} i_a (\sin \psi - \cos \psi \cot \alpha) \quad (E10)$$

With the per-unit synchronous reactance defined as

$$x_d = \frac{x_A I_B}{V_B}$$

Equation E10 becomes:

$$e_f = v_t + x_d i_a (\sin \psi - \cos \psi \cot \alpha) \quad (E11)$$

If equation E11 is divided by e_f and simplified, the following relationship is produced:

$$\frac{v_t}{e_f} = 1 - x_a i_a (\sin \psi - \cos \psi \cot \alpha) \quad (E12)$$

Where x_a , the internally normalized per-unit synchronous reactance is defined as:

$$x_a = \frac{x_A I_B}{E_F} = \frac{x_A I_A}{E_F} \quad (E13)$$

Converting equation E12 from per-unit to absolute values yields:

$$\frac{V_T}{E_F} = 1 - x_a (\sin \psi - \cos \psi \cot \alpha) \quad (E14)$$

Equation E13 may be expressed as:

$$x_a = \frac{\omega e^{(L_a - L_{ab}) I_A}}{E_F} \quad (E15)$$

Using equation B25 for $(L_a - L_{ab})$ and equations E2 and E3, equation E15 becomes:

$$x_a = \frac{3\sqrt{2}}{4} \frac{\ell_a}{\ell_m} \frac{J_a}{J_f} \frac{\sin(\frac{p\theta_{wa}}{2})}{\sin(\frac{p\theta_{wf}}{2})} \left(\frac{R_{ao}}{R_{fo}}\right)^{2p} \frac{1}{(1-y^{2p})} \frac{C_{sp}}{C_{lpf}} \quad (E16)$$

All terms in equation E8 are now defined in terms of machine currents and geometry. Utilizing expressions developed in this and other appendices, it is possible to determine the compensator current density required for a given machine configuration and power level for any given value of α .

Using equation C38, torque on the armature may be expressed as:

$$T_a = \frac{24\mu_0 J_a}{n^2 \pi} \left(\frac{1}{\alpha_0 R_{si}} \right) \left(\frac{R_{ao}^{2+k} - R_{ai}^{2+k}}{2+k} \right) \sin\left(\frac{k\theta_{wa}}{2}\right) \\ [J_f \Omega_f \sin\left(\frac{k\theta_{wf}}{2}\right) \sin(k\phi) + J_c \Omega_c \sin\left(\frac{k\theta_{wc}}{2}\right) \sin k(\phi-\alpha)] \quad (C38)$$

where Ω_c and Ω_f are defined by equation A56.

As a matter of convenience groups of terms in equation C38 may be defined as:

$$\Delta_1 \equiv \frac{24\mu_o J_a}{n^2\pi} \left(\frac{1}{\alpha_o R_{si}} \right) \left(\frac{R_{ao} - R_{ai}}{2+k} \right)^{2+k} \sin \left(\frac{k\theta_{wa}}{2} \right) \quad (E17)$$

$$\Delta_2 \equiv J_f \Omega_f \sin \left(\frac{k\theta_{wf}}{2} \right) \quad (E18)$$

$$\Delta_3 \equiv \ell_c \sin \left(\frac{k\theta_{wc}}{2} \right) \quad (E19)$$

Equation C38 may now be written as:

$$T_a = \Delta_1 [\Delta_2 \sin k\phi + \Delta_3 J_c \sin k(\phi - \alpha)] \quad (E20)$$

Torque on the armature may also be expressed as

$$\left. \begin{aligned} T_a &= \frac{p(\text{PWR})}{2\pi F} \\ \text{where} \\ \text{PWR} &= P \cos \psi \end{aligned} \right\} \quad (E21)$$

Substituting equation E21 into E20 and simplifying, a set of quadradic equations in terms of $\sin(k\phi)$ results:

$$Q_A \sin^2(k\phi) + Q_B \sin(k\phi) + Q_C = 0 \quad (E22)$$

Where,

$$Q_A \equiv \Delta_1^2 [J_C^2 \Delta_3^2 + \Delta_2^2 + 2\Delta_2 \Delta_3 J_C \cos(k\alpha)] \quad (E23)$$

$$Q_B \equiv -\frac{p(\text{PWR}) \Delta}{\pi F} [J_C \Delta_3 \cos(k\alpha) + \Delta_2] \quad (E24)$$

$$Q_C \equiv \frac{p^2(\text{PWR})^2}{4\pi^2 F^2} - J_C^2 \Delta_1^2 \Delta_3^2 \sin^2(k\alpha) \quad (E25)$$

Using the equation for zero torque on the superconducting field winding (C38 or C33) written as

$$\cos(k\phi) = J_C \bar{\Lambda} \cos(k\alpha) \quad (E26)$$

Equation E22 reduces to:

$$\Delta_5 J_C^4 + \Delta_4 J_C^3 + \Delta_3 J_C^2 + \Delta_2 J_C + \Delta_1 = 0 \quad (E27)$$

where,

$$\bar{\Lambda} = \begin{cases} \Delta_1 & R_{ci} < R_{fi} \text{ (equations C29 or C30)} \\ \Delta_2 & R_{ci} < R_{fi} \text{ (equations C34 or C35)} \end{cases} \quad (E28)$$

$$\Delta_5 \equiv \Delta_1^2 \Delta_3^2 \bar{\Lambda}^2 \sin^2(k\alpha) \quad (E29)$$

$$\Delta_4 \equiv 2\bar{\Lambda}^2 \Delta_1^2 \Delta_2 \Delta_3 \sin^2(k\alpha) \cos(k\alpha) \quad (E30)$$

$$\Delta_3 \equiv \bar{\Lambda}^2 \Delta_1^2 \Delta_2^2 \sin^2(k\alpha) - \frac{p(\text{PWR}) \Delta_1 \Delta_3 \bar{\Lambda} \cos(k\alpha) \sin(k\alpha)}{\pi F} - \Delta_1^2 \Delta_3^2 \sin^2(k\alpha) \quad (E31)$$

$$A_2 \equiv -\frac{\Delta_1 \Delta_2 \bar{A} p(\text{PWR}) \sin(k\alpha)}{\pi F} \quad (E32)$$

$$A_1 \equiv \frac{p^2 (\text{PWR})^2}{4\pi^2 F^2} \quad (E33)$$

For a four pole machine with angle α fixed at 45° (90° electrically) with an iron shield boundary (assume $\mu_s = .009 \text{ hy/m}$), a first harmonic analysis of equations E29 through E33 yields:

$$\left. \begin{array}{l} A_5 = \Delta_1^2 \Delta_3^2 \bar{A}^2 \\ A_4 = 0 \\ A_3 = \bar{A}^2 \Delta_1^2 \Delta_2^2 - \Delta_1^2 \Delta_3^2 \\ A_2 = -2\Delta_1 \Delta_2 \bar{A} (\text{PWR}) \\ A_1 = \frac{(\text{PWR})^2}{\pi^2 F^2} \end{array} \right\} \quad (E34)$$

Equation E26 implies a set of conditions for zero torque on the superconducting field; one condition for each odd integer value of k . Higher order effects of the third and higher harmonics are not addressed herein.

Consider equation E8 written as

$$P = K_1 J_a J_f \left(\frac{V_T}{E_F} \right) \quad (E35)$$

where,

$$K_1 = \frac{24}{\pi\sqrt{2}} \omega_e u_o \ell_m (1-y^{2+p}) R_{fo}^4 C_{lpf} \sin\left(\frac{p\theta_{wf}}{2}\right) \sin\left(\frac{p\theta_{wa}}{2}\right) \quad (E36)$$

also, consider equation E16 written as

$$x_a = K_2 \frac{J_a}{J_f} \quad (E37)$$

where,

$$K_2 = \frac{3\sqrt{2}}{4} \frac{\ell_a}{\ell_m} \frac{\sin\left(\frac{p\theta_{wa}}{2}\right)}{\sin\left(\frac{p\theta_{wf}}{2}\right)} \left(\frac{R_{ao}}{R_{fo}}\right)^{2p} \frac{1}{(1-y^{2p})} \frac{C_{sp}}{C_{lpf}} \quad (E38)$$

Substituting equation E14 and E37 into E35 yields:

$$P = K_1 J_a J_f \left[1 - K_2 \frac{J_a}{J_f} (\sin \psi - \cos \psi \cot \alpha) \right] \quad (E39)$$

Equation E39 may be reduced to:

$$P = K_3 J_a - K_4 J_a^2 (\sin \psi - \cos \psi \cot \alpha) \quad (E40)$$

where

$$\left. \begin{aligned} K_3 &\equiv K_1 J_f \\ K_4 &\equiv K_1 K_2 \end{aligned} \right\} \quad (E41)$$

Using equations E7 and E40, an expression for J_a in terms of J_f , ψ and α may be found:

$$J_f = K_5 + K_4 J_a (\sin \psi - \cos \psi \cot \alpha) \quad (E42)$$

where,

$$K_5 \equiv \frac{3V_T \theta_{wa} R_{ao}^2 (1-x^2)}{K_1 N_{ta}} \quad (E43)$$

If λ is defined as $\sin \psi - \cos \psi \cot \alpha$, equation E42 may be written as:

$$J_a = \left(\frac{1}{K_4 \lambda} \right) J_f - \frac{K_5}{K_4 \lambda} \quad \left. \right\} K_4, K_5 > 0 \quad (E44)$$

An examination of Figures 7, 8, and 9 reveals that the angle ϕ between the armature phase a field and the superconducting main field is equivalent to the angle $(\psi + 90^\circ)$ electrically at the zero torque condition. Therefore, equation E26 may be written as

$$\cos k (\psi + 90^\circ) = J_C \bar{A} \cos (k\alpha) \quad (E45)$$

which reduces to

$$\cos (k\psi) = J_C \bar{A} \cos (k\alpha) \quad (E46)$$

Angle ψ in equation E46 is a mechanical angular value analogous to angle ϕ in Figure 1. Employing the analytical techniques which earlier resulted in equations E29 through E34, it is also possible to obtain a fourth order equation in $\cos k\alpha$ or $\sin k\alpha$ as

$$B_5 \cos^4(k\alpha) + B_4 \cos^3(k\alpha) + B_3 \cos^2(k\alpha) + B_2 \cos(k\alpha) + B_1 = 0 \quad (E47)$$

where B_1 through B_5 are functions of machine geometry, J_a , ψ , and J_c .

Machine Length Parameters

Based on machine lengths developed in reference 6, Table E1 represents the parameters used in this paper.

Armature end turn length	$\Delta\ell = R_{ai} + R_{ao}$
Armature self-inductance effective length	$\ell_a = \ell + \Delta\ell$
Field-to-armature mutual inductance effective length	$\ell_m = \ell$
Compensator-to-armature mutual inductance effective length	$\ell_c = \ell$
Eddy current loss effective length	$\ell_{ed} = \ell$
Conduction loss effective length	$\ell_c = \ell + 2\Delta\ell$

TABLE E1 Effective Lengths

APPENDIX F

PROGRAM LISTING

The program used in the development of this thesis, THESIS I, accepts input data and provides output data as described in Table F1. The program as listed herein provides output data for any given number of machine geometries and for each machine geometry provides data for armature current densities ranging from $.25 \times 10^6$ to 2.5×10^6 a/m². Any input parameter may be incremented as required by inserting a proper ∞ loop. The program accepts any number of pole pairs, any harmonic desired, and any value for shield permeability. Table F2 describes the arrangement of the input deck.

DATA CLASS	ALGEBRAIC SYMBOL	FORTRAN WORD
Input	p	P
	n	N
	θ_{wa}	TWA
	θ_{wc}	TWC
	θ_{wf}	TFW
	α	ALP
	f	F
	J_a	JA
	J_f	JF
	I_a	IA
	μ_s	MUS
	$\cos \psi$	PF
	R_{ai}	RAI
	R_{ao}	RAO
	R_{fi}	RFI
	R_{fo}	RFO
	R_{ci}	RCI
	R_{co}	RCO
	R_{si}	RSI
	R_{so}	RSO
	ℓ	L
Output	all input quantities	as above
	C_2	C2
	C_{2f}	C2F
	x_a	XA

DATA CLASS	ALGEBRAIC SYMBOL	FORTRAN WORD
	x_d	XD
	E_f	EF
	N_{ta}	NTA
	V_t	VT
	PWR	APWR
	T_a	TA
	Λ	F4
	$\Delta_1, \Delta_2, \Delta_3$	DELT1, DELT2, DELT3
	J_c	JC

TABLE F1. Input/Output Data for THESIS I Program

DATA CARD #	COLUMNS	CONTAINS	FORMAT
1	1-10	p	F10.3
	11-20	N	F10.3
	21-30	θ_{wa}	F10.3
	31-40	θ_{wc}	F10.3
	41-50	θ_{wf}	F10.3
	51-60	α	F10.3
	61-70	F	F10.3
2	1-10	J_a	E10.3
	11-20	J_f	E10.3
3	1-10	I_A	F10.3
4	1-10	μ_s	F10.3
5	1-10	PF	F10.3
6	1-5	IMUS	I5
	6-10	KY	I5
7	1-10	R_{ai}	F10.3
	11-20	R_{ao}	F10.3
	21-30	R_{fi}	F10.3
	31-40	R_{fo}	F10.3
	41-50	R_{ci}	F10.3
	51-60	R_{ω}	F10.3
	61-70	R_{si}	F10.3
	71-80	R_{so}	F10.3

DATA CARD #	COLUMNS	CONTAINS	FORMAT
8	1-10	L	F10.3

TABLE F2. Arrangement of Input Data Deck

Data cards 7 and 8 are sequentially repeated (without cards 1-6) depending upon the number of machines desired. KY is the number of machines being analyzed on each run. KY may, of course, be set artificially high and the program terminates once all data is processed. By setting IMUS = ϕ on card 6, α_0 is set equal to -1, assuming a laminated iron shield of high permeability; otherwise, IMUS = any integer not ϕ allows α_0 to be computed.

THESES
 LT. D. M. REYNEDSON, WSN SPRING 1975
 A SUPERCONDUCTING SYNCHROCCUS TORQUE-COMPENSATED MOTOR FOR NAVAL APPLICATIONS
 A TYPICAL, THA, TWC, TWF, ALP, F, JA, JC, JE, TA, MUS, P, TMS, KY, DAT, FAD, RFI, 370, PCT, PC
 C, RAST, RSO, I, OUTPUT ALL INPUTS AND FTM, C2, C2F, XA, XD, EE, VT, NTA, FADP, DPMI, ADUR, MA, DELT1, DELT
 C, 2, DELT3, 74, JCF (4 ROOTS)
 DRC3BAM ALLOWS FOR END TURN EFFECTS
 INPUT UNITS BELOW IN PAREN
 D=DATA'S OF EFFECTS
 N=HARMONIC THEORY
 TWA=ARMATURE INCLUDED ANGLE (DEGREES)
 TYC=COMPENSATOR INCLUDED ANGLE (DEGREES)
 THE=MAIN FIELD INCLUDED ANGLE (DEGREES)
 TAE=OUTER RADIUS OF ARMATURE (INCHES)
 TAO=OUTER RADIUS OF ARMATURE (INCHES)
 TCT=INNER RADIUS OF COMPENSATOR (INCHES)
 TCO=OUTER RADIUS OF COMPENSATOR (INCHES)
 TFI=INSIDE RADIUS OF FIELD (INCHES)
 TFO=OUTER RADIUS OF FIELD (INCHES)
 TSI=INNER RADIUS OF SHIELD (INCHES)
 TSO=OUTER RADIUS OF SHIELD (INCHES)
 T= MACHINE LENGTH (INCHES)
 F= FREQUENCY (HZ)
 JA=ARMATURE CURRENT DENSITY (A/SQ. METER)
 JCE=COMPENSATOR CURRENT DENSITY (A/SQ. METER)
 JF=FIELD CURRENT DENSITY (A/SQ. METER)
 NTA= # TURNS FOR ARMATURE EACH PATH
 NTC= # TURNS FOR COMPENSATOR PATH, PAIR
 NTE= # TURNS FOR FIELD PATH PAIR
 TA=ARMATURE CURRENT (AMPS RMS)
 MS=SHIELD PERMEABILITY (HY/METER)
 DE=POWER FACTOR
 IUS=FLUX: If IUS INPUT AS 0, ASSUME SHIELD PERMEABILITY LARGE, ALDO=-1; If
 IUS INPUT ANY INTEGRED OTHER THAN 0, ALDO COMPUTED.
 SUPP=PERFECTION COEF AT RST


```

C KY=4 OF MACHINERY COMPUTED
C PDM=REV PER MINUTE OF PROPELLER SHAFT
C C2=ANALYTICAL CONSTANT
C XA=INTENALLY NORMALIZED SYNCHRONOUS REACTANCE
C XD=2PIR-UNIT SYNCHRONOUS REACTANCE
C FP=INTENNAL THREE PHASE VOLTAGE (VOLTS RMS)
C PWR=INTERNAL MACHINE POWER IN KW
C PWRIM=IMAGINARY POWER IN KWASS
C ADRG=MACHINE POWER IN HORSEPOWER
C TA=MACHINE OUTPUT TORQUE (FT-LBS)
C VT=EXTENSIONAL VOLTAGE PER PHASE (VOLTS RMS)
C C COMPLEX*16 A(5),B(5)
C DOUBLE PRECISION R(5),C(5)
C READ,IA,IL,IC,IA,JA,JC,TF,MUS,N,MUO,NTA,NTB,K,R2
C
C =4
C
C I=PTN=1
C READ(5,100) N,TWA,TWC,TWF,ALP,F
C READ(5,200) JA,JP
C READ(5,300) TA
C WRITE(6,400) P,N,TWA,TWF,TWC,ALP,F
C READ(5,500) MUS
C READ(5,600) P2
C PI=3.14159
C READ(5,700) TMUS,KY
C KY=N*D
C K2=2.*K
C AK2=K+2.
C 2K=K-2.
C P2=P*2.
C A72=7+2.
C A2P=2-2.
C MU0=4.*PI*(1.E-07)
C DO 12 KX=1,KY
C READ(5,800) RAI,RAO,PT,FFO,RCI,RCC,RSI,RSO

```



```

READ(5,900) L
WRITE(6,1000) PAT, RAO, RFI, RFO, RCI, RCO, RSSI, RSO
WPT=(6,110) PPT, L
DFIT=L+BAT+AO
LA=L+DELTI
TM=L
LC=L
LF=L
C7=.0254
R=1=C7*PPT
B7C=P7C*CE
PCT=PCT*CF
RCO=P7C*CE
BAT=PAT*CF
RAC=PAO*CE
RST=GST*CF
RSO=R7S*CE
L=L*CF
IA=IA*CE
LE=L*CE
LV=L*CE
LC=LC*CE
R=7ST/PSO
X=PAT/RAC
Y=29T/PSO
7=FCI/RCO
TA=PI*TA/180.
TWC=PI*TWC/180.
TWF=PI*WFT/180.
ALD=PI*ALD/180.
STC=STN(PI*TNC/2.)
STA=STN(PI*TNA/2.)
STR=STN(PI*TNE/2.)
SKA=STN(PI*ALD)
CKA=COS(PI*ALF)
EFM=60.*D/P

```



```

      WRITE(5,1200) JA,IP,PPW
      DO 11 KV=1,10
      T=(MUS*EC.C) GO TO 1
      P1=(MUS/MUS)*(1.+W**K2)
      F2=(1.-W**K2)+W1
      F3=(1.+W**K2)+W1
      ALD0=(1.+WUS/WU0)*(F2/F3)/(1.-(MUS/MU0)*(F2/F3))
      GO TO 2
      ALD0=-1.
      1 2 T=(PCT*G.F.*PFO) GO TO 3
      P4=(.5667*STC*(EC0**AK2-RCT**AK2)/(JA*STA*(RAO**AK2-PAI**AK2))
      GO TO 4
      3 T=(K.*W0*2.*)GC TO 4
      P4=(.6667*STC*(PFO**AK2-RPI**AK2)*(RCC**AK2-RCT**AK2-ALD0*(AK2/A2K
      1)*(S1**2)*(RC0**AK2-RCT**AK2)))/(JA*STA*(RAO**AK2-PAI**AK2)*(RFO
      1*AK2-RCT**AK2-ALD0*(AK2/A2K)*(S1**K2)*(S1**AK2))*
      GO TO 5
      4 P4=(.5667*STC*(PFO**4-RFT**4)*(RCO**4-RCI**4-4.*ALD0*(RST**4)*ALOG
      1(1.07)))/(JA*STA*(RAO**4-PAI**4)*RFO**4-RFT**4-4.*ALD0*ALOG(1./Y)
      1)
      5 T=(K.*EC.2.) GO TO 6
      CMC=(PCO**AK2-RCT**AK2)/AK2-(ALD0*(RST**K2)*(RFO**AK2-PAI**AK2))/A
      12K
      CMC=(RFO**AK2-RFT**AK2)/AK2-(ALD0*(RST**K2)*(RFO**AK2-PAI**AK2))/A
      12K
      GO TO 7
      6 CMC=(RFO**4-RFT**4)/4.-ALD0*(RST**4)*ALOG(1./Y)
      CMC=(PCO**4-PAI**4)/4.-ALD0*(RST**4)*ALOG(1./Z)
      7 DATA(6,1200) TA
      NTA=(JA*TA*(1.-X*X)*PAC*PA0)/(2.*TA)
      TA(K.*79.2.) GC TO 8
      C25=(1.-(Y**A2D)-(A2P/AE2)*ALD0)*(1.-XAP2)*(RAO/RST)**P2)/(P*(4.-
      1P*xP))
      C2=(2.-K-4.*X**AK2)+AK2*(Y**4)-(AK2/AK2)*(1.-X**AK2)*(RAO/RST)**P2)
      C25=(1.-(Y**A2D)-(A2P/AE2)*ALD0)*(1.-XAP2)*(RAO/RST)**P2)
      GO TO 9

```


α C2F=-.125*ALOG(X)+((1.-Y**4)*PAO**4)/(32.*PSI**4)
 $C2=5*(X**4)*ALOG(X)+(1.-X**4)/8.+((1.-X**4)*(PAO**4))/(16.*RST**4)
1)
 α KPTTS(6,1400)C2,C2,F
 α Y1PA=(32.*LM**NJO*C2F*STA*STF*(1.-Y**AK2)*(PAO/PAO)**P)/(DI*TWA*T
 α 19D*(1.-Y**Y)*(1.-X**Y)*ALPO
 α YA=(7.61*LA*TA*STA*C2*((PAO/370)**NP2))/(LM*JF*STA*(1.-Y**AP2)*C2
1E)
 α WPTT(6,1400)YA
 α FFA=ABCCS(PF)
 α SINP=STN(PA)
 α VTFP=1.-X1*(STN2-P2*(CKA/SKA))
 α XD=XA*VT
 α YD=XTT(6,1400)YD
 α RF1=.707*NT*P17A*JF*STW*(1.-Y*Y)*REQ*PFO*F
 α EH=EE1*NT
 α VT=VTF*EP
 α KPTT(6,1700)EP,NTA,VT
 α PW=33.94*P*W*JA*JF*LM*(1.-Y**AP2)*(PAO**AP2)*C2F*VTE*STA*STF*P
1E/(PAO**AP2)
 α PW2=PW2/1500.
 α P5P1=P5P1*STNP/DP
 α MPTT(6,1400)
 α KPTT(6,1400)PW,R,PWPT
 α APWF=PW*302134
 α TA=(P*AW**55C.)/(2.*PT*F)
 α WPTT(6,2000)APR,TA
 α DELT1=(24.*TA*WIC*JA*STA*(PAO**AK2)-PAT**AK2)/(N*N*PI*AK2*AL20*(PST
1*AK2))
 α DELT2=JE*CH*STF
 α DELT3=ONC*STC
 α KPTT(6,2100)DELT1,DELT2,DELT3,E4
 α P(1)=(P*D*PWR*DMP)/(4.*ET*PT*F)
 α B(2)=-(DELT1*DELT2*F4*D*PWR*SKA)/(PT*F)
 α B(3)=F4*D*DELT1*DELT2*DELT2*DELT3*DELT1*DELT3*SKA*SKA
 α 1KA*SKA)/(ET*F)-(DELT1*DELT3*SKA*SKA$


```

B(4)=2.*F4*F4*DPLT1*DPLT2*DPLT3*DPLT3*SKA*SKA*SKA
B(5)=DPLT1*DPLT1*DPLT3*DPLT3*SKA*SKA*SKA*F4*F4
C(1)=0.*D
C(2)=C.*E
C(3)=0.*D
C(4)=0.*D
C(5)=0.*D
DO 10 T=1,5
A(I)=DCNTRY(B(I),C(I))
10  CCNTNIT
      CALL CCNTNIT(A,M,TDPIN,SOCT)
      11 CCNTNIT
      12 CCNTNIT
      100 FOPMAT(7E10,3)
      200 FCMPMAT(2E10,3)
      300 FCMPMAT(5E10,3)
      400 FCMPMAT(/5X,1P=1,1X,F5.2,3X,'N=1,1X,F5.2,3X,'TWA=1,1X,F8.2,3X,'TWF=1,1X,F8.2,3X,'TWC=1,1X,F8.2,3X,'ALDHA=1,1X,F8.2,1REQ=1,1X,F8.2)
      500 FCMPMAT(7E10,3)
      600 FOPMAT(F10,3)
      700 FCMPMAT(2E15)
      800 FCMPMAT(8E10,3)
      900 FCMPMAT(7E10,3)
      1000 FOPMAT(/5X,'PAT=1,1X,F7.2,3X,'RAO=1,1X,F7.2,3X,'RCI=1,1X,F7.2,3X,'RCI=1,1X,F7.2,3X,'RFO=1,1X,F7.2,3X,'RST=1,1X,F7.2,3X,'RST=1,1X,F7.2,3X)
      1100 FOPMAT(/5X,'POWER?FACTCR=1,1X,F7.5,5X,'L=1,1X,F7.2)
      1200 FCMPMAT(/5X,'JA=1,1C.4,3X,'JF=1,1X,E10.4,3X,'RDM=1,1X,F10.3)
      1300 FOPMAT(/5X,'TA=1,1X,F10.2)
      1400 FOPMAT(/5X,'C2=1,1X,F12.5,3X,'C2E=1,1X,F12.5)
      1500 FOPMAT(/5X,'XA=1,1X,F12.5)
      1600 FCMPMAT(/5X,'PER UNIT SYNC.'REACTANC=1,1X,F10.7)
      1700 FOPMAT(/5X,'PE=1,1X,F10.3,3X,'NTA=1,1X,F12.5,3X,'VT=1,1X,E12.5)
      1800 FOPMAT(/5X,'REAL POWER IN KW; 'EFFECTIVE POWER IN KWAD')
      1900 FOPMAT(/5X,'REAL POWER=1,1X,F12.5,3X,'REAL POWER=1,1X,F12.5)

```


2000 FC2X, *POWERP (HP)=*, 1X, 312.5, 3X, *TOT_QUE (FT-L,BS)=*, 1X, F12.5)
2100 FORMAT (/5X, *DELT1=*, 1X, E12.5, 3X, *DELT2=*, 1X, F12.5, 3X, *DELT3=*, 1X, E

TH2S0217
TH2S0218
TH2S0219

REFERENCES

1. Hildebrand, Francis B., *Advanced Calculus for Applications*, Prentice-Hall, Inc., Englewood Cliffs, N.J., May 1965.
2. Steeves, Michael, "A Generalized Two-Dimensional Field Analysis of Air-Core Synchronous Machines", Internal Memorandum #19, Electric Power Systems Engineering Laboratory, M.I.T., Cambridge, Massachusetts, June 1973.
3. Kirtley, James L., "Surface Coefficient for Multipolar Magnetic Field Boundary Condition Problems", presented to IEEE Winter Power Meeting, New York, January 27 - February 1, 1974, to be published in *Transactions Power Apparatus and Systems*, paper #T 74 220-0.
4. Stekly, Z.J.J. and Halas, E., "A Study of Alternators With Superconducting Field Windings: I - Analysis", *IEEE Transactions Power Apparatus and Systems*, Vol. PAS-85, No. 3, March, 1966.
5. Kirtley, James L., "Basic Formulas for Air-Core Synchronous Machines", IEEE Conference Paper #71 CP 155-PWR.
6. Kirtley, James L., "Design and Construction of an Alternator with a Superconducting Field Winding", Ph.D. Thesis, Department of Electrical Engineering, M.I.T., August 1971.
7. Minervini, Joseph V., "Analysis and Design of Multipole, Superconducting Rotating Electric Machines", S.M.M.E. Thesis, Department of Mechanical Engineering, M.I.T., January 1974.
8. Crandall, Stephen H. and Norman C. Dahl, *An Introduction to the Mechanics of Solids*, McGraw-Hill, New York, 1959.
9. M.I.T. Electrical Engineering Department Staff, *Magnetic Circuits and Transformers*, M.I.T. Press, Cambridge, Massachusetts, January 1965.

Thesis

R3665

Reynerson

A superconducting
synchronous torque-
compensated motor
for naval applications.

133788

